Isolation of antimutator yeast strains: an exploration of DNA replication fidelity

Lindsey N. Williams

A dissertation
submitted in partial fulfillment of the
requirements for the degree of

Doctor of Philosophy

University of Washington

2012

Reading Committee:

Brad Preston, Chair

Matt Kaeberlein

Nancy Maizels

Program Authorized to Offer Degree:

Molecular and Cellular Biology

University of Washington

ABSTRACT

Isolation of antimutator yeast strains: an exploration of DNA replication fidelity

Lindsey Williams

Chair of Supervisory Committee:
Professor Bradley Preston
Department of Pathology

DNA polymerases (Pols) ε and δ perform the bulk of eukaryotic nuclear DNA replication. Both Pols are high-fidelity enzymes with intrinsic proofreading exonucleases that remove errors during DNA synthesis. Errors that elude proofreading are extended into duplex DNA and excised by the mismatch repair (MMR) system. Cells that lack Pol proofreading or MMR exhibit a mutator phenotype, manifested as a 10- to 100-fold increase in spontaneous mutation rate. Haploid yeast strains with combined defects in Pol proofreading and MMR initially divide, but succumb to error-induced extinction and fail to form viable colonies. We exploited error-induced extinction to isolate suppressors of lethal mutation rates (*eex* mutants). In screens for mutants that suppress *pol3-01 msh6Δ* or *pol2-4 msh2Δ* error-induced extinction, thirty-five- and six-percent of *eex* mutations, respectively, encoded 'antimutator' polymerases that increased replication fidelity. The locations of antimutator amino-acid changes and their effects on mutation spectra suggest multiple mechanisms of mutator suppression. The remaining *eex* alleles were extragenic to the polymerase genes, suggesting that factors in addition to polymerase base selectivity, proofreading and MMR influence replication fidelity. Previous

studies (Datta *et al.* 2000) showed that the mutator phenotype of proofreading-deficient Pol δ depends on Dun1, a protein kinase that mediates damage-inducible gene expression and up-regulates dNTP synthesis during the S-phase checkpoint. We demonstrated that deletion of Dun1 (*dun1Δ*) rescues cells from error-induced extinction caused by combined defects in Pol ε proofreading and base selectivity (*pol2-4,M644G*) or Pol ε proofreading and mismatch repair (*pol2-4 msh2Δ*). *dun1Δ* suppressed the mutator phenotypes of *pol2-4* (encoding proofreading-deficient Pol ε) and *pol2-M644G* (encoding a Pol ε variant with altered base selectivity) 5- to 10-fold. Our findings, together with those of Datta *et al.*, suggest that Pol ε and Pol δ errors are sensed as stressors that trigger Dun1 activation. Our data present a complex picture of DNA replication fidelity, where misincorporations during replication trigger Dun1-dependent mutagenesis. We propose that Dun1 stimulation of dNTP synthesis enhances mispair extension to ensure continued DNA replication. Thus, it appears that mutator phenotypes are inducible and suppressible through multiple mechanisms. We speculate that transient mutator phenotypes promote microbial adaptation and mammalian oncogenesis.

TABLE OF CONTENTS

LIST OF FIGURES

Page

LIST OF TABLES

Page

ACKNOWLEDGMENTS

I would like to thank Brad Preston for giving me the freedom to explore the questions that I found most interesting, for his unwavering enthusiasm, and for insisting on scientific excellence and rigor. I would like to thank Alan Herr for being a patient and giving teacher, for listening to me curse too much, for advice when I needed it, and for leaving me alone when I did not. And to many others for their kindness and generosity: Donovan Anderson, Jean Campbell, Eddie Fox, Brian Hayes, Dongqing Huang, Scott Kennedy, Larry Loeb, Chris Murakami, Brian Piening and Donna Prunkard.

Last but not least, I would like to acknowledge the best committee in the world. Bonny Brewer, Matt Kaeberlein, Nancy Maizels and Toshi Tsukiyama: thank you.

CHAPTER I: THE DETERMINANTS OF DNA REPLICATION FIDELITY

To propagate, every organism must first duplicate its chromosomes. Normal cells duplicate their DNA with extraordinary fidelity (~10^{-10} mutations per nucleotide per cell division) and, thus, maintain genomic stability and cellular function (Drake *et al.* 1998). Replicative DNA polymerases make errors approximately once every 10^{-5} nucleotides polymerized (reviewed in (Kunkel and Bebenek 2000)). Despite this exceptional base selectivity, each time a yeast cell divides, ~120 polymerase errors occur; in mammalian cells, ~100,000 errors occur. These base-base mispairs and slippage events must be corrected at nearly 100% efficiency to maintain a spontaneous mutation rate of 10^{-10}. This is accomplished with the combined efforts of polymerase exonucleolytic proofreading and mismatch repair (MMR).

Loss of proofreading or MMR increases the spontaneous mutation rate, resulting in a mutator phenotype (Greene and Jinks-Robertson 2001; Morrison *et al.* 1991; Morrison *et al.* 1993; Morrison and Sugino 1992; Morrison and Sugino 1994; Simon *et al.* 1991; Tran *et al.* 1999b). In diploid yeast, combined defects in proofreading and MMR result in a multiplicative increase in mutation rate, suggesting that proofreading and MMR act in a series to repair polymerase errors (Morrison *et al.* 1993; Tran *et al.* 1999b). In contrast, defects in other repair pathways such as base-excision repair or nucleotide-excision repair result in normal mutation rates unless cells are challenged with DNA damaging agents (Friedberg and Meira 2003; Hanawalt 2002; Memisoglu and Samson 2000). Therefore, base selectivity, proofreading and MMR are the major determinants of replication fidelity.

Polymerase base selectivity and proofreading

DNA polymerases (Pols) are enzymes that catalyze the polymerization of deoxyribonucleotides (dNTPs) into a DNA strand. Pols have a highly conserved structure,

and based on sequence homology, are subdivided into one of seven families: A, B, C, D, X, Y and RT (reviewed in (Pavlov *et al.* 2006b)). All known eukaryotic pols belong to the A, B, X or Y families (Hubscher *et al.* 2002; Pavlov *et al.* 2006b). Family B polymerases perform the bulk of nuclear DNA synthesis in eukaryotes: Pols δ and Pol ε replicate the lagging- and leading-strands, respectively (Larrea *et al.* 2010; Nick Mcelhinny *et al.* 2008; Pavlov and Shcherbakova 2010; Pursell *et al.* 2007). Replicative pols require speed, processivity and accuracy to faithfully replicate large genomes. Pol γ, which replicates mitochondrial DNA, belongs to the A-family. Other specialized eukaryotic DNA polymerases copy only short stretches of DNA during repair or translesion synthesis and are members of the X or Y families (Pavlov *et al.* 2006b).

Amino acid sequence alignments and crystal structures indicate that A, B, D, Y and RT family polymerases have a core structure analogous to a cupped right hand (Beese *et al.* 1993; Ding *et al.* 1998; Eom *et al.* 1996; Huang *et al.* 1998a; Wang *et al.* 1997) (Li *et al.* 1998) (Franklin *et al.* 2001) (Ling *et al.* 2001). The palm contains the catalytic residues, the fingers coordinate incoming dNTPs, and the thumb positions primed DNA in the active site. C- and X-family polymerases are 'left-handed' based on the orientation of DNA synthesis relative to the thumb and fingers (Sawaya *et al.* 1997; Wing *et al.* 2008). DNA polymerization occurs in a stepwise manner (Kunkel and Bebenek 2000). First, a dNTP binds the fingers, inducing a conformational change that rotates the fingers towards the palm (Doublie *et al.* 1999; Franklin *et al.* 2001; Kiefer *et al.* 1998; Sawaya *et al.* 1997). A binding pocket is formed between the fingers and the palm, positioning the incoming dNTP for bond formation. Phosphoryl transfer occurs after the fingers close. The fingers then flip to an open conformation and, lastly, the polymerase translocates. Watson-Crick base pairs are remarkably similar with respect to size and geometry, and these spatial characteristics can be monitored to maintain fidelity (Saenger 1984). For highly accurate pols, inherent at every

step of polymerization are measures that limit incorporation and extension of mispairs (reviewed in (Kunkel and Bebenek 2000) and (Johnson 1993)).

Discrimination against incorrect nucleotides occurs as dNTPs bind and induce finger rotation. Correct dNTPs bind with 10- to >1,000- times higher affinity than incorrect dNTPs (Hubscher *et al.* 2002). This may reflect differential release of correct and incorrect dNTPs from the fingers. The fingers remain in an open conformation until a dNTP is bound (Bailey *et al.* 2006; Eom *et al.* 1996; Wang *et al.* 1997). Studies of T7 Pol indicate that correct nucleotides commit the fingers to conformational rotation, and slow dNTP release (Tsai and Johnson 2006). Once in a closed conformation, high-fidelity DNA pols form a tight nucleotide binding pocket that limits solvent access and selects base pairs that specifically conform to Watson-Crick geometry (Beese *et al.* 1993; Doublie *et al.* 1998; Eom *et al.* 1996; Franklin *et al.* 2001; Swan *et al.* 2009; Wing *et al.* 2008). Watson-Crick base pairs have similar distances between the C1' atoms of the sugars, equivalent glycosidic bond angles, and identically positioned hydrogen bond acceptors (O2 of pyrimidines and N-3 of purines) in the minor groove (Saenger 1984). The overall geometry of mispairs differs dramatically and thus, mispairs can be excluded based on size, shape and position of minor groove contacts (Beard and Wilson 2003; Echols and Goodman 1991). Additionally, template DNA is bent 90° between the fingers and thumb, ensuring that only the template nucleotide contacts the active site, reducing stacking interactions that might otherwise stabilize mispairs (Swan *et al.* 2009).

The rate of phosphodiester bond formation is slower for an incorrect nucleotide (Tsai and Johnson 2006). All DNA polymerases contain two highly conserved carboxylate residues that coordinate divalent metal ions (Metal A and Metal B) to facilitate catalysis (Beard and Wilson 2003; Steitz *et al.* 1994). Metal A promotes nucleophile formation of the 3'-OH. Metal B stabilizes the pentacovalent intermediate and both metals balance the

negative charge on the pyrophosphate to facilitate a leaving group (Steitz *et al.* 1994). A proper pentacovalent intermediate is required for efficient chemistry (Beard and Wilson 2003). In the T7 Pol studies, phosphoryl transfer was 100-times faster for correct base pairs, suggesting that incorrect nucleotides are misaligned in the active site, slowing phosphoryl transfer (Tsai and Johnson 2006).

A mispaired primer terminus, resulting from a misincorporation error, compromises the rate of DNA extension by a hundred- to a million-fold (Bebenek and Kunkel 1995; Echols and Goodman 1991; Goodman *et al.* 1993). Thus, the polymerase pauses, allowing the mispaired terminus to be partitioned to exonucleases for proofreading. Pols ε and δ have integral exonucleases. The pols shuttle between polymerase and exonuclease mode, and balance between the activities is regulated by competition for the 3' end of the primer (Hubscher *et al.* 2002). Movement between the polymerase and exonuclease domains is aided by the thumb tip (Shamoo and Steitz 1999) and proofreading is processive, allowing the polymerase to remain bound to DNA (Hubscher *et al.* 2002). Point mutations that inactivate Pol ε or Pol δ proofreading (Exo-) increase the mutation rate up to 100-fold, creating a mutator phenotype characterized by increased base-substitutions and frameshift mutations (Fortune *et al.* 2005; Morrison *et al.* 1993; Simon *et al.* 1991; Tran *et al.* 1999b). Inactivation of both exonuclease domains is synthetically lethal in haploid yeast, indicating that pol proofreading is synergistic (Morrison and Sugino 1994). Thus, yeast Pol ε and Pol δ act on the same pool of replication errors and proofread for one another. However, this does not appear to be the case in mammals (Albertson *et al.* 2009). Additionally, yeast Pol δ and Pol ε likely proofread for polymerases that lack exonuclease domains, such as Pol α (Albertson and Preston 2006; Pavlov *et al.* 2004).

There is still a chance for excision if a mispair is extended. Distortions in the helix can be detected by the thumb, which has extensive contacts with the primer-template and the

active site. Decreased contacts between the thumb and duplex DNA correlate to increased mismatch extension (Hubscher *et al.* 2002). Additionally, structural studies of an A-family polymerase showed that mispairs up to 4 base pairs from the primer terminus can cause distortions in the DNA helix. Distortions disrupt the arrangement of the primer-template in the active site, thereby slowing catalysis and allowing exonuclease switching. Thus, the polymerase has a short 'memory' that can be monitored for misinsertion (Johnson and Beese, 2004).

Mismatch repair

Mismatches that are extended into duplex DNA are recognized by MMR (reviewed in (Iyer *et al.* 2006)). In yeast, complexes of MutS homologs (Msh2-Msh6 or Msh2-Msh3) bind mispairs, insertions and deletions. MutL homodimers (Mlh1-Pms1 or Mlh1-Mlh3) are then recruited to bound lesions. Pms1 and Mlh3 contain a latent endonuclease activity that nicks the nascent strand, allowing excision and re-synthesis (Kadyrov *et al.* 2006; Kadyrov *et al.* 2009; Kunkel and Erie 2005). Defects in MMR increase mutation rates between 10- to 1000-fold in organisms as diverse as bacteria, yeast, worms, mice, and humans (De Wind *et al.* 1995; Denver *et al.* 2005; Fishel *et al.* 1993; Morrison *et al.* 1993; Parsons *et al.* 1993; Reitmair *et al.* 1997; Schaaper 1993). Simultaneous inactivation of both proofreading and MMR can increase mutation rates by more than 10,000-fold ((Morrison *et al.* 1993; Schaaper 1993).

Discovery of polymerase antimutators

The first polymerase antimutators were discovered in the *43* gene of bacteriophage T4 (Drake and Allen 1968; Drake *et al.* 1969). Gene *43* encodes the viral replicase, a B-family polymerase with homology to the eukaryotic replicative pols (Pol α, Pol ε, and Pol δ).

While characterizing temperature sensitive phages with mutations in gene *43*, Drake and Allen discovered two mutants that exhibited lower mutation rates than wild-type. The revelation that polymerase fidelity could be improved was startling. Given that most mutations are deleterious, why wouldn't evolution select these higher fidelity polymerase variants? Early biochemical analyses in the Bessman and Nossal labs observed that T4 antimutators function by hydrolyzing more dNTPs per base pair synthesized than wild-type polymerases (Muzyczka *et al.* 1972), thereby increasing fidelity at the expense of processivity (Gillin and Nossal 1976a; Gillin and Nossal 1976b). Further characterization revealed that the antimutator T4 phages replicated poorly in strains with lower dNTP pools, hinting that increased proofreading efficiency comes with a fitness cost. Although a large collection of antimutator T4 Pol variants was later isolated, it remained unclear whether any amino acid changes increased the base selectivity of the polymerase (Reha-Krantz 1988; Reha-Krantz and Nonay 1994).

Pol III variants isolated in *E. coli* were the first indication that fidelity could be improved without hyper-editing. Pol III performs the bulk of chromosomal synthesis in *E. coli* (Johnson and O'Donnell 2005) and consists of tightly associated subunits that comprise the holoenzyme. The *dnaE* gene encodes the polymerase subunit α and the *dnaQ* gene encodes the proofreading exonuclease subunit ε. The first Pol III antimutator variant was identified as a suppressor of the proofreading-compromised *dnaQ* mutator allele, *mutD5* (Schaaper and Cornacchio 1992). *mutD5* cells grow slowly, and Schaaper isolated a spontaneous, faster growing clone of *mutD5* cells. The mutation mapped to *dnaE* and suppressed the *mutD5* mutator phenotype, as well as the growth defect. The discovery that changes in the polymerase subunit could offset proofreading defects prompted screens for antimutators that could suppress MMR defects (Fijalkowska *et al.* 1993). In bacteria, MutS homodimers recognize mismatched DNA and recruit MutL homodimers, which in turn recruit

the MutH endonuclease (Iyer *et al.* 2006). *dnaE* mutants that suppressed the *mutL* mutator phenotype were recovered, indicating that most mutations in the strain derive from Pol III errors that escape proofreading, thus reducing the frequency of the most common Pol III-derived MMR substrates (Fijalkowska and Schaaper 1993). To confirm that the newly identified antimutators did not lower mutation rates by increasing proofreading efficiency, Schaaper and colleagues moved the *dnaQ* antimutators into the *mutD5* strain (Fijalkowska and Schaaper 1995). The *mutD5* mutator phenotype was also suppressed, suggesting that these antimutators did not require subunit ε for their increased replication fidelity. Further, mutations that completely abrogate ε proofreading activity are lethal, and the α-encoded antimutators rescued this lethality, confirming that the amino acid substitutions in Pol III lower mutation rates independently of proofreading activity (Fijalkowska and Schaaper 1996). Evidence of altered nucleotide selectivity comes from the observation that certain Pol III antimutators suppress the mutator phenotype of *mutT*, which encodes an 8-oxo-dGTPase. By 'cleansing' the nucleotide pools, the *mutT* protein minimizes transversions caused by A•8-oxo-dGTP base pairs (Schaaper 1996). Schaaper identified two Pol III antimutator variants that suppressed the *mutT* mutator phenotype 10-fold, and these were also effective at suppressing *mutL* (Schaaper 1996).

The first eukaryotic antimutator allele was discovered serendipitously in yeast by combining the Pol δ frameshift mutator allele *pol3-t* (Tran *et al.* 1995) with the proofreading defective allele *pol3-01* (Morrison *et al.* 1993). Rather than producing a compound mutator phenotype, the double mutant exhibited a three-fold reduction in mutation rate relative to *pol3-01* (Tran *et al.* 1999a). Pavlov *et al.* demonstrated that another weak mutator allele (*pol3-Y708A*) suppressed *pol3-01* frameshift mutations, although not base-substitution errors (Pavlov *et al.* 2004). Curiously, the analogous substitution (Y831A) in proofreading deficient Pol ε (encoded by *pol2-4*) suppressed both types of errors (Pavlov *et al.* 2004). The

contrasting effects of antimutator substitutions on proofreading-defective Pol ε and Pol δ may reflect intrinsic polymerase differences or the ability to alternate replication enzymes that correct or extend errors on the leading and lagging strands.

Reha-Krantz and colleagues identified additional antimutator alleles of Pol δ. Introduction of a G447S substitution into a beta-hairpin structure in the exonuclease domain of Pol δ produced a frameshift suppression phenotype (Hadjimarcou *et al.* 2001). The analogous change in T4 Pol (G255S) inhibits hyper-editing of the primer strand to the exonuclease domain (Stocki *et al.* 1995). This suggests that yeast Pol δ G477S suppresses misalignment errors that cause frameshifts by minimizing primer-DNA dissociation. In a separate study, Reha-Krantz identified suppressors of the PAA-sensitive L612M allele in an MMR-deficient (*msh2Δ*) background (Li *et al.* 2005). Interestingly, while the L612M mutant is a modest mutator in yeast, substitution of the L612-equivalent in human Pol δ with lysine (L606K) increased polymerase fidelity *in vitro* in the presence or absence of proofreading activity (Schmitt *et al.* 2010).

Error-induced extinction and escape from lethal mutation rates

In haploid yeast with a Pol δ proofreading deficiency (*pol3-01*), the inactivation of mismatch repair is lethal. Evidence for this replication 'error-induced extinction' came from early studies demonstrating that proofreading and MMR acted sequentially to correct DNA polymerase errors (Morrison *et al.* 1993; Morrison and Sugino 1994; Tran *et al.* 1999b). The *pol3-01* allele confers a mutation rate up to 100-fold over wild-type, as does inactivation of MMR (Morrison *et al.* 1993; Prolla *et al.* 1994; Simon *et al.* 1991). Diploids defective in both Pol δ proofreading and MMR (*pol3-01/pol3-01 pms1/pms1*) grew slowly and exhibited a 1,000-fold increase in spontaneous mutation rates, suggesting that loss of both pathways results in unrestrained replication errors (Morrison *et al.* 1993; Tran *et al.* 1999b). Double-

mutant haploid spores derived from *POL3/pol3-01 PMS1/pms1* diploids germinated, but failed to form colonies. Further examination of the germinated spores revealed microcolonies of around 100 cells arrested at all stages of the cell cycle (Morrison *et al.* 1993; Tran *et al.* 1999b). The phenotypic distribution of morphologies in *pol3-01 pms1* microcolonies mirrored the distribution observed in a systematic inactivation of all essential yeast genes (Yu *et al.* 2006), suggesting that random mutations in essential genes drives error extinction. As further evidence of this, we defined the maximal mutation rate in haploids using a plasmid shuffling scheme (Boeke *et al.* 1984; Simon *et al.* 1991) that created a conditional mutator phenotype (Herr *et al.* 2011a). The yeast strain for these studies carried chromosomal gene deletions of the catalytic subunit of Pol δ (*pol3Δ*) and an essential component for repair of most base-base mismatches (*msh6Δ*) (Marsischky *et al.* 1996). When we shuffled in a collection of mutant *pol3* plasmids carrying hypomorphic or proofreading-defective alleles of *POL3*, some *pol3 msh6Δ* combinations were viable. However, the stronger *pol3* mutator alleles were synthetically lethal with *msh6Δ*. By measuring the mutation rates of viable combinations and calculating the theoretical mutation rates of lethal combinations, we determined that the threshold for error-induced extinction is around 1×10^{-3} *can1* mutants/cell division. Our studies provided evidence for an error threshold. Assuming *CAN1* (1500 base pairs) represents an average yeast gene, this mutation rate predicts a mutational target size of 1000 essential genes, which is very close the number of essential genes determined by systematic gene inactivation (Winzeler *et al.* 1999). Thus, mutation accumulation throughout the genome likely drives replication error-induced extinction in yeast.

While defining the threshold of mutagenesis, we also isolated mutants that survived error-induced extinction driven by *pol3-01 msh6Δ*. A large-scale screen for *pol3-01 msh6Δ* suppressors revealed that one third of these error-induced extinction (*eex*) mutants carried mutations that encode single amino acid changes in Pol δ. The rest mapped to the nuclear

genome, implicating other genes in antimutagenesis. The amino acid substitutions in Pol δ conferred an antimutator phenotype, suppressing *pol3-01* between 3- and 50-fold, and were scattered throughout the polymerase domains. Surprisingly, even though the Pol δ exonuclease was inactivated in the *pol3-01 msh6Δ* strain, numerous suppressors altered the exonuclease domain. Because error-induced extinction is due to random mutations in multiple genes, the antimutators likely reduce Pol δ errors in many different sequence contexts (Herr *et al.* 2011a; Herr *et al.* 2011b).

Significance

Mutator phenotypes are hypothesized to provide the genetic diversity necessary for emergence of malignant clones during cancer progression (Loeb *et al.* 1974). Indeed, inherited defects in polymerase proofreading or MMR confer mutator phenotypes and increase cancer risk (Albertson *et al.* 2009; Goldsby *et al.* 2002; Goldsby *et al.* 2001; Peltomäki 2005; Wei *et al.* 2002). The total number of mutations in a cancer has been estimated at more than 10^{12} (Tomlinson *et al.* 2002), providing support for the mutator hypothesis of cancer. However, mutation accumulation in normal cells prior to cancer progression combined with the large number of generations required for tumor growth may be sufficient to obtain such staggering numbers of mutations (Tomlinson *et al.* 2002).

Whether most tumors exhibit a mutator phenotype is unclear. Several groups investigating genetic instability and cancer have concluded that mutation rates are not elevated in cancer cell lines (Finette *et al.* 2001; Wang *et al.* 2002). Critics of these studies argue that since only clonal mutations were examined, these groups are determining mutation frequencies rather than mutation rates (Bielas and Loeb 2005). An alternative explanation for these findings is that mutator phenotypes are transient and subject to suppression after adaptive growth. Supporting this hypothesis are studies demonstrating that

mutator alleles are favorable under conditions of stress when there are selective pressures for cellular growth, but confer reduced fitness during normal growth (Funchain *et al.* 2000; Giraud *et al.* 2001a; Giraud *et al.* 2001b; Miller *et al.* 1999). These observations have led to a transient mutator model for cancer progression, where growth of a precancerous lesion would be limited by multiple factors *in vivo* (Loeb 1997a). Mutator phenotypes that are advantageous during periods of adaptive selection would be suppressed during periods of steady-state growth when mutators are detrimental. Thus, mutator suppression may occur during the outgrowth of tumors or following the adaptation of tumor cells to cell culture conditions.

Our studies described above demonstrate that suppressors of lethal mutation rates arise frequently in yeast, providing a tractable system to study mutator suppression. By exploiting synthetic lethality to isolate mutants with altered DNA replication fidelity, we hope to further our understanding of DNA polymerase function and identify novel pathways that affect replication fidelity. Since proteins involved in DNA metabolism are generally conserved, these pathways might also inform our understanding of DNA replication fidelity in humans.

CHAPTER II: EMERGENCE OF DNA POLYMERASE ε ANTIMUTATORS THAT ESCAPE ERROR-INDUCED EXTINCTION IN YEAST

DNA polymerases (Pols) ε and δ perform the bulk of yeast leading- and lagging-strand DNA synthesis. Both Pols possess intrinsic proofreading exonucleases that edit errors during polymerization. Rare errors that elude proofreading are extended into duplex DNA and excised by the mismatch repair (MMR) system. Strains that lack Pol proofreading or MMR exhibit a 10- to 100-fold increase in spontaneous mutation rate (mutator phenotype), and inactivation of both Pol δ proofreading (*pol3-01*) and MMR is lethal due to replication error-induced extinction (*EEX*). It is unclear whether a similar synthetic lethal relationship exists between defects in Pol ε proofreading (*pol2-4*) and MMR. Using a plasmid shuffling strategy in haploid *Saccharomyces cerevisiae*, we observed synthetic lethality of *pol2-4* with alleles that completely abrogate MMR (*msh2Δ*, *mlh1Δ*, *msh3Δ msh6Δ*, or *pms1Δ mlh3Δ*) but not with partial MMR loss (*msh3Δ*, *msh6Δ*, *pms1Δ* or *mlh3Δ*), indicating that high levels of unrepaired Pol ε errors drive extinction. However, variants that escape this error-induced extinction (*eex* mutants) frequently emerged. Five percent of *pol2-4 msh2Δ* escape mutants encoded second-site changes in Pol ε that reduced the *pol2-4* mutator phenotype between 3- and 23-fold. The remaining *eex* alleles were extragenic to *pol2-4*. The locations of antimutator amino-acid changes in Pol ε and their effects on mutation spectra suggest multiple mechanisms of mutator suppression. Our data indicate that unrepaired leading- and lagging-strand polymerase errors drive extinction within a few cell divisions and suggest there are polymerase-specific pathways of mutator suppression. The prevalence of suppressors extragenic to the Pol ε gene suggests that factors in addition to proofreading and MMR influence leading-strand DNA replication fidelity.

INTRODUCTION

Organisms must accurately duplicate their genomes to avoid loss of long-term fitness. Consequently, cells employ high-fidelity DNA polymerases (Pols) equipped with proofreading exonucleases to replicate their DNA (reviewed in (McCulloch and Kunkel 2008; Reha-Krantz 2010)). Mismatch repair (MMR) further ensures the integrity of genetic information by targeting mismatches for excision from newly replicated DNA (reviewed in (Iyer *et al.* 2006; Kolodner and Marsischky 1999; Paulovich and Hartwell 1995)). These polymerase error-correcting mechanisms, together with DNA damage repair (Friedberg *et al.* 2006), maintain the genome with less than one mutation per 10^9 nucleotides per cell division (Drake *et al.* 1998). Defects in proofreading or MMR result in mutator phenotypes characterized by increased rates of spontaneous mutation (Iyer *et al.* 2006; Kolodner and Marsischky 1999; McCulloch and Kunkel 2008; Paulovich and Hartwell 1995; Reha-Krantz 2010).

Mutator phenotypes can be an important source of genetic diversity, which facilitates adaptation to environmental change. In bacterial and yeast populations, unstable environments favor mutator strains that readily acquire adaptive mutations (Chao and Cox 1983; Desai *et al.* 2007; Giraud *et al.* 2001a; Mao *et al.* 1997; Nilsson *et al.* 2004; Notley-Mcrobb *et al.* 2002; Sniegowski *et al.* 1997; Thompson *et al.* 2006). In mammals, mutator phenotypes are proposed to accelerate the process of somatic cell evolution during tumorigenesis (Loeb *et al.* 2008; Loeb *et al.* 1974). Deep sequencing of spontaneous tumors provides evidence for a mutator phenotype (Fox *et al.* 2009; Loeb 2011), and genetic defects in MMR or Pol proofreading elevate cancer susceptibility (Peltomäki 2005; Preston *et al.* 2010; Wei *et al.* 2002). However, mutator phenotypes do not persist indefinitely. Loss of fitness accompanies sustained expression of a mutator phenotype in a variety of organisms, including viruses (Smith *et al.* 2005), bacteria (Funchain *et al.* 2000; Giraud *et al.* 2001a), yeast (Herr *et al.* 2011a; Wloch *et al.* 2001; Zeyl and De Visser 2001), worms (Estes *et al.*

2004) and mammals (Albertson *et al.* 2009). Thus, following adaptation, selection pressure favors restoration of low mutation rates, which can occur through the elimination of mutator alleles or the acquisition of mutator suppressors (*i.e.,* antimutators). A limited number of antimutator variants in the DNA replication machinery have been described (reviewed in (Herr *et al.* 2011b)).

In the budding yeast *Saccharomyces cerevisiae*, DNA polymerases epsilon (Pol ε) and delta (Pol δ) are thought to perform the bulk of leading- and lagging-strand DNA synthesis, respectively (Kunkel and Burgers 2008; Larrea *et al.* 2010; Nick Mcelhinny *et al.* 2008; Pavlov and Shcherbakova 2010; Pursell *et al.* 2007). Both polymerases are accurate and possess intrinsic proofreading exonucleases that edit mispaired primer termini during polymerization (Fortune *et al.* 2005; Morrison *et al.* 1991; Shcherbakova *et al.* 2003; Shimizu *et al.* 2002; Simon *et al.* 1991). Defects in Pol ε or Pol δ proofreading increase the spontaneous mutation rate in a manner consistent with major roles for these polymerases in leading- and lagging-strand synthesis (Greene and Jinks-Robertson 2001; Karthikeyan *et al.* 2000; Morrison *et al.* 1991; Morrison and Sugino 1994; Shcherbakova *et al.* 1996; Simon *et al.* 1991; Tran *et al.* 1999b). Interestingly, the Pol δ proofreading defect generates a mutator phenotype 5- to 30-fold greater than that observed in Pol ε proofreading-deficient strains (Datta *et al.* 2000; Greene and Jinks-Robertson 2001; Karthikeyan *et al.* 2000; Morrison and Sugino 1994; Pavlov *et al.* 2004; Shcherbakova *et al.* 1996; Tran *et al.* 1999b), and the spectra of spontaneous mutations that arise in Pol ε and Pol δ proofreading-deficient strains differ, which may reflect distinct error specificities of the polymerases as well as strand-specific effects (Fortune *et al.* 2005; Karthikeyan *et al.* 2000; Morrison and Sugino 1994; Pavlov *et al.* 2003; Pavlov *et al.* 2002; Shcherbakova *et al.* 2003). Mouse cells with defects in Pol ε or Pol δ proofreading also exhibit increased mutation rates (Albertson *et al.* 2009; Goldsby *et al.* 2002), and, consistent with distinct roles in DNA replication, the types of

tumors that develop in Pol ε and Pol δ proofreading-deficient mice differ markedly (Albertson *et al.* 2009). Thus, avoidance of errors during eukaryotic DNA replication depends on both Pol ε and Pol δ proofreading (McCulloch and Kunkel 2008; Preston *et al.* 2010).

The extent that Pol ε and Pol δ proofreading contribute to DNA replication fidelity is obscured by MMR. The eukaryotic MMR machinery consists of homologs of bacterial MutS and MutL proteins (reviewed in (Iyer *et al.* 2006; Paulovich and Hartwell 1995)). MutS homolog 2 (Msh2) associates with Msh6 or Msh3 to form two different heterodimers with partially overlapping activities. Msh2-Msh6 recognizes and binds to base-base and small insertion/deletion mispairs, while Msh2-Msh3 recognizes small and larger insertion/deletion mispairs and a subset of base-base mispairs (Harrington and Kolodner 2007). Once bound to mismatched DNA, the Msh proteins recruit heterodimers of MutL homologs (Mlh). Mlh1 is the common subunit for two complexes. Mlh1-Pms1 (Mlh1-Pms2 in mammals) functions with both Msh2-Msh6 and Msh2-Msh3, while Mlh1-Mlh3 works primarily with Msh2-Msh3. Pms1 and Mlh3 contain latent endonucleases that cleave the nascent DNA strand, providing entry points for removal of mismatches and error-free DNA re-synthesis (Chabes *et al.* 2000; Huang and Elledge 1997; Kadyrov *et al.* 2006).

Consistent with these biochemical properties, genetic studies in yeast reveal overlapping mutator phenotypes when individual MMR genes are deleted. Deletion of *MSH2* eliminates both Msh6- and Msh3-dependent repair, effectively abrogating MMR and conferring a strong base-substitution and frameshift mutator phenotype. Deletion of *MSH6* or *MSH3* alone only partially inactivates MMR. *msh6Δ* mutants are strong base-substitution but weak frameshift mutators, *msh3Δ* strains are weak frameshift and duplication/deletion mutators (with increases in some base substitutions), and *msh3Δ msh6Δ* double-mutants recapitulate the strong mutator phenotype of *msh2Δ* (Flores-Rozas and Kolodner 1998; Greene and Jinks-Robertson 1997; Harrington and Kolodner 2007; Johnson *et al.* 1996;

Marsischky *et al.* 1996; Reenan and Kolodner 1992; Reichard 1988a; Sancar *et al.* 2004; Tran *et al.* 1999b). Similar to *msh2Δ*, deletion of *MLH1* inactivates MMR, resulting in a strong base-substitution and frameshift mutator phenotype. *pms1Δ* mutants are also strong base-substitution and frameshift mutators, while *mlh3Δ* strains are weak frameshift and duplication/deletion mutators (Elledge and Davis 1987; Flores-Rozas and Kolodner 1998; Greene and Jinks-Robertson 1997; Harrington and Kolodner 2007; Prolla *et al.* 1994; Sanchez *et al.* 1999; Strand *et al.* 1993; Williamson *et al.* 1985). Yeast *pms1Δ mlh3Δ* double-mutants have strong mutator phenotypes, similar to or stronger than *pms1Δ* and *mlh1Δ* single-mutants (Flores-Rozas and Kolodner 1998). In mice, deletion of both *Mlh3* and *Pms2* (equivalent to yeast *PMS1*) is required to recapitulate the strong mutator and cancer phenotypes caused by deletion of *Mlh1* alone (Sabouri *et al.* 2008). Collectively, these studies indicate that Msh2-Msh6 and Mlh1-Pms1 (Mlh1-Pms2 in mammals) are the primary complexes that function in eukaryotic MMR, while Msh2-Msh3 and Mlh1-Mlh3 play important secondary roles.

Elimination of MMR in Pol ε or Pol δ proofreading-deficient cells results in a multiplicative increase in mutation rate in diploid yeast, suggesting that proofreading and MMR act in series to correct polymerase errors (Morrison *et al.* 1993; Morrison and Sugino 1994). In haploids, combined inactivation of Pol δ proofreading (*via* the *pol3-01* allele) and any one of several MMR components (*msh6Δ, msh2Δ,* or *pms1Δ*) is lethal, presumably due to unrestrained mutagenesis during replication (Greene and Jinks-Robertson 2001; Morrison *et al.* 1993; Tran *et al.* 1999b). We recently used a collection of *pol3* mutator alleles to define the maximal mutation rate compatible with haploid yeast viability (Herr *et al.* 2011a). Cell populations become inviable when mutation rates exceed ~10^{-3} inactivating mutations/gene/cell division. This 'error-induced extinction' (*EEX*) phenotype is readily suppressed by antimutator mutations encoding amino-acid substitutions in the catalytic

subunit of Pol δ, as well as suppressor mutations in undefined genes. Thus, variants that escape error-induced extinction (*eex* mutants) provide a means to probe mechanisms of adaptation to mutator phenotypes (Herr *et al.* 2011a; Herr *et al.* 2011b).

Whether Pol ε errors are also sufficient to trigger error-induced extinction remains unclear. Morrison and Sugino reported that the *pol2-4* allele, which inactivates Pol ε proofreading, was not synthetically lethal with *pms1*Δ in haploid yeast, but noted that the resulting colonies were heterogeneous in size and grew slowly (Morrison and Sugino 1994). Interestingly, *pol2-4 pms1Δ* isolates exhibited varying mutation rates, suggesting that mutator suppressors may arise in these strong mutator strains. Tran *et al.* also described haploid strains with Pol ε proofreading and MMR defects: *pol2-4 msh2Δ* and *pol2-4 msh3Δ msh6Δ* (Tran *et al.* 1999b). Mutation rate increases relative to *pol2-4*, *msh2Δ* and *msh3Δ msh6Δ* strains were consistent with a multiplicative relationship between MMR and Pol ε proofreading (Tran *et al.* 1999b). However, Greene and Jinks-Robinson later reported that they could not obtain a viable *pol2-4 msh2Δ* strain using either gene disruption or plasmid shuffling methods (Greene and Jinks-Robertson 2001). Thus, it remains unresolved whether the magnitude of Pol ε errors is sufficient for error-induced extinction.

Here, we show that defective Pol ε proofreading is lethal to haploid yeast in the absence of MMR, providing evidence that, when left unrepaired, leading-strand errors exceed a mutation threshold. Moreover, we show that spontaneous mutants escape this Pol ε error-induced extinction and that escape alleles function as antimutators. We discuss possible mechanisms of escape and mutator suppression. Our studies corroborate the unstable nature of mutators and provide a tractable system to investigate adaptive antimutator mutations that influence leading-strand DNA replication fidelity.

RESULTS

Synthetic lethal interactions of Pol ε proofreading and MMR defects

To investigate error-induced extinction due to Pol ε replication errors, we introduced *pol2-4*, which encodes proofreading-deficient Pol ε, into newly constructed haploid strains containing deletions of individual MMR genes (*msh2Δ, msh3Δ, msh6Δ, mlh1Δ, mlh3Δ or pms1Δ*). A plasmid shuffling strategy was used, starting with MMR mutant strains that also carry a chromosomal deletion of the Pol ε gene (*pol2Δ*) covered by a *POL2–URA3* plasmid. Following transformation with a *pol2-4–LEU2* plasmid, cells were plated on 5-fluoroorotic acid (FOA)-containing media to select for spontaneous loss of *POL2–URA3*, and the viabilities of the resultant *pol2-4 mmrΔ* double-mutants were assessed following incubation at 30°C for 2-3 days.

We observed that *pol2-4* was synthetically lethal with *msh2Δ* or *mlh1Δ*, but not with *msh3Δ*, *msh6Δ*, *pms1Δ*, or *mlh3Δ* (Figure 1). The *pol2-4 msh6Δ* and *pol2-4 pms1Δ* strains exhibited slow-growth phenotypes, as evidenced by the reduced size and number of colonies compared to *POL2 msh6Δ* and *POL2 pms1Δ* strains (Figure 1A). In contrast, when *pol3-01* (which encodes proofreading-deficient Pol δ) was introduced by plasmid shuffling into analogous MMR mutant strains (*pol3Δ mmrΔ*), synthetic lethality occurred with all MMR gene deletions except *msh3Δ* and *mlh3Δ* (Figure 1).

The pattern of *pol2-4* (in)viability with each of the single MMR gene deletions suggested that complete loss of MMR is required for synthetic lethality. To further investigate this relationship, we shuffled *pol2-4* into strains lacking both Msh2 partners (*msh3Δ* and *msh6Δ*) or both Mlh1 partners (*pms1Δ* and *mlh3Δ*). *pol2-4 msh3Δ msh6Δ* and *pol2-4 pms1Δ mlh3Δ* triple mutants were inviable (Figure 1B). Considered together, these data suggest that Msh2-Msh3, Msh2-Msh6, Mlh1-Pms1 and Mlh1-Mlh3 complexes all play important roles in

suppressing lethal Pol ε errors and that the Msh2-Msh6 and Mlh1-Pms1 complexes predominate.

The reduced growth of strains lacking Pol ε proofreading and either Msh2-Msh6 (*msh6Δ*) or Mlh1-Pms1 (*pms1Δ*) suggests that these strains accumulate deleterious mutations that compromise replicative fitness. *pol2-4 msh6Δ* cells were most compromised (Figure 1A, top left), resembling strong mutator variants previously shown to exist near the maximum tolerated mutation rate of haploid yeast (Herr *et al.* 2011a). *msh2Δ* and *mlh1Δ* are stronger mutator alleles than *msh6Δ* (Flores-Rozas and Kolodner 1998; Greene and Jinks-Robertson 1997; Li *et al.* 2005; Tran *et al.* 1999b), suggesting that *pol2-4 msh2Δ* and *pol2-4 mlh1Δ* cells are inviable because they exceed the maximum tolerated rate. Although *pol2-4 msh2Δ* cells did not form visible colonies (Figure 1B, top left), when viewed under the microscope we found abundant microcolonies of approximately 100 cells. Thus, *pol2-4 msh2Δ* cells initially divide but fail to continue after 6-7 mitotic cycles. This pattern of abortive growth typifies cells undergoing replication error-induced extinction (Herr *et al.* 2011a; Morrison *et al.* 1993).

Pols ζ and η do not mediate pol2-4 msh2Δ synthetic lethality

The mutator phenotypes of many DNA replication mutants are dependent on the specialized DNA polymerase, Pol ζ (Alcasabas *et al.* 2001; Barlow *et al.* 2008; Northam *et al.* 2006; Northam *et al.* 2010; Pavlov *et al.* 2001; Shcherbakova *et al.* 1996). This dependency may reflect a role for Pol ζ in rescuing stalled DNA replication forks (Northam *et al.* 2010) and may relate to Pol ζ's ability to efficiently extend primers with 3´-terminal mismatches (Barlow *et al.* 2008; Chabes *et al.* 2003b; Johnson *et al.* 2000; Tsaponina *et al.* 2011). To determine whether Pol ζ is required for *pol2-4 msh2Δ* lethal mutagenesis, we used our plasmid shuffling strategy to introduce *pol2-4* into *msh2Δ* cells that also lack *REV3* (which encodes the

catalytic subunit of Pol ζ). *rev3Δ* did not rescue *pol2-4 msh2Δ* synthetic lethality (Figure 2). Similarly, deletion of *RAD30*, which encodes the translesion DNA polymerase η (Domkin *et al.* 2002), also failed to rescue *pol2-4 msh2Δ* synthetic lethality (Figure 2). These data show that Pols ζ and η do not mediate *pol2-4 msh2Δ* synthetic lethality.

Mutants escape pol2-4 msh2Δ synthetic lethality

We occasionally observed macroscopic colonies that survived when *pol2-4* was shuffled into the *msh2Δ, mlh1Δ*, *msh3Δ msh6Δ*, or *pms1Δ mlh3Δ* strains. In light of our recent discovery of Pol δ antimutators (Herr *et al.* 2011a), we hypothesized that these surviving colonies may have acquired suppressor mutations that improve Pol ε fidelity. Thus, we systematically screened for *error-induced extinction* (*eex*) mutants that survived *pol2-4 msh2Δ* synthetic lethality. Using the plasmid shuffling strategy, multiple independent *pol2-4 msh2Δ* transformants were separately plated on FOA-containing medium so that rare survivors could be detected and counted (Figure 3A and B). There was wide fluctuation in the number and size of surviving colonies, suggesting that escape variants arise randomly prior to selection on FOA.

After eliminating clones with *pol2-4* → *POL2* gene conversions or other mutations conferring FOA resistance (*e.g.*, *ura3*), 81 independent *eex* mutants were isolated (Table 2.1). To distinguish between *eex* mutations in the plasmid-borne *pol2-4* gene ('intragenic *eex*') and *eex* mutations located elsewhere in the yeast genome ('chromosomal *eex*'), *pol2-4* plasmids were rescued from the *eex* mutants and used to transform a fresh *msh2Δ* strain. Among the 81 *eex* mutants characterized, 76 (94%) carried plasmids that were lethal when re-shuffled into *msh2Δ* cells. Thus, the majority of *eex* mutants contained suppressor mutations extragenic to *pol2-4*. Five mutants carried *pol2-4* plasmids that did not induce *pol2-4 msh2Δ* synthetic lethality. DNA sequencing revealed that, in addition to the

pol2-4 allele, each of these plasmids encoded a single amino-acid substitution in Pol ε: G435C, V522A, T850M, K966Q, or A1153D. The amino-acid changes were located in regions that are moderately or highly conserved in DNA polymerases ε and δ (Figure 4). When the corresponding mutations were re-engineered into fresh *pol2-4* plasmid backbones and shuffled into *msh2Δ* cells, they conferred an *eex* phenotype (Figure 5A). *pol2-4,eex msh2Δ* strains were viable, forming small clearly visible colonies (Figure 5A, right). Moreover, the *eex* alleles completely rescued the slow-growth phenotype of *pol2-4 msh6Δ* cells (Figure 5A, center). These data show that secondary amino-acid substitutions within proofreading-deficient Pol ε can rescue *pol2-4 msh2Δ* synthetic lethality and restore normal growth to *pol2-4 msh6Δ* cells.

Strain-dependent differences in pol2-4 msh2Δ suppression

In our screen for *eex* mutants, we used two related yeast strains derived from S288C: BY4733 (Brachmann *et al.* 1998) and Y7092 (Tong and Boone 2007). *eex* alleles intragenic and extragenic to *pol2-4* were recovered from both strains (Table 2.1). However, BY4733 displayed a reproducibly lower frequency of *pol2-4 msh2Δ* suppression than Y7092 (compare Figures 3A and B). Independent *pol2-4 msh2Δ* clones from either genetic background yielded variable numbers of escape mutants (compare different grid positions on the same plate), further indicating that suppressors originate during clonal expansion prior to plating on FOA. Accordingly, intragenic escape mutants isolated from a common parent clone (*i.e.*, from the same grid position) harbored identical *eex* mutations. Based on these observations, we used fluctuation analyses to calculate the rates of escape from error-induced extinction in each strain. Transformation of *POL2–URA3 msh2Δ* cells with wild-type *POL2–LEU2* plasmid served as a control to assess shuffling efficiencies and estimate the number of cell divisions during colony outgrowth (see Materials and Methods). Escape mutants arose at a rate of

2 x 10^{-4} per cell division in the BY4733 strain and at a 20-fold higher rate in the Y7092 strain (4 x 10^{-3} escape mutants per cell division). These results show that genetic background influences the propensity of strains to escape the synthetic lethal interaction of *pol2-4* and *msh2Δ*.

To compare rates of escape from Pol ε and Pol δ proofreading-deficiency, we quantified *eex* mutants in *pol3-01 msh2Δ* Y7092 cells using an analogous plasmid shuffling strategy (Herr *et al.* 2011a) (Figure 3C). Suppressors arose at a rate 450-times lower in the *pol3-01 msh2Δ* strain (9 x 10^{-6} escape mutants per cell division) compared to *pol2-4 msh2Δ* (4 x 10^{-3}) in the same genetic background. Thus, escape from error-induced extinction occurs more readily in Pol ε than Pol δ proofreading-deficient *msh2Δ* cells.

Intragenic eex mutants suppress mutation rates

If *pol2-4 msh2Δ* synthetic lethality is due to error-induced extinction, then Pol ε *eex* substitutions may promote escape by increasing the fidelity of Pol ε. To determine whether the *eex* substitutions suppressed the *pol2-4* mutator phenotype, we compared mutation rates conferred by *pol2-4* and *pol2-4,eex* alleles in an *msh6Δ* strain derived from BY4733. All of the *eex* mutations suppressed the *pol2-4 msh6Δ* mutator phenotype between 3- and 23-fold (Figure 5B, gray box). Thus, the *eex* mutations likely promote escape from *pol2-4 msh2Δ* synthetic lethality by lowering mutation rates below an error threshold. We also determined whether the *eex* alleles influence mutation rates in the presence of Pol ε proofreading by introducing each *eex* mutation into the otherwise wild-type *POL2* gene. The resultant *pol2-eex* alleles had modest effects on background *msh6Δ* mutation rates (Figure 5B, right). *pol2-G435C msh6Δ* and *pol2-A1153D msh6Δ* were indistinguishable from *POL2 msh6Δ*. *pol2-K966Q* and *pol2-T850M* increased the *msh6Δ* mutation rate 2- to 3-fold, while *pol2-V522A* lowered the rate three-fold.

Distinct mutation spectra of eex mutants

To gain insight into how the *eex* substitutions suppress mutation rates, we determined the types of mutations that spontaneously arise in *pol2-4 msh6Δ* and *pol2-4,eex msh6Δ* strains (Figure 6 and Table 2.2). Multiple independent canavanine-resistant (Can^r) colonies were isolated (~50 per strain), and the *CAN1* genes were sequenced to determine the spectrum of spontaneous mutations in each strain. Mutations were distributed throughout the *CAN1* sequence (Figure 6), with recurrent mutations observed at several nucleotide positions (*i.e.*, 'hotspots'). In all strains, the majority of mutations were base substitutions (Table 2.2), consistent with the expected synergy of a proofreading-deficient polymerase with *msh6Δ* (Tran *et al.* 1999b). The *CAN1* locus (nucleotides 33466 to 31694 on Chromosome V) is flanked by two confirmed DNA replication origins: ARS507, located ~26 kb centromeric to *CAN1*, and ARS504, located ~24 kb telomeric (Raghuraman *et al.* 2001; Siow *et al.* 2012; Yabuki *et al.* 2002). Thus, *CAN1* could be replicated by forks emerging from either origin, and the mutation spectra probably reflect a mixture of Pol ε errors made on both strands.

We analyzed the mutation spectra using iMARS (Morgan and Lewis 2006) to compare each *pol2-4,eex msh6Δ* spectrum to that produced by *pol2-4 msh6Δ* in a pair-wise fashion. This statistical analysis considers both the type of mutation and its position in the *CAN1* sequence (Figure 6). All but one *eex* mutant, *pol2-4,A1153D msh6Δ* ($p = 0.10$), displayed significantly different mutation spectra from the *pol2-4 msh6Δ* strain ($p \leq 0.05$; Monte Carlo hypergeometric test). When only base substitutions are considered with no regard to sequence position (Table 2.2), the distributions of mutation types in *pol2-4,T850M msh6Δ* and *pol2-4,K966Q msh6Δ* were significantly different from the distribution in *pol2-4 msh6Δ*. Specifically, *K966Q* increased the percentage of T→C mutations, and *T850M* increased the C→A percentage while decreasing the proportion of G→T base substitutions. *T850M* also

increased the percentage of -1 frameshifts, and *G435C* and *K966Q* decreased the proportion of +1 frameshifts.

To quantify the effects of *eex* alleles on individual mutation types, we converted mutation frequencies (Table 2.2) to mutation rates (Table 2.3). Only the most frequent mutation types were included in this analysis. When type-specific rates in *pol2-4 msh6Δ* and *pol2-4,eex msh6Δ* strains were compared (parenthetic values in Table 2.3), several patterns of mutator suppression were evident. The two strongest *eex* alleles (*T850M* and *A1153D*) suppressed all mutation types to a similar degree (95-99% suppression relative to *pol2-4 msh6Δ*). *K966Q* also exhibited a nearly uniform pattern of suppression (70-90%) with some preference for +1 frameshifts (94%). In contrast, *G435C* only weakly suppressed base substitutions (50-60%) while strongly suppressing +1 frameshifts (>95%), and *V522A* preferentially suppressed both G→A base substitutions and +1 frameshifts (94-96%) with a somewhat weaker effect on C→T and G→T mutations (80%). Collectively, the data in Tables 2 and 3 indicate there are multiple mechanisms of mutator suppression.

DISCUSSION

Adaptation necessitates genetic diversity. Large cell populations with low DNA replication error rates may contain sufficient variation to surmount a single selective barrier. However, rapid environmental changes impose additional selection pressures that may exceed the ability of wild-type cells to adapt. Natural populations of bacteria and yeast often harbor low levels of mutator cells that emerge under such conditions (Elena and Lenski 2003; Giraud *et al.* 2001b). However, sustained expression of mutator phenotypes compromises long-term fitness through the accumulation of deleterious mutations. Thus, following adaptation to external pressures, selection would favor cells that have either evolved mutator

suppressors or eliminated the mutator allele. In this manner, mutator phenotypes rise and fall as cells shift between periods of relative stability and environmental change (Giraud *et al.* 2001b; Taddei *et al.* 1997).

Here we investigated pathways of mutator suppression that restore fidelity to an error-prone variant of Pol ε, the primary leading-strand DNA polymerase in yeast (Nick Mcelhinny *et al.* 2008; Pursell *et al.* 2007). We show that cells defective for both Pol ε proofreading and MMR are inviable (Figure 1). However, spontaneous mutants readily escape this synthetic lethality (Figure 3). Five percent of these escape mutants encode secondary amino-acid substitutions in Pol ε (Figure 4) that suppress the Pol ε proofreading-deficient phenotype (Figure 5). This study complements our recent investigation of Pol δ (Herr *et al.* 2011a), where we defined the maximal mutation rate sustainable by haploid yeast cells and described variants that suppress the mutator phenotype of cells deficient for Pol δ proofreading. Our findings highlight the unstable nature of mutator phenotypes and suggest multiple mechanisms for their suppression.

Pol ε errors and lethal mutagenesis

It is well established that combined defects in Pol δ proofreading and MMR are synthetically lethal in haploid yeast (Greene and Jinks-Robertson 2001; Morrison *et al.* 1993; Tran *et al.* 1999b). Loss of Msh6 or Pms1 (*msh6Δ* or *pms1Δ*) is sufficient to extinguish Pol δ proofreading-deficient (*pol3-01*) cells (Figure 1), the apparent consequence of mutation accumulation during DNA replication (Herr *et al.* 2011a; Morrison *et al.* 1993). Consistent with a mechanism of error-induced lethality, yeast cells with Pol δ proofreading and MMR defects form microcolonies of approximately 100 cells arrested in various stages of the cell cycle (Morrison *et al.* 1993) and with diverse cell morphologies resembling inactivation of different essential genes (Yu *et al.* 2006). The maximum tolerated mutation rate in haploid

yeast (~10^{-3} inactivating mutations/gene/cell division ≈ 3 x 10^{-6} mutations/bp/cell division) is consistent with random inactivation of essential genes as the cause of extinction (Herr *et al.* 2011a).

In contrast to Pol δ, the combined loss of Pol ε proofreading (*pol2-4*) and Msh6 (*msh6Δ*) is not synthetically lethal, although it does compromise growth (Figure 1). The different fates of *msh6Δ* cells with defects in Pol δ proofreading (inviable) or Pol ε proofreading (slow-growing, strong mutators) are likely due to quantitative differences in cellular mutation burden. While *pol3-01 msh6Δ* cells exceed the maximum tolerated mutation rate (Herr *et al.* 2011a), *pol2-4 msh6Δ* cells mutate at a rate 10-times lower than the maximum (10^{-4} Can^r mutants/cell division ≈ 10^{-4} inactivating mutations/gene/cell division; Figure 5B). We observe that *pol2-4* cells become inviable when both Msh6- and Msh3-dependent MMR are disrupted (Figure 1B). Thus, the additional burden of unrepaired Msh2-Msh3 substrates is sufficient to push *pol2-4 msh6Δ* cells over the lethal threshold. Similarly, *pol2-4 pms1Δ* cells become inviable when *MLH3* is deleted. Our finding that unrepaired Pol ε errors are lethal provides additional evidence that Pol ε plays a substantial role in genome replication (Pursell and Kunkel 2008). Our data also indicate that loss of genetic information on either DNA strand (Pol ε errors on leading- and Pol δ errors on lagging-strands; (Nick Mcelhinny *et al.* 2008; Pursell *et al.* 2007)) is sufficient to drive extinction of a population of cells.

MMR pathways suppressing lethal Pol ε errors

The MMR pathways that suppress deleterious Pol ε errors are sharply delineated in proofreading-MMR double mutants (Figure 1). Pol ε's bias for generating more base substitutions than frameshifts (Shcherbakova *et al.* 2003) is consistent with our observation that *pol2-4* cells defective for base-base mismatch repair (*msh6Δ* or *pms1Δ*) exhibit slow-growth phenotypes, while *pol2-4* cells defective primarily for frameshift repair (*msh3Δ* or

mlh3Δ) grow normally (Figure 1). Morrison and Sugino also observed compromised growth of *pol2-4 pms1Δ* cells (Morrison and Sugino 1994). Surprisingly, we found that deletion of *MSH6* impacted cell growth more severely than deletion of *PMS1* (Figure 1A), even though Msh2-Msh6 mediates repair through its interaction with Mlh1-Pms1 (Iyer *et al.* 2006; Paulovich and Hartwell 1995; Yamaguchi *et al.* 2001b). This indicates that some Msh6-dependent repair can occur in the absence of Mlh1-Pms1, perhaps by using Mlh1-Mlh3 in place of Mlh1-Pms1 (Guittet *et al.* 2001). Our observation that *pol2-4 pms1Δ* cells become inviable when *MLH3* is deleted (Figure 1) further implicates Mlh1-Mlh3 in the repair of deleterious Pol ε errors. Thus, both Pms1 and Mlh3 play important protective roles. Synthetic lethality with *pol2-4* occurs only when both Mlh1-Pms1 and Mlh1-Mlh3 are eliminated by deleting either *MLH1* alone or *PMS1* and *MLH3* together (Figure 1). Mouse *Mlh1*, *Mlh3* and *Pms2* (equivalent to yeast *PMS1*) have a similar relationship in preventing spontaneous mutations and cancer (Sabouri *et al.* 2008). Considered together, our data show that multiple MMR components protect cells from deleterious Pol ε errors, which include base substitutions, frameshifts and possibly other mutation types (Harrington and Kolodner 2007).

Contribution of Pol ε errors to cellular mutation burden

What accounts for the differences in synthetic phenotypes of *pol2-4* and *pol3-01* with MMR defects? Biochemical studies indicate that exonuclease-deficient Pols ε and δ have similar overall fidelities *in vitro* (Fortune *et al.* 2005; Shcherbakova *et al.* 2003; Shimizu *et al.* 2002). They generate distinct mutational spectra, but both primarily produce base-base mispairs and frameshift errors, the preferred substrates for MMR (Iyer *et al.* 2006; Kolodner and Marsischky 1999; Paulovich and Hartwell 1995). Nevertheless, in MMR-proficient cells, the *pol3-01* mutation rate is 5- to 30-times higher than that of *pol2-4* (Datta *et al.* 2000;

Greene and Jinks-Robertson 2001; Karthikeyan *et al.* 2000; Morrison and Sugino 1994; Pavlov *et al.* 2004; Shcherbakova *et al.* 1996; Tran *et al.* 1999b). MMR preferentially repairs lagging-strand errors (Hombauer *et al.* 2011; Pavlov *et al.* 2003). Consistent with this bias, we observe that deletion of *MSH6* increases the mutation rate *of pol3-01* variants ~160 fold (Herr *et al.* 2011a) and the *pol2-4* mutation rate ~50 fold (Figure 5B). Shcherbakova *et al.* see a similar impact of *msh6Δ* on *pol2-4* mutation rates (40- to 50-fold; (Shcherbakova *et al.* 2003)). However, this preference of MMR for Pol δ errors contradicts the observation that loss of Pol δ proofreading results in higher mutation rates than loss of Pol ε proofreading.

There are several possible explanations for this apparent discrepancy. As previously suggested by others (Morrison and Sugino 1994; Pavlov and Shcherbakova 2010), Pol ε may replicate less of the genome than Pol δ. Replacement of Pol ε with Pol δ near the end of a replicon may be necessary to enable ligation of the leading strand to the downstream Okazaki fragment from an adjacent replicon (Garg *et al.* 2004). If replacement occurs randomly or in response to Pol ε errors or pausing at DNA lesions (Pavlov and Shcherbakova 2010), then Pol δ would synthesize variable amounts of each leading-strand fragment and overall more of the genome than Pol ε. Gap-filling synthesis is also catalyzed predominantly by Pol δ during DNA repair, recombination, and telomere replication (Pavlov *et al.* 2006b).

Another possibility is that Pol ε creates fewer mutations *in vivo* than predicted by *in vitro* measurements of fidelity. The overall error rate of Pol ε *in vivo* should approximately correspond to the mutation rate of cells that lack both Pol ε proofreading and MMR. *pol2-4 msh6Δ* cells generate 10^{-4} Can^r mutants/cell division or ~3 x 10^{-7} mutations/bp/cell division (calculated as described in (Herr *et al.* 2011a)). However, this likely underestimates the Pol ε error rate. Other enzymes may excise Pol ε errors (*e.g.*, Pol δ may proofread for Pol ε; (Pavlov and Shcherbakova 2010)), and Msh2-Msh3-mediated MMR, which is still active in these cells, also repairs some Pol ε errors. Tran *et al.* show that loss of Msh2-Msh3 (*msh3Δ*)

further increases the mutation rate of *pol2-4 msh6Δ* cells about 3-fold (Tran *et al.* 1999b), while we find that *msh3Δ* is lethal in *pol2-4 msh6Δ* cells and therefore must increase mutations ≥10-fold. A 10-fold increase corresponds to ~3 x 10^{-6} mutations/bp, which is substantially lower than the error rate of proofreading-deficient Pol ε *in vitro* (~3 x 10^{-4} errors/bp; (Shcherbakova *et al.* 2003)). Furthermore, the spectra of mutations observed *in vivo* and *in vitro* are quite different (Figure 6, Table 2.2 and (Shcherbakova *et al.* 2003)). These differences are not likely due to differential extension of mispairs *in vitro*, because Pol ε is present in large excess to maximize mispair extension in the M13 fidelity assay (Bebenek and Kunkel 1995; Shcherbakova *et al.* 2003). Thus, *in vitro* fidelity measurements do not recapitulate the mutational events caused by Pol ε *in vivo*. As previously suggested (Shcherbakova *et al.* 2003), Pols ε and δ may replicate similar amounts of the yeast genome, but may do so with different accuracies, perhaps by utilizing strand- or polymerase-specific accessory factors or repair pathways that decrease mutations from Pol ε, or by triggering the mutagenic Dun1 pathway which increases mutations from Pol δ (Datta *et al.* 2000; Reha-Krantz *et al.* 2011). Interestingly, the error-prone DNA polymerases ζ and η do not significantly impact mutagenesis by proofreading-deficient Pol ε or Pol δ (Figure 2; (Datta *et al.* 2000; Shcherbakova *et al.* 1996)). Additional studies are required to examine in greater detail the roles of Pol ε and Pol δ *in vivo* and the pathways that mediate mutagenesis when these polymerases err.

Escape from Pol ε error-induced extinction

In our plasmid shuffling experiments, colonies frequently emerged that escape *pol2-4 msh2Δ* lethality (Figure 3). This escape from Pol ε error-induced extinction is similar to that recently described for Pol δ (Herr *et al.* 2011a). Morrison and Sugino also observed mutator suppression in a *pol2-4 pms1* clone, but this clone was not further characterized (Morrison

and Sugino 1994). In our studies, escape results from genetic suppressors that are either second-site mutations within the proofreading-deficient Pol ε gene ('intragenic suppressors') or alleles affecting unknown genes elsewhere in the genome and extragenic to *pol2-4* ('chromosomal suppressors'; Table 2.1). Five intragenic suppressors were identified (Figure 4). Each of these individually confer escape from *pol2-4 msh2Δ* lethality (Figure 5A) and suppress the mutator phenotype of Pol ε proofreading deficiency 3- to 23-fold (Figure 5B). These data strongly suggest that *pol2-4 msh2Δ* inviability results from lethal mutagenesis, and that intragenic suppressors lower the spontaneous mutation rate below the maximum tolerated threshold. The existence of a relatively narrow lethal threshold was previously shown using a collection of *pol3* mutator and antimutator alleles (Herr *et al.* 2011a). Our new data with *pol2* alleles validate this threshold and are consistent with a maximal mutation rate in haploid yeast of ~10^{-3} inactivating mutations/gene/cell division (Herr *et al.* 2011a).

Both *pol3-01 msh6Δ* and *pol2-4 msh2Δ* strains exceed the lethal error threshold, and antimutator variants that lower mutation rates below the threshold were readily obtained in both strains (data herein and (Herr *et al.* 2011a)). Yet chromosomal suppressors of *pol2-4 msh2Δ* lethality represented a greater proportion of *eex* mutants (94%; Table 2.1) than those that suppressed *pol3-01 msh6Δ* lethality (65%; (Herr *et al.* 2011a)). We also observed that *eex* mutants arise more readily in Pol ε than Pol δ proofreading-deficient *msh2Δ* cells (Figure 3B and C). This may reflect differences in how close the mutation rates of the strains are to the lethal threshold. Both weak and strong antimutators would rescue *pol2-4 msh2Δ* and *pol3-01 msh6Δ* cells, which reside relatively close to the threshold (see above and (Herr *et al.* 2011a)). In contrast, the combination of *pol3-01* and *msh2Δ* imparts a much higher mutation rate, which would be overcome by only the strongest antimutators. It is also possible that a wider array of genes influences Pol ε replication fidelity than Pol δ fidelity, and

thus the probability of isolating chromosomal suppressor alleles is greater for Pol ε. *pol3-01 msh6Δ* cells still have Msh2-Msh3 MMR activity that protects against frameshift mutations (Marsischky *et al.* 1996; Palombo *et al.* 1996), while Pol ε error-induced extinction depends on abrogation of the Msh2-Msh3 pathway (Figure 1). Thus, the higher proportion of chromosomal suppressors in *pol2-4 msh2Δ* cells may also be due to mutations in genes encoding replication components that affect frameshift mutagenesis.

An unexpected finding from our study is that different strains escape from error-induced extinction at different rates (Figure 3). The facile emergence of *pol2-4 msh2Δ eex* mutants in Y7092 compared to BY4733 cells suggests that the former strain acquired a weak antimutator prior to our screening experiments. A pre-existing weak antimutator allele may be insufficient to trigger escape but could cooperate with a second nascent antimutator to shift mutation rates below the lethal threshold and into the viable range. Alternatively, a pre-existing weak mutator allele in Y7092 cells may generate suppressors at a higher rate. However, the infrequency of FOA resistance due to *ura3* and other mutations is inconsistent with a higher overall mutation rate in Y7092 (Table 2.1). The Y7092 strain has undergone a number of genetic manipulations (Tong and Boone 2007), thus providing opportunity for variants to arise. These data suggest that strain differences or the presence of unknown suppressor alleles may explain inconsistencies in the literature regarding Pol ε proofreading and MMR synthetic lethal interactions (Greene and Jinks-Robertson 2001; Morrison and Sugino 1994; Tran *et al.* 1999b).

Possible mechanisms of mutator suppression by Pol ε variants

Our screen for suppressors uncovered five novel Pol ε antimutator variants: G435C, V522A, T850M, K966Q and A1153D (Figure 4). The Pol ε structure is unknown, but the positions of antimutator residues in Pol ε can be deduced from structures of related B-family

DNA polymerases (Swan *et al.* 2009; Wang *et al.* 1997). Mapping the Pol ε *eex* substitutions onto a ribbon diagram of the *S. cerevisiae* Pol δ structure indicates that the Pol ε substitutions are scattered throughout the domains of the protein (Figure 7A), similar to the wide distribution of *eex* substitutions found in Pol δ (Figure 7B; (Herr *et al.* 2011a)). No *eex* mapped to the C-terminal half of Pol ε, which performs an essential, non-catalytic role in yeast cells (Dua *et al.* 1999; Feng and D'urso 2001; Kesti *et al.* 1999) and is not present in Pol δ or other B-family DNA polymerases.

The locations of the *eex*-encoded amino-acid substitutions (Figure 7) and the mutation spectra resulting from each (Figure 6 and Table 2.2) suggest several possible antimutator mechanisms for the Pol ε variants. Two amino-acid substitutions, T850M and K966Q, are within the predicted palm domain of Pol ε (Figure 7A). T850 corresponds to Pol δ V727 in conserved Motif B (Figure 4), proximal to the polymerase active site in the Pol δ structure (Figure 7A and C). Substitution of T850 to methionine in proofreading-deficient Pol ε changes the spectrum of spontaneous *CAN1* mutations (Figure 6 and Table 2.2), suggesting that T850M alters nucleotide selectivity. Pol δ V727 contacts tyrosines Y613 and Y708 (corresponding to Pol ε Y645 and Y831, respectively). These tyrosines are highly conserved in B-family DNA polymerases (Figure 4) and are key components of the minor-groove binding pocket where incoming dNTPs base pair with the template (Figure 7C; (Swan *et al.* 2009)). The minor groove structures of all correct base pairs are remarkably similar (Saenger 1984) and are monitored during polymerization for proper Watson-Crick base-pair geometry (Kool 2002). Pavlov *et al.* showed that site-directed mutation of Pol ε Y831 to alanine also suppresses the *pol2*-4 mutator phenotype (Pavlov *et al.* 2004). Thus, T850M likely increases Pol ε fidelity through its interaction with Y831, thereby tightening the geometry of the binding pocket to exclude certain mispairs. The most dramatic change in the *pol2-4,T850M msh6Δ* mutation spectrum was a 100-fold reduction in the rate of G→T mutations (Table 2.3), which

would be caused by G•dATP mispairs if Pol ε synthesizes leading-strand DNA from forks originating at ARS504 or C•dTTP mispairs from forks originating at ARS507 (Kumar *et al.* 2011; Raghuraman *et al.* 2001; Yabuki *et al.* 2002). Substantial reductions in the mutation rates of G→A (G•dTTP or C•dATP), C→T (C•dATP or G•dTTP) and +1 frameshift mutations were also observed (Table 2.3). Thus, the T850M variant limits formation of a range of mutation types.

The K966Q *eex* substitution, also located in the palm domain, maps to the first lysine in the absolutely conserved KKRYA sequence found in all B-family DNA polymerases (K813 in Pol δ) (Figure 4). In the Pol δ crystal structure, the basic residues in this sequence form a loop between two β-strands and interact with the minor groove of duplex DNA (Figure 7A and D). Specifically, K813 contacts the phosphate of the template strand 4 bp from the polymerase active site. The spontaneous mutation spectrum of *pol2-4,K966Q msh6Δ* cells displayed a significant decrease in +1 frameshift mutations (Tables 2 and 3), suggesting that K966Q lowers the propensity for strand slippage events. K966Q may decrease Pol ε pausing through homonucleotide runs, thereby reducing the opportunity for slippage (Johnson *et al.* 2003; Viguera E. 2001). Alternatively, the *pol2-4,K966Q* polymerase may more readily dissociate from looped DNAs that result from frameshifting errors, allowing editing by an alternative exonuclease (*i.e.*, extrinsic proofreading (Albertson and Preston 2006; Nick Mcelhinny 2006; Pavlov *et al.* 2006a).

Interestingly, the T850M and K966Q antimutator variants confer a mild mutator phenotype (2- to 3-fold) in *msh6Δ* cells when the catalytic residues of Pol ε's exonuclease are restored to wild type (Figure 5B). Several scenarios could explain this paradox. Polymerase variants with enhanced fidelity often have reduced overall activity (Loh *et al.* 2007). While decreases in catalytic activity or processivity might improve accuracy (Elledge and Davis 1990; Herr *et al.* 2011b; Huang *et al.* 1998b; Johnson 2010; Joyce and Benkovic 2004), they

can also increase polymerase error rates for specific mutation types (Huang *et al.* 1998b) and may trigger mutagenic replication processes in the cell (Barlow *et al.* 2008; Northam *et al.* 2006; Northam *et al.* 2010). Alternatively, T850M and K966Q could suppress proofreading if partitioning to the exonuclease active site is affected (Kumar *et al.* 2010b; Reha-Krantz 2010). Finally, these amino acid substitutions may change the binding pocket to enhance discrimination against some errors but weaken discrimination against others, resulting in weak mutators (Drake 1993).

The remaining Pol ε antimutator substitutions affect other domains in the polymerase structure (Figures 4 and 7). V522A maps to the amino domain in an α-helix previously implicated in *pol3-01* mutator suppression (Figure 7A, B and E; (Herr *et al.* 2011a)). The same types of spontaneous mutations arise in *pol2-4 msh6Δ* cells with or without the *V522A* allele (Table 2.2). Thus, V522A suppresses the most prevalent mutations generated by proofreading-deficient Pol ε to a similar degree. This pattern of suppression is consistent with a mutant polymerase that exhibits either increased overall nucleotide selectivity or an increased facility to undergo extrinsic proofreading. The G435C antimutator maps to the exonuclease domain of Pol ε between the conserved Exo II and Exo III motifs (Figure 4). It is unlikely that G435C restores proofreading activity, since the *pol2-4*-encoded exonuclease lacks two essential catalytic residues (D290A and E292A) (Morrison *et al.* 1991; Shcherbakova *et al.* 2003). G435 aligns with R475 in Pol δ (Figure 4), which is in a loop that extends into and interacts with the thumb domain (Figure 7A and F). We previously identified R475 substitutions in Pol δ that suppress *pol3-01 msh6Δ* synthetic lethality (Herr *et al.* 2011a). The recurrence of *eex* mutants with substitutions at this position is striking and suggests that Pols δ and ε share structural features that govern fidelity. In the Pol δ structure, R475 buttresses residue R840 (equivalent to Pol ε R989), which contacts the backbone of the primer strand 3 bp from the polymerase active site (Figure 7A and F).

Consistent with a role in DNA binding, G435C significantly reduces the rate of frameshift mutations by Pol ε (Tables 2 and 3), suggesting that G435C may lower the propensity for strand slippage events or facilitate the repair of DNA loops created by Pol ε. Lastly, the Pol ε A1153D antimutator likely resides in the thumb domain of the polymerase (Figure 4), although the structure of this region in Pol δ is unknown (Swan *et al.* 2009). *A1153D* suppresses the mutation rate of *pol2-4 msh6Δ* cells 17-fold (Figure 5B), but the types of mutations in *pol2-4,A1153D msh6Δ* and *pol2-4 msh6Δ* cells are not significantly different (Table 2.2). Thus, similar to T850M and V522A (see above), A1153D may uniformly increase dNTP selectivity by Pol ε or may promote uniform extrinsic proofreading of Pol ε errors.

Perspectives and Conclusions

Previous studies identified antimutator variants of bacteriophage T4 and *E. coli* DNA polymerases (reviewed in (Herr *et al.* 2011b; Reha-Krantz 1995; Schaaper 1998)). Similar to the yeast variants we describe (data herein and (Herr *et al.* 2011a)), *E. coli* antimutators were isolated in the absence of native proofreading and are due to individual amino-acid substitutions throughout the polymerase structures (Herr *et al.* 2011b; Loh *et al.* 2007; Schaaper 1998). Accordingly, Schaaper and colleagues proposed two general mechanisms for polymerase antimutators: 1) increased dNTP discrimination, and 2) increased dissociation from DNA to allow editing by alternate pathways (Fijalkowska and Schaaper 1995). Our data are consistent with these mechanisms. Biochemical analyses will be required to assess the fidelities and processivities of our Pol ε variants and the potential contribution of these parameters to antimutagenesis.

The idea of dissociation and alternative editing raises the question: what other enzymes might remove Pol ε errors in the antimutator strains? One candidate is proofreading by Pol δ.

Yeast defective for both Pol δ and Pol ε proofreading exhibit a synergistic increase in mutation rate, suggesting one or both polymerases may proofread for the other (Morrison and Sugino 1994). Pavlov and Shcherbakova present evidence that mistakes made by Pol ε are corrected by the proofreading activity of Pol δ, but not *vice versa* (Pavlov and Shcherbakova 2010). Other candidates for extrinsic proofreading include the 3′→5′ exonuclease activities of Mre11 (Trujillo and Sung 2001) and Apn2 (Unk *et al.* 2001) or endonucleases such as Rad1/Rad10 or Mus81/Mms4 that cleave 3′ flap structures during replication fork restart (Bardwell *et al.* 1994; Bastin-Shanower *et al.* 2003; Boddy *et al.* 2001; Chen *et al.* 2001; Kaliraman *et al.* 2001).

The majority of *eex* mutants isolated in our screen were extragenic to *pol2-4* (Table 2.1). What genes mediate antimutagenesis in these *eex* mutants, what are the functions of the proteins affected by these *eex* alleles, and what are their roles in eukaryotic DNA replication? Antimutators could result from up-regulation of DNA repair or recombination proteins that, when over-expressed, are able to remove nascent 3′ mispairs or mismatches in duplex DNA. MMR proteins, other 3′ nucleases (see above), and recombination proteins and resolvases are potential candidates for this mechanism. Antimutators could also result from changes in proteins that function at the DNA replication fork. Proteins directly affecting stalled replication forks are candidates as are checkpoint sensors and indirect effectors of these processes. The error-prone Pols ζ and η are unlikely *eex* candidates, because neither polymerase is required for *pol2-4 msh2Δ* synthetic lethality (Figure 2). Previous studies show that the mutator phenotype caused by defective Pol δ proofreading (*pol3-01)* is partially dependent on Dun1 (Datta *et al.* 2000), a checkpoint kinase that up-regulates dNTP synthesis (Kumar *et al.* 2010a; Zhao and Rothstein 2002; Zhou and Elledge 1993). However, the *pol2-4* mutator phenotype does not appear dependent on Dun1 (Datta *et al.* 2000). Thus, mutations in *DUN1* are unlikely *eex* candidates. There are a number of other possible

antimutagenesis mechanisms involving multiple pathways and candidate genes (Herr *et al.* 2011b). Whole-genome sequencing should greatly facilitate identification of the chromosomal *eex* alleles (Navadgi-Patil and Burgers 2009; Poli *et al.* 2012; Puddu *et al.* 2011). These *eex* may reveal novel pathways of mutation suppression and help clarify the division of labor between Pols ε and δ at the replication fork.

Our studies illustrate the inherent instability of eukaryotic mutators. Antimutators readily emerge from yeast harboring defects in either Pol ε or Pol δ proofreading (Figure 3; (Herr *et al.* 2011a)). Suppressors of diverse mutator phenotypes (proofreading, MMR and DNA damage repair) also frequently arise in *E. coli* (Fijalkowska *et al.* 1993; Fijalkowska and Schaaper 1995; Giraud *et al.* 2001b; Notley-Mcrobb *et al.* 2002; Schaaper 1996; Schaaper and Cornacchio 1992; Tröbner and Piechocki 1984). Thus, it appears that mutator phenotypes in general are prone to suppression. We speculate that antimutators moderate high mutation rates and minimize deleterious mutations during microbial adaptation and mammalian oncogenesis.

MATERIALS AND METHODS

Media and growth conditions

Standard media and growth conditions were used in the propagation of yeast strains (Sherman 2002). Cells were grown non-selectively using YPD or synthetic complete (SC) media with 2% dextrose. Selective growth was on SC media containing 2% dextrose and lacking the appropriate amino acid(s). Pre-formulated SC amino acid supplement was purchased from Bufferad, and supplements lacking defined amino acids were made from individual components as described (Sherman 2002). *URA3*-deficient cells were selected with 5-fluoroorotic acid (FOA, 1 mg/ml, Zymo Research) media (Boeke *et al.* 1984). *can1* mutants were selected on SC lacking arginine and supplemented with 60 μg/ml of

canavanine. Unless otherwise specified, reagents were purchased from Sigma-Aldrich or Fisher Scientific.

Plasmids and strain constructions

POL2 Plasmids. pRS416, a *CEN6/ARS4/URA3* plasmid (Brachmann *et al.* 1998), was engineered to carry the wild-type *POL2* gene under control of its native promoter. The genomic sequence of *POL2* was amplified from BY4733 yeast using Expand Hi-Fidelity DNA polymerase (Roche) and the following primers and PCR conditions: Pol2-XhoI (5´-ACTCGGTACTCGAGGCGCTCTGCCCTAGTTGGAATG-3´; XhoI site underlined) and PolED2 (5´-GATATTCCGAGCTCGCAACTTCCGGAGTGGTCAC-3´; SacI site underlined); 94°C, 1 min; 29x (94°C, 15 sec; 58°C, 20 sec; 68°C, 8 min); 68°C, 16 min. The resulting 7.5-kb fragment and pRS416 were digested with SacI and XhoI, ligated together with T4 DNA ligase (Gibco BRL), and then introduced into *E. coli*. Transformed clones were isolated, and a correct *POL2*-containing plasmid was confirmed by sequencing the entire insert. This vector (pRS416*POL2-5´YIF1*) did not fully complement the growth deficiency of our *pol2Δ* mutants. pRS416*POL2-5´YIF1* contains the entire *POL2* coding sequence as well as 592 bp of upstream sequence, including 371 bp of non-coding sequence containing the promoter and 221 bp of the 5' end of the *YIF1* gene, transcribed in the opposite direction. We hypothesized that transcription of the truncated *YIF1* gene may suppress *POL2* expression in our vector. Thus, we eliminated the *YIF1* sequences by replacing the XhoI-SalI 5´ fragment of pRS416*POL2-5´YIF1* with DNA amplified from this plasmid using PCR primers Pol2-7386bp-XhoIF (5´-ATGACTCGAGGTATGGGCCTTTGGTTTTCGT-3´) and Pol2-8161bpR (5´-GTTACACGCAATAAAGAAGTATGG-3´). The PCR product and pRS416*POL2-5´YIF1* were digested with BamHI and SalI and ligated together, and *E. coli* were transformed with the ligation product. The entire *POL2* gene from a transformant was again sequenced to verify its integrity, and this new vector (pRS416*POL2*) fully complemented the growth

deficiency of *pol2Δ* yeast. We sub-cloned the functional *POL2* fragment from pRS416*POL2* into the XhoI and SalI sites of the related plasmid pRS415 (*CEN6/ARS4/LEU2*) (Brachmann *et al.* 1998) to obtain pRS415*POL2*. pRS416*POL2* and pRS415*POL2* contain the full-length *POL2* coding sequence plus 368 bp upstream of the *POL2* start site (corresponding to nucleotides 147844 to 155125 of yeast chromosome XIV). The *pol2-4* mutation and all *eex* mutations were introduced into pRS415*POL2* using primers listed in Table 2.4, the QuikChange protocol (Wang and Malcolm 1999), Phusion polymerase (New England Biolabs), and the following PCR conditions: 95°C, 1 min; 16x (95°C, 40 sec; 53°C, 1 min; 68°C, 7 min). The entire *pol2* gene was sequenced in each case to verify the presence of desired mutations and the absence of other mutations. All Pol δ-expressing plasmids are previously described (Herr *et al.* 2011a). pRS vectors (Brachmann *et al.* 1998) were used as templates for chromosomal gene disruptions (see below). pUG6 served as a template for *kanMX* (Guldener *et al.* 1996) and pFv199 as a template for *natMX* (Stulemeijer *et al.* 2011).

Strains. BY4733 and Y7092 haploid yeast strains were engineered to carry alleles of DNA polymerase and MMR genes (Table 2.5). BY4733 (*MATa leu2Δ0 ura3Δ0 met15Δ0 trp1Δ63 his3Δ200*), a S288C descendent (Brachmann *et al.* 1998), was obtained by sporulating a BY4733 X BY4734 diploid (kindly provided by Tim Formosa, University of Utah). All engineered BY4733 strains (Table 2.5) originated from the same spore. Y7092 (*MAT*α *can1Δ::STE2pr-his5 lyp1Δ ura3Δ0 leu2Δ0 his3Δ1 met15Δ0*), also a S288C descendent, is a BY4742 derivative (Brachmann *et al.* 1998) modified by Boone and colleagues to use in Synthetic Genetic Array analyses (Tong and Boone 2007). Chromosomal gene disruptions were made using PCR products generated with Phusion polymerase (New England Biolabs) and the primers, templates and PCR conditions indicated in Table 2.6. Yeast were transformed with the resulting PCR products using lithium acetate transformation (Gietz and Woods 2002). Cells from transformant colonies were treated with Zymolyase (ICN

Biomedicals; 50 u/ml in 10 mM Tris•HCl/0.1 mM EDTA, pH 7.5 at 37°C for 30 min, then 95°C for 10 min) and subjected to junction-specific PCR with primers in the transgenes and flanking endogenous loci to detect correct insertion/deletion mutants (primers and PCR conditions available upon request).

Plasmid shuffling

Plasmid shuffling strains contained either *pol2Δ::kanMX* or *pol3Δ::HIS3* chromosomal gene disruptions and the *URA3* plasmids pRS416*POL2* or pGL310 (*POL3*) (Simon *et al.* 1991) to provide the essential activity of Pol ε or Pol δ (Table 2.5). Following transformation with CEN/LEU2 plasmids encoding mutant polymerases (YCplac111*pol3-01*, pRS415*pol2-4*, pRS415*pol2-4,eex,* or pRS415*pol2-eex*), transformants were selected on SC media lacking leucine and uracil (SC -URA -LEU). YCplac111*POL3*, pRS415*POL2* and the pRS415-unmodified plasmid were used as positive and negative controls. Colonies (1-2mm) from the selection plates were picked and suspended in 200 μl sterile water, and 25 μl was plated onto FOA-containing media (Boeke *et al.* 1984) in serial dilutions to select for spontaneous loss of the *URA3* plasmid expressing the wild-type polymerase.

eex mutant screen

eex mutants were isolated using the shuffling protocol. *pol2Δ msh2Δ* strains with the pRS416*POL2–URA3* plasmid were transformed with pRS415*pol2-4–LEU2*. Forty-eight individual colonies (1–2 mm) were picked from the SC -URA -LEU transformation plates and separately suspended in 240 μl sterile water, and 25-μl aliquots from each independent transformant were spotted in separate patches on FOA-containing media in a 6 x 8 grid. pRS415*POL2–LEU* and unmodified pRS415–*LEU* plasmids were used as positive and negative controls, respectively. After incubation at 30°C for 3 days, individual colonies were isolated and genotyped to identify clones carrying the *pol2-4* allele and no wild-type *POL2*. Sequences encoding the Pol ε exonuclease domain were amplified using primers Pol2-4U

(5'-ATAACACTCTCAGGGGACAAGTATAT-3') and Pol2s5 (5'-AGAATATTCGGAAAGGTGCTG-3') and the following PCR conditions: 98°C, 1 min.; 30x (98°C, 10 sec.; 54°C, 60 sec.; 72°C, 90 sec.); 72°C, 60 sec. PCR products were then digested with Alu1 at 37°C for at least 6 hours. The wild-type *POL2* allele results in a prominent 824-bp product as well as a number of smaller DNA fragments (275, 114, 84, 79, 53, and 17 bp). The *pol2-4* mutation introduces an additional AluI site within the 824-bp fragment, resulting in 447-bp and 377-bp products. Using this assay, we eliminated strains with *pol2-4* to *POL2* gene conversions (colonies with only the *POL2* allele) or other mutations (*e.g.*, *ura3*) that allow cells to retain *POL2* when grown on FOA (colonies with both *pol2-4* and *POL2*). Strains containing only the *pol2-4* allele were considered *bona fide eex* mutants. To identify *eex* mutants that are intragenic to *pol2-4*, plasmids were recovered from each mutant, introduced into *E. coli*, purified, and reshuffled into a fresh *pol2Δ msh2Δ* yeast strain. Plasmids that retained the ability to induce *pol2-4 msh2Δ* synthetic lethality were considered to be from strains with an *eex* mutation extragenic to the *pol2-4* plasmid ('chromosomal *eex*'). Plasmids that failed to recapitulate the *pol2-4 msh2Δ* synthetic lethality were hypothesized to carry *eex* mutations within *pol2-4* ('intragenic *eex*'). These mutations were identified by sequencing the *pol2* gene. All intragenic *eex* alleles were re-engineered into fresh pRS415*POL2* and pRS415*pol2-4* plasmids and re-shuffled for final confirmation of suppression. The re-engineered *eex* plasmids were used for all subsequent analyses.

Mutation and suppression rates

Mutation rates. Canavanine resistance (Can^r) mutation rates were measured as described (Herr *et al.* 2011a). Briefly, a freshly streaked *pol2Δ msh6Δ* strain containing pRS416*POL2* was transformed with pRS415*POL2,* pRS415*pol2-4,* pRS415*pol2-eex*, or pRS415*pol2-4,eex*, and multiple transformants were plated onto FOA media to obtain shuffled colonies. Twenty-four colonies for each allele were picked, suspended in water, and vigorously

vortexed to disperse the cells. Diluted aliquots from each colony were then plated onto SC (to estimate the number of cell divisions during colony formation) and canavanine selection plates (to determine the number of Can^r mutants). Colonies were counted after 3–4 days at 30°C. Mutation rates were calculated by the MMS maximum likelihood method using the web-based program Fluctuation AnaLysis CalculatOR (FALCOR; http://www.keshavsingh.org/protocols/FALCOR.html) (Hall *et al.* 2009).

Rates of escape from error-induced extinction. Rates of escape were determined from the plates shown in Figure 3 by counting the number of colonies in grid positions with verified *eex* mutants (patches with colonies that had *pol2-4* → *POL2* gene conversions or other FOA-resistant mutations were not included in this calculation) and the number of colonies from wild-type controls. The shuffling efficiency was assessed by plating aliquots of cells from an individual colony onto FOA (to determine the number of viable cells that lose the *ura3* plasmid) and synthetic complete media (to determine the total number of viable cells plated). The percentage of cells that lose the *ura3* plasmid (*i.e.*, the shuffling efficiency) was approximately 1% in our system. Therefore, colony counts were multiplied by 100, and FALCOR was used to calculate the rate of escape from error-induced extinction (Hall *et al.* 2009). Totals from the grid positions with verified *eex* mutants were entered into FALCOR as number of mutants (r), and totals from wild-type control positions were entered as number of viable cells (Nt). The FALCOR program uses these values to calculate a maximum likelihood estimate of mutation rate expressed per cell division (see (Hall *et al.* 2009) and references therein).

***CAN1* mutation spectra**

For each strain, ~55 Can^r colonies were isolated from 55 independent shuffling experiments. Cells were treated with Zymolyase, and the *can1* gene was PCR-amplified and sequenced as

previously described (Herr *et al.* 2011a). Mutation spectra were compared statistically using iMARS (Morgan and Lewis 2006) and Fisher's exact test.

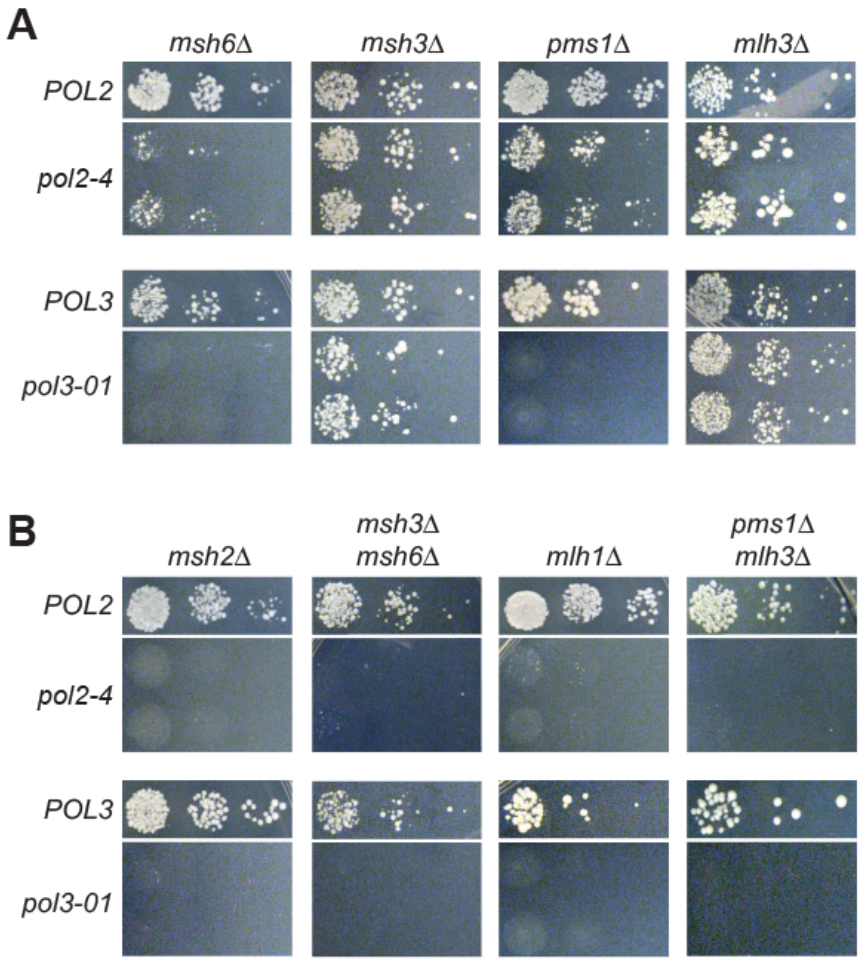

Figure 2.1 Genetic interactions between Pol ε and Pol δ proofreading and MMR. Using a plasmid shuffling strategy, proofreading-deficient variants of Pol ε (encoded by *pol2-4*) or Pol δ (encoded by *pol3-01*) or wild-type controls (*POL2* or *POL3*) were introduced *via LEU2* plasmids into BY4733 *pol2Δ* or *pol3Δ* strains harboring deletion mutations that partially (A) or completely (B) abrogate MMR. Serial dilutions were plated on FOA-containing media to select for loss of complementing *POL2*– or *POL3*–*URA3* plasmids and reveal the synthetic phenotype. *POL* and *MMR* alleles are indicated at left and above the corresponding panels, respectively.

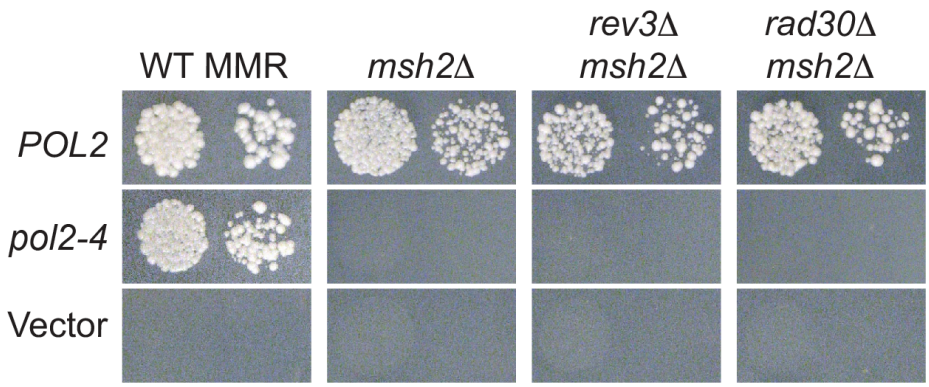

Figure 2.2 Effects of Pols ζ and η on *pol2-4 msh2Δ* synthetic lethality. *pol2Δ msh2Δ POL2–URA3* cells defective for Pol ζ (*rev3Δ*) or Pol η (*rad30Δ*) were transformed with *POL2–* or *pol2-4–LEU2* plasmids, and 10-fold serial dilutions of isolated transformants were plated onto FOA-containing media as in Figure 1. For comparison, the *POL2–* and *pol2-4–LEU2* plasmids were similarly shuffled into strains that were wild-type for Pols ζ and η (*REV3 RAD30*) and either *msh2Δ* or *MSH2* (WT MMR). *LEU2* plasmid with no *POL2* or *pol2-4* gene served as the vector-only control. Colony formation was assessed after incubation at 30°C for 3 days. Neither *rev3Δ* nor *rad30Δ* rescued *pol2-4 msh2Δ* synthetic lethality.

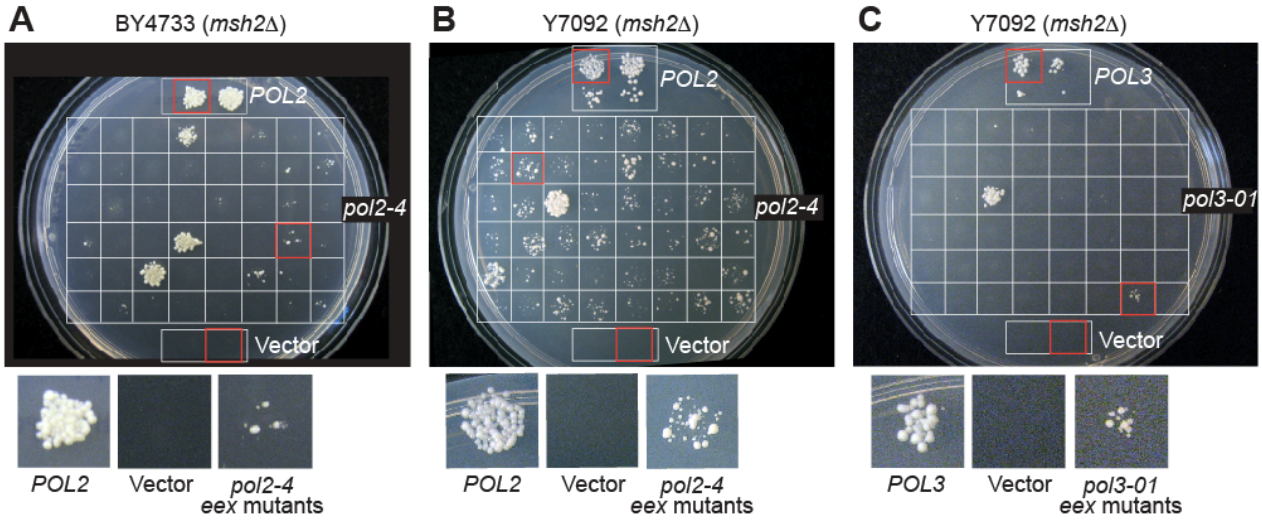

Figure 2.3 Escape from error-induced extinction. (A and B) Plasmid shuffling was used to screen for *error-induced extinction* (*eex*) mutants that suppress *pol2-4 msh2Δ* synthetic lethality. *pol2Δ msh2Δ POL2–URA3* strains derived from (A) BY4733 and (B) Y7092 were transformed with *pol2-4*, *POL2* or vector-only *LEU2* plasmids. Approximately 10^4 – 10^5 cells from 48 independent *pol2-4* transformants of each strain were spotted separately in a 6 x 8 grid on FOA-containing media to select for loss of the *POL2–URA3* plasmid and to isolate suppressor mutants. *Bona fide* suppressors containing *pol2-4* as the sole source of Pol ε arose at a rate of 1.9×10^{-4} *eex* mutants/cell division in the BY4733 strain (95% confidence interval (CI) = 2.6×10^{-4} – 1.3×10^{-4}), and 4.0×10^{-3} in the Y7092 background (95% CI = 4.4×10^{-3} – 3.6×10^{-3}). (C) A similar plasmid shuffling strategy was used to estimate the rate of escape from *pol3-01 msh2Δ* synthetic lethality in the Y7092 background (8.8×10^{-6} *eex* mutants/cell division; 95% CI = 2.0×10^{-5} – 1.6×10^{-6}). In panel (C), 10-fold fewer viable cells were plated in each grid position compared to panels (A) and (B). The *POL2* control patches in panel (A) are two independent transformants. The *POL2* and *POL3* control patches in panels (B) and (C) are also from replicate transformants and include 10-fold dilutions of each. Rates (*eex* mutants/cell division) were calculated as described in Materials and Methods. Red boxes indicate grid positions magnified below each plate.

Figure 2.4

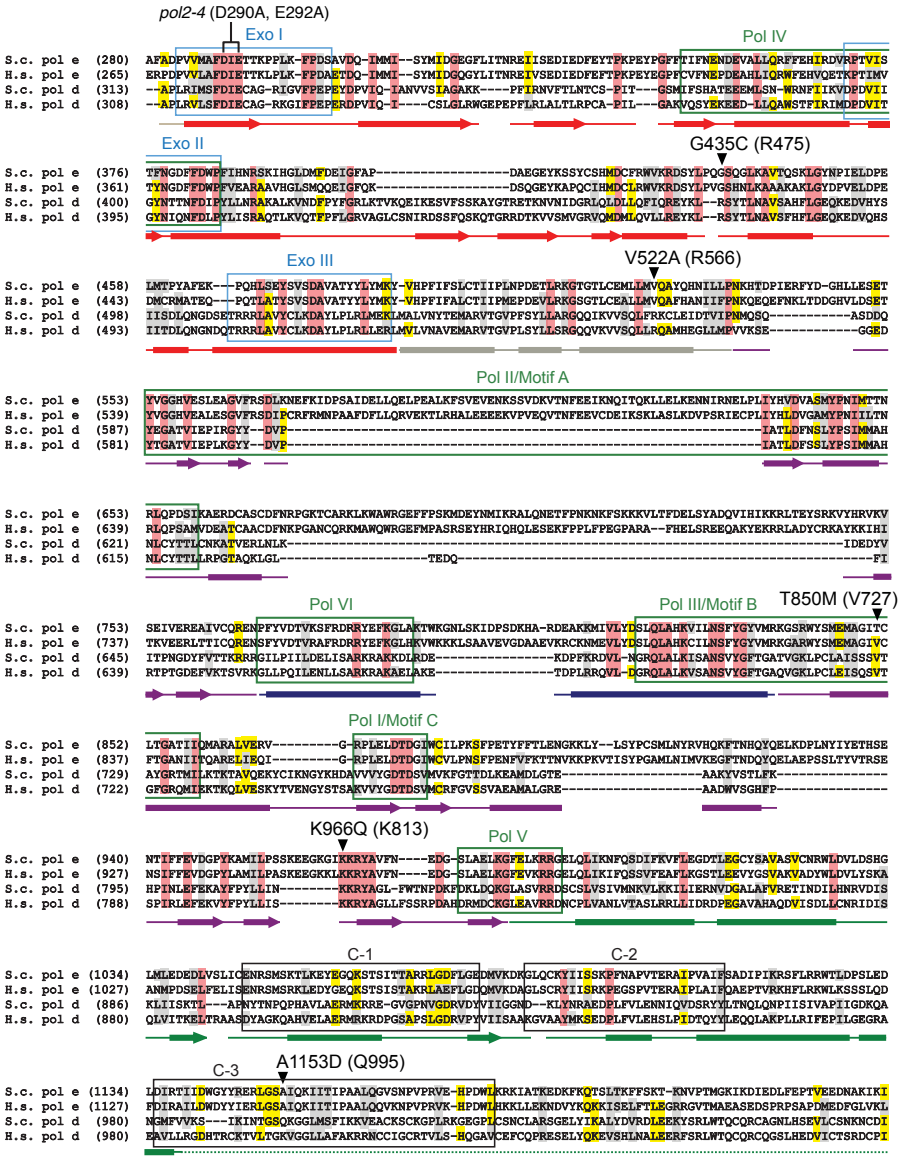
pol2-4 (D290A, E292A)
Exo I
Pol IV
Exo II
G435C (R475)
Exo III
V522A (R566)
Pol II/Motif A
Pol VI
Pol III/Motif B
T850M (V727)
Pol I/Motif C
K966Q (K813)
Pol V
C-1
C-2
C-3
A1153D (Q995)

Figure 2.4 Amino acid changes in Pol ε *eex* mutants. Aligned amino-acid sequences of the catalytic subunits of Pols ε and δ (S.c. pol e, *Saccharomyces cerevisiae* Pol ε; H.s. pol e, *Homo sapiens* Pol ε; S.c. pol d, *Saccharomyces cerevisiae* Pol δ; H.s. pol d, *Homo sapiens* Pol δ). Secondary structural elements of yeast Pol δ (Swan *et al.* 2009) are indicated below the alignment and color coded to depict their domain location (as in Figure 7): rectangles, α-helices; arrows, β-strands; solid lines, loops; dotted line, structure unknown. Amino-acid substitutions encoded by Pol ε *eex* mutations are shown in black above the sequence, with the corresponding yeast Pol δ residues in parentheses. Conserved polymerase and exonuclease motifs are framed in green and blue, respectively (Bernad *et al.* 1989; Wang *et al.* 1989). Three additional regions of homology (C-1, C-2, and C-3) are framed in black (Huang *et al.* 1999). Amino acid conservation is indicated using the following color scheme: red, residues conserved in all 4 sequences; yellow, residues conserved in 3 sequences; gray, similar amino acids in at least 3 sequences.

Figure 2.5

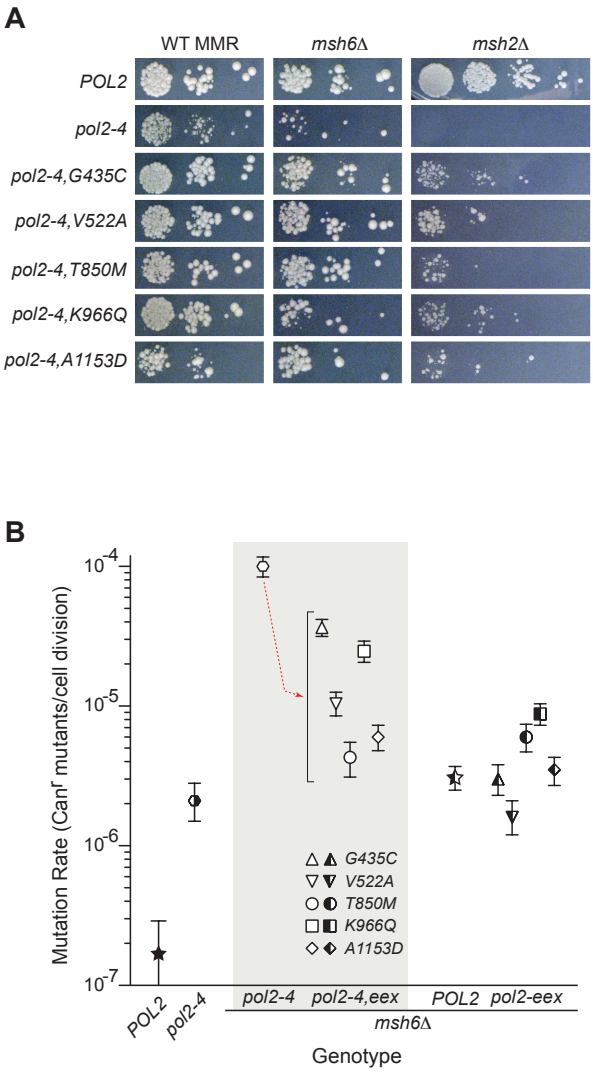
A
WT MMR
msh6Δ
msh2Δ
POL2
pol2-4
pol2-4,G435C
pol2-4,V522A
pol2-4,T850M
pol2-4,K966Q
pol2-4,A1153D
B
Mutation Rate (Canr mutants/cell division)
10-4
10-5
10-6
10-7
G435C
V522A
T850M
K966Q
A1153D
POL2
pol2-4
pol2-4
pol2-4,eex
POL2
pol2-eex
msh6Δ
Genotype

Figure 2.5 Growth and antimutator phenotypes conferred by *pol2-4* intragenic *eex*. (A) *eex* mutations reverse synthetic growth defects associated with *pol2-4*. The *pol2-4,eex* mutations were re-engineered into fresh *pol2-4–LEU2* plasmids and introduced into wild-type (WT) MMR, *msh6Δ* or *msh2Δ* strains for plasmid shuffling. Strains harboring *POL2*– or *pol2-4–LEU2* plasmids served as controls. Transformants were serially diluted and spotted onto FOA-containing media to assess colony forming capacity after incubation at 30°C for 3 days (WT MMR and *msh6Δ*) or 4 days (*msh2Δ*). (B) *eex* mutations confer antimutator phenotypes. Rates of spontaneous mutation, expressed as canavanine resistant (Can^r) mutants/cell division, were determined from multiple independent fluctuation analyses of each strain. Confidence intervals (95%) for each mutation rate are shown as error bars. The downward red arrow in the gray box indicates the antimutator effect of *eex* alleles on the *pol2-4* mutator phenotype. Symbol fill patterns indicate *POL2* and *MSH6* allele status: black left half, *POL2*; black right half, *MSH6*; solid black, *POL2 MSH6*; unfilled left half, *pol2-4*; unfilled right half, *msh6Δ*; completely unfilled, *pol2-4 msh6Δ*. Symbol shapes indicate *eex* allele status (see key insert): star and hexagon, no *eex*; triangle, *G435C*; inverted triangle, *V522A*; circle, *T850M*; square, *K966Q*; diamond, *A1153D*.

Figure 2.6

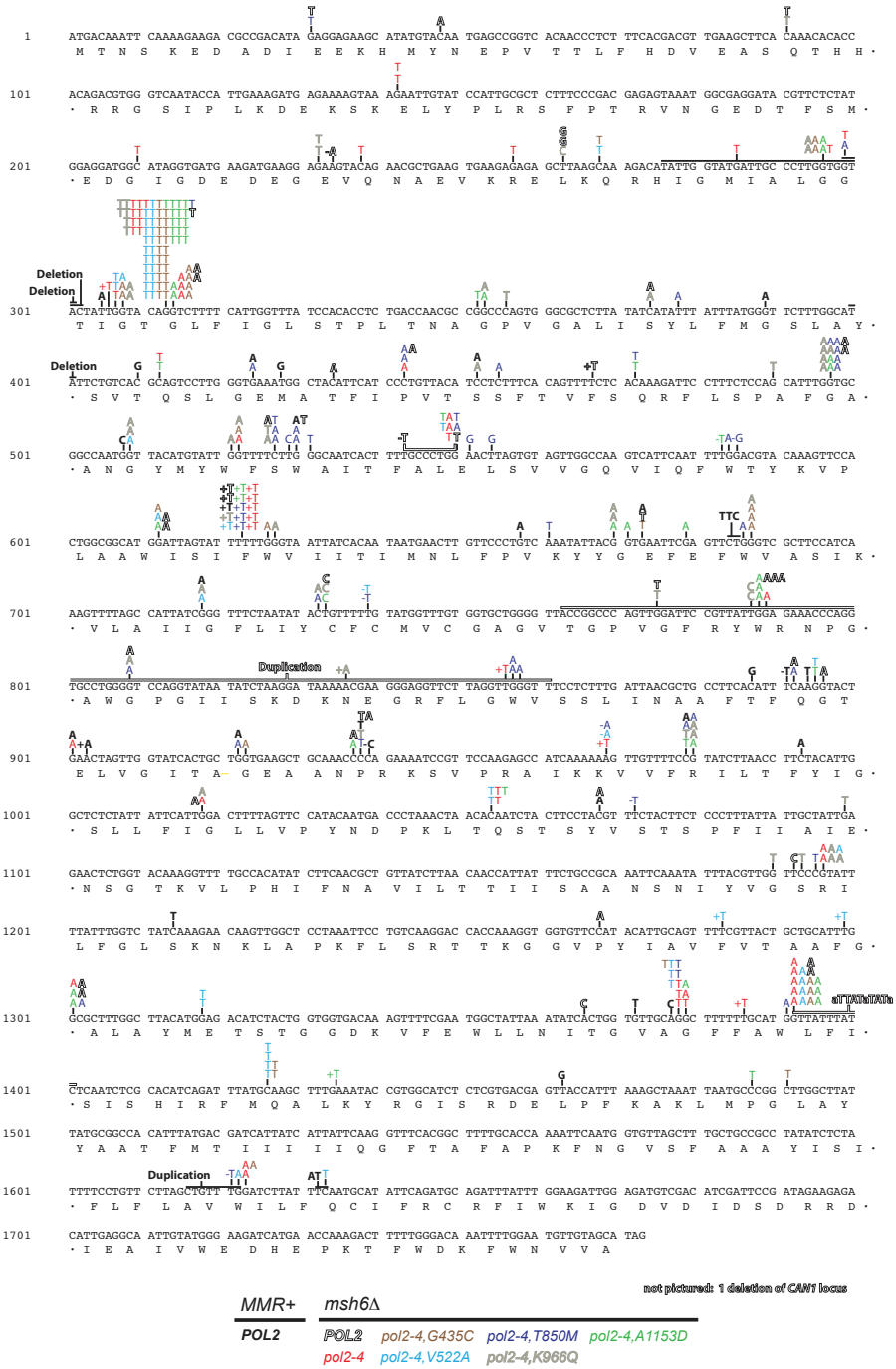
Deletion
Deletion
Deletion
Duplication
Duplication
not pictured: 1 deletion of CAN1 locus
MMR+
msh6Δ
POL2
POL2
pol2-4,G435C
pol2-4,T850M
pol2-4,A1153D
pol2-4
pol2-4,V522A
pol2-4,K966Q

Figure 2.6 Spontaneous *CAN1* mutations from *pol2-4* and *pol2-4,eex msh6Δ* cells. The *can1* genes from about 50 independent canavanine-resistant mutants of each strain were PCR-amplified and sequenced. Mutations identified in different strains are color-coded according to the key at the bottom. Each base letter above the wild-type *CAN1* sequence indicates an independent base substitution or frameshift (+ or -) mutation. Horizontal lines indicate *CAN1* sequences involved in complex mutations, duplications and deletions. The wild-type *POL2* and *POL2 msh6Δ* spectra are from Herr et al. (Herr *et al.* 2011a).

Figure 2.7

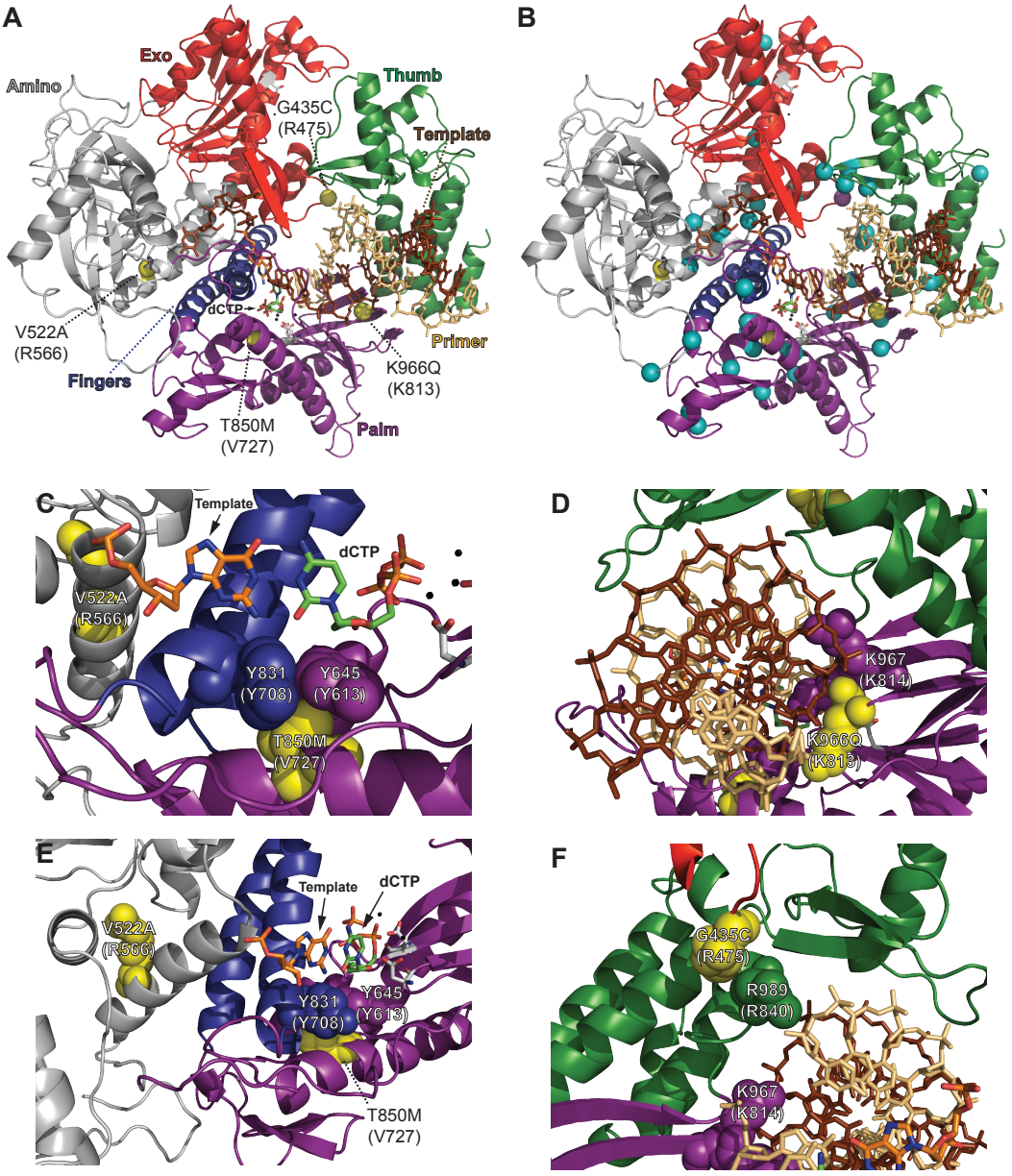
A
Exo
Amino
Thumb
G435C
(R475)
Template
dCTP
V522A
(R566)
Primer
Fingers
K966Q
(K813)
T850M
(V727)
Palm
B
C
Template
dCTP
V522A
(R566)
Y831
(Y708)
Y645
(Y613)
T850M
(V727)
D
K967
(K814)
K966Q
(K813)
E
Template
dCTP
V522A
(R566)
Y831
(Y708)
Y645
(Y613)
T850M
(V727)
F
G435C
(R475)
R989
(R840)
K967
(K814)

Figure 2.7 Locations of Pol ε *eex* amino-acid substitutions mapped onto the Pol δ structure. (A) Overall distribution of Pol ε *eex* amino-acid substitutions. The catalytic subunit of yeast Pol δ is depicted as a ribbon diagram with the following color-coded elements: exonuclease domain, red; thumb domain, green; fingers domain, blue; palm domain, purple; amino domain, gray; DNA template strand, brown sticks; primer strand, tan sticks; catalytic carboxylate residues in the polymerase and exonuclease active sites, gray CPK sticks; metal ions, small black spheres; incoming dCTP, green CPK sticks; template G nucleotide, orange CPK sticks. Locations of *eex*-encoded changes are shown as yellow spheres and labeled by the Pol ε amino-acid substitution with the corresponding Pol δ residue in parentheses. The A1153D substitution is not pictured because it falls in a region where the Pol δ structure is unknown. (B) Locations of Pol ε *eex* substitutions (yellow spheres) relative to Pol δ *eex* substitutions (aqua spheres; see (Herr *et al.* 2011a)). The purple sphere at the Exo-Thumb interface is Pol ε G435C, which aligns with Pol δ R475I/G. (C, D, E and F) Close-up depictions of Pol ε *eex* substitutions. Important residues are highlighted as space-filling spheres, with yellow indicating positions corresponding to Pol ε *eex* substitutions. Structure of *S. cerevisiae* Pol δ from Swan *et al.* ((Swan *et al.* 2009); Protein Data Bank accession code 3IAY).

Table 2.1 Genotypes of candidate *eex* mutants

Class of FOA^r Mutant	Mutants Isolated from:		Total # of Mutants
	BY4733	Y7092	
eex			
intragenic to *pol2-4*	4	1	5
extragenic to *pol2-4*	50	26	76
	54	27	81
pol2-4 → *POL2* conversion	26	3	29
other (*e.g.*, *ura3* mutations)	23	0	23
Total	103	30	133

FOA-resistant (FOA^r) colonies from 133 different *pol2-4–LEU2 POL2–URA3 msh2Δ* parent clones were isolated, and *POL2* was genotyped to distinguish genuine *eex* mutants from *pol2-4* → *POL2* gene conversions and other mutations that confer FOA resistance (*e.g.*, *ura3*). Clones harboring only *pol2-4* were considered *eex* mutants. Plasmids from *eex* mutants were recovered and retested in a fresh *msh2Δ* strain to distinguish second-site suppressors within *pol2-4* ('intragenic *eex*') from *eex* mutations located extragenic to *pol2-4* ('chromosomal *eex*'). *eex* mutants were isolated from two different strains: BY4733 and Y7092 (Figure 3A and B).

Table 2.2 Types of spontaneous *CAN1* mutations in *pol2-4,eex msh6Δ* strains [a]

	WT [b]	*msh6Δ* [b]	*pol2-4 msh6Δ*	*pol2-4,eex msh6Δ*				
				G435C	*V522A*	*T850M* [c]	*K966Q* [c]	*A1153D*
Transitions								
G→A	8 (24)	16 (34)	20 (36)	19 (41)	10 (19)	21 (41)	26 (48)	21 (41)
C→T	3 (9)	2 (4)	5 (9)	4 (9)	8 (15)	4 (8)	6 (11)	4 (8)
A→G	0 (0)	0 (0)	0 (0)	0 (0)	0 (0)	1 (2)	0 (0)	0 (0)
T→C	0 (0)	3 (6)	0 (0)	0 (0)	0 (0)	1 (2)	4 (7) [d]	1 (2)
	11 (33)	21 (45)	25 (45)	23 (50)	18 (35)	26 (51)	36 (67) [d]	26 (51)
Transversions								
G→T	2 (6)	5 (11)	21 (38)	23 (50)	29 (56)	6 (12) [d]	12 (22)	19 (37)
C→A	3 (9)	10 (21)	1 (2)	0 (0)	0 (0)	8 (16) [d]	4 (7)	1 (2)
G→C	1 (3)	0 (0)	0 (0)	0 (0)	0 (0)	0 (0)	0 (0)	1 (2)
C→G	2 (6)	0 (0)	0 (0)	0 (0)	0 (0)	0 (0)	0 (0)	0 (0)
A→C	1 (3)	1 (2)	0 (0)	0 (0)	0 (0)	0 (0)	0 (0)	0 (0)
T→G	1 (3)	2 (4)	0 (0)	0 (0)	0 (0)	1 (2)	0 (0)	0 (0)
A→T	1 (3)	0 (0)	0 (0)	0 (0)	0 (0)	1 (2)	0 (0)	0 (0)
T→A	1 (3)	0 (0)	0 (0)	0 (0)	0 (0)	1 (2)	0 (0)	0 (0)
	12 (36)	18 (38)	22 (39)	23 (50)	29 (56)	17 (33)	16 (30)	21 (41)
Frameshifts								
+1	2 (6)	3 (6)	9 (16)	0 (0) [d]	3 (6)	3 (6)	2 (4) [d]	3 (6)
–1	2 (6)	1 (2)	0 (0)	0 (0)	2 (4)	5 (10) [d]	0 (0)	1 (2)
	4 (12)	4 (9)	9 (16)	0 (0) [d]	5 (10)	8 (16)	2 (4) [d]	4 (8)
Other	6 (18)	4 (9)	0 (0)	0 (0)	0 (0)	0 (0)	0 (0)	0 (0)
Multiple	0 (0)	0 (0)	1 (2)	1 (2)	1 (2)	0 (0)	1 (2)	0 (0)
Total	33	47	56	46	52	51	54	51

[a] The *CAN1* gene was sequenced from Can^r mutants of each strain. The numbers of mutations of each subtype are shown with percentages in parentheses. 'Other' includes duplications, deletions, and complex mutations. Some mutants had two mutations separated by more than 10 bp (61–1150 bp). These are reported under 'Multiple'; each mutation in this category was scored as an independent event and added to the relevant subclass tally, although they may be mechanistically linked. See Figure 6 for locations of mutations in the *CAN1* gene.

[b] WT and *msh6Δ* data from Herr *et al.* (Herr *et al.* 2011a).

[c] Distribution of base substitutions significantly different from *pol2-4 msh6Δ* (p≤0.05, Monte Carlo hypergeometric test).

[d] Significantly different from *pol2-4 msh6Δ* (p≤0.05, Fisher's exact test).

Table 2.3 Rates of spontaneous *CAN1* mutations in *pol2-4,eex msh6Δ* strains [a]

	pol2-4 msh6Δ	*pol2-4,eex msh6Δ*				
		G435C	*V522A*	*T850M*	*K966Q*	*A1153D*
Transitions						
G→A	360 (1.0)	150 (0.4)	20 (0.06)	18 (0.05)	120 (0.3)	25 (0.07)
C→T	90 (1.0)	~32 (~0.4)	16 (0.2)	~3 (~0.04)	27 (0.3)	~5 (~0.05)
Transversions						
G→T	380 (1.0)	180 (0.5)	58 (0.2)	5 (0.01)	55 (0.1)	22 (0.06)
C→A	~18 (1.0)	<8 (ND)	<2 (ND)	7 (ND)	~18 (ND)	~1 (ND)
Frameshifts						
+1	160 (1.0)	<8 (<0.05)	~6 (~0.04)	~3 (~0.02)	~9 (~0.06)	~4 (~0.02)
–1	<18 (1.0)	<8 (ND)	~4 (ND)	4 (ND)	<5 (ND)	~1 (ND)
Overall	1001 (1.0)	365 (0.36)	104 (0.10)	43 (0.04)	247 (0.25)	60 (0.06)

[a] Expressed as the number of Can^r mutants per cell division (x 10^{-7}). Rates for individual mutation types were calculated by multiplying the overall Can^r mutation rate of a strain (last row of table) by the percentage of the corresponding mutation in the *CAN1* mutation spectrum from that strain (Table 2.2). Rates relative to those in *pol2-4 msh6Δ* are in parentheses. Values were calculated to three decimal places and then rounded to one or two significant figures. < or ~: incidence values (Table 2.2) were zero or not significantly different from zero, respectively ($p>0.05$, Fisher's exact test). ND: relative rates could not be reliably determined because mutations of this type were not detected at significant levels in the *pol2-4 msh6Δ* strain (Table 2.2).

Table 2.4 Oligonucleotides used for site-directed mutagenesis

Allele	PCR Primer Name	PCR Primer Sequence
pol2-4	pol2-4F1	5′-CTGTGGTAATGGCATTTGCTATAGCTACCACGAAGCCGCC-3′
	pol2-4R1	5′-GGCGGCTTCGTGGTAGCTATAGCAAATGCCATTACCACAG-3′
pol2-G435C	eex51qcF	5′-ATTCTTATTTACCACAATGTTCCCAGGGTTTAAAA-3′
	eex51qcR	5′-TTTTAAACCCTGGGAACATTGTGGTAAATAAGAAT-3′
pol2-V522A	eex20qcR	5′-GAAATGTTGTTGATGGCTCAAGCTTATCAACAT-3′
	eex20qcR	5′-ATGTTGATAAGCTTGAGCCATCAACAACATTTC-3′
pol2-T850M	eex26qcF	5′-GAAATGGCGGGGATTATGTGTTTAACAGGTGCC-3′
	eex26qcR	5′-GGCACCTGTTAAACACATAATCCCCGCCATTTC-3′
pol2-K966Q	eex55qcF	5′-GAAGGAAAAGGTATACAGAAAAGATATGCTGTC-3′
	eex55qcR	5′-GACAGCATATCTTTTCTGTATACCTTTTCCTTC-3′
pol2-A1153D	eex12qcF	5′-GAAAGACTTGGATCTGATATACAAAAGATAATT-3′
	eex12qcR	5′-AATTATCTTTTGTATATCAGATCCAAGTCTTTC-3′

Mutations were introduced into pRS415POL2 or pRS415pol2-4 using the QuickChange protocol (Wang and Malcolm 1999), Phusion Polymerase (New England Biolabs), the indicated primers, and PCR conditions of 95°C, 1 min; 16x (95°C, 40 sec.; 53°C, 60 sec., 68°C, 7 min.).

Table 2.5 Yeast strains

Strain	Relevant Genotype	Reference
LW01[a]	*pol2::kanMX msh2::HIS3* + pRS416*POL2*	This study
LW02[a]	*pol2::kanMX msh3::MET15* + pRS416*POL2*	This study
LW03[a]	*pol2::kanMX msh6::HIS3* + pRS416*POL2*	This study
LW04[a]	*pol2::kanMX mlh1::HIS3* + pRS416*POL2*	This study
LW05[a]	*pol2::kanMX pms1::HIS3* + pRS416*POL2*	This study
LW06[a]	*pol2::kanMX mlh3::MET15* + pRS416*POL2*	This study
LW07[a]	*pol2::kanMX msh6::HIS3 msh3::LEU2* + pRS416*POL2*	This study
LW08[a]	*pol2::kanMX pms1::HIS3 mlh3::TRP1* + pRS416*POL2*	This study
LW09[a]	*pol2::kanMX msh2::HIS3 rev3::TRP1* + pRS416*POL2*	This study
LW10[a]	*pol2::kanMX msh2::HIS3 rad30::TRP1* + pRS416*POL2*	This study
BP0109[b]	*pol3::HIS3 msh2::TRP1* + pGL310 [*URA3/POL3*]	(Herr *et al.* 2011a)
BP0210[b]	*pol3::HIS3 msh3::TRP1* + pGL310 [*URA3/POL3*]	This study
BP0301[b]	*pol3::HIS3 msh6::TRP1* + pGL310 [*URA3/POL3*]	This study
BP0412[b]	*pol3::HIS3 mlh1::TRP1* + pGL310 [*URA3/POL3*]	This study
BP0502[b]	*pol3::HIS3 pms1::TRP1* + pGL310 [*URA3/POL3*]	This study
LW09[b]	*pol3::HIS3 mlh3::TRP1* + pGL310 [*URA3/POL3*]	This study
LW10[b]	*pol3::HIS3 msh6::TRP1 msh3::MET15* + pGL310 [*URA3/POL3*]	This study
LW11[b]	*pol3::HIS3 pms1::TRP1 mlh3::MET15* + pGL310 [*URA3/POL3*]	This study
LW12[c]	*pol2::NAT1 msh2::MET15* + pRS416*POL2*	This study
LW13[c]	*pol3::NAT1 msh2::MET15* + pGL310 [*URA3/POL3*]	This study

[a] Strains engineered from the BY4733 strain (*MATa leu2Δ0 ura3Δ0 met15Δ0 trp1Δ63 his3Δ200*), an S288C descendent (Brachmann *et al.* 1998) that we re-derived via sporulation of a BY4733 X BY4734 diploid (kindly provided by Tim Formosa, University of Utah). The *pol2::kanMX* strains were constructed from this re-derived BY4733 strain by first introducing pRS416*POL2* (to provide a wild-type plasmid copy of *POL2*) and then replacing the entire chromosomal *POL2* gene with a *kanMX* cassette. pRS416*POL2* is the *CEN6/ARSH4/URA3* plasmid pRS416 (Brachmann *et al.* 1998) carrying wild-type *POL2* with its natural promoter.

[b] These strains were engineered from P3H3a described in (Herr *et al.* 2011a).

[c] These strains were engineered from the Y7092 strain (*MATα can1Δ::STE2pr-his5 lyp1Δ ura3Δ0 leu2Δ0 his3Δ1 met15Δ0*), an S288C descendent modified by the Boone lab to be used as a query strain in Synthetic Genetic Analysis (Tong and Boone 2007).

Table 2.6 Oligonucleotides used for construction of chromosomal gene disruptions

Allele	PCR Primer Name	PCR Primer Sequence	PCR Template [a]
pol2Δ::kanMX	Pol2-kanMXkoF	5′-ATGATGTTTGGCAAGAAAAAAAACAACGGAGGATCTTCCACTGCAAGATATTCAGCTGGCGAAGTTATTAGGTCTAGAGATCTG-3′	pUG6 (Guldener *et al.* 1996)
	Pol2-kanMXkoR	5′-TCATATGGTCAAATCAGCAATACAACTCAATAATATATCAAAACCGTAATACTTGGCTACTACGAAGTTATATTAAGGGTTCTCG-3′	
pol2Δ::natMX	Pol2::nat1-for2	5′-AGAGCATATGATGATGAAAGAGCACATTCTATCAAGATAACACTCTCAGGGGACAAGTATACATGGAGGCCCAGAATACCCT-3′	pFvL99 (Stulemeijer *et al.* 2011)
	Pol2::nat1-rev2	5′-TTTTTTTTTTTTTTTTTTTCATGGTAAAGAGGCCATTGAACCTCGCGTTATATACTGCTTACCAGTATAGCGACCAGCATTCAC-3′	
pol3Δ::natMX	Pol3MXF	5'-ATAGATATTGAGCACTTGCTATTAAGCATTAATCTTTATACATATACGCACAGCAACATGGAGGCCCAGAATACCCT-3'	pFvL99 (Stulemeijer *et al.* 2011)
	Pol3MXR	5′-GCAAAAAGTTGTTAGCCTTTCTTAATCCTAATATGATGTGCCACCCTATCGTTTTCAGTATAGCGACCAGCATTCAC-3′	
msh2Δ::HIS3 or *msh2Δ::TRP1*	Msh2U	5′-AAAAATCTCTTTATCTGCTGACCTAACATCAAAATCCTCAGATTAAAAGTAGATTGTACTGAGAGTGCAC-3′	pRS413 or pRS414 (Brachmann *et al.* 1998)
	Msh2D	5′-TTATAACAACAAGGCTTTTATATATTTCAGGTAATTATCGTTTTCCTTTTCTGTGCGGTATTTCACACCG-3′	
msh2Δ::MET15	Msh2::Met15F	5′-AAAAATCTCTTTATCTGCTGACCTAACATCAAAATCCTGCTGGCTTAACTATGCGGCATC-3′	pRS411 (Brachmann *et al.* 1998)
	Msh2::Met15R	5′-TTATAACAACAAGGCTTTTATATATTTCAGGTAATTATGTTTACAATTTCCTGATGCGGT-3′	
msh6Δ::HIS3 or *msh6Δ::TRP1*	Msh6U	5′-TTTAATTGGAGCAACTAGTTAATTTTGACAAAGCCAATTTGAACTCCAAAGAAGTTATTAGGTCTAGAGATCTG-3′	pRS413 or pRS414 (Brachmann *et al.* 1998)
	Msh6D	5′-ACTTTAAAAAAAATAAGTAAAAATCTTACATACATCGTAAATGAAAATACACGAAGTTATATTAAGGGTTCTCG-3′	
mlh1 Δ::HIS3 or *mlh1Δ::TRP1*	Mlh1U	5′-ATAGTGATAGTAAATGGAAGGTAAAAATAACATAGACCTATCAATAAGCAATGTCTCTCAGAATAAAAGCAGATTGTACTGAGAGTGCAC-3′	pRS413 or pRS414 (Brachmann *et al.* 1998)
	Mlh1D	5′-CTCAGGAAATAAACAAAAAACTTTGGTATTACAGCCAAAACGTTTTAAAGTTAACACCTCTCAAAAACTTTACTGTGCGGT ATTTCACACCG-3′	
pms1Δ::HIS3 or *pms1Δ::TRP1*	Pms1U	5′-GAACGCGAAAAGAAAAGACGCGTCTCTCTTAATAATCATTATGCGATAAAATGTTTCACCACATCGAAAAAGATTGTACTGAGAGTGCAC-3′	pRS413 or pRS414 (Brachmann *et al.* 1998)
	Pms1D	5′-TGTATATAATGTATTTGTTAATTATATAATGAATGAATATCAAAGCTAGATCATATTTCGTAATCCTTCGACTGTGCGGTATTTCACACCG-3′	

CHAPTER III: SYNTHETIC GENETIC ARRAY (SGA) ANALYSIS TO IDENTIFY DELETIONS THAT SUPPRESS ERROR-INDUCED EXTINCTION

DNA polymerases (Pols) ε and δ perform the bulk of nuclear DNA synthesis. Both Pols are high-fidelity enzymes with intrinsic proofreading exonucleases that edit errors during polymerization. Errors that elude proofreading are extended into duplex DNA and excised by the mismatch repair (MMR) system. Strains with combined defects in Pol proofreading and MMR initially divide, but succumb to error-induced extinction and fail to form viable colonies. Using a plasmid shuffling strategy in haploid *Saccharomyces cerevisiae*, we exploited error-induced extinction to isolate suppressors of lethal mutation rates (*eex* mutants). In screens for mutants that suppress *pol3-01 msh6Δ* or *pol2-4 msh2Δ* error-induced extinction, thirty-five- and five-percent of *eex* mutations, respectively, encoded 'antimutator' polymerases, that increased replication fidelity. The remaining *eex* alleles were extragenic to the polymerase genes, suggesting that factors in addition to polymerase base selectivity, proofreading and MMR influence replication fidelity. To identify extragenic factors of DNA replication fidelity, we screened a collection of 4,811 viable gene deletion mutants for deletions that suppress error-induced extinction. We found that no single nonessential gene deletion suppressed *pol3-01 msh2Δ* error-induced extinction. Our data suggest that *pol3-01 msh2Δ eex* mutants extragenic to *pol3* are gain-of-function mutations or hypomorphic mutations in essential genes.

INTRODUCTION

Eukaryotic cells employ high-fidelity DNA polymerases (Pols) for genome replication (McCulloch and Kunkel 2008). In budding yeast, Pols ε and δ replicate the leading- and lagging-strands, respectively (Larrea *et al.* 2010; Nick Mcelhinny *et al.* 2008; Pavlov and Shcherbakova 2010; Pursell *et al.* 2007). While inherently accurate, both polymerases also possess intrinsic exonuclease domains that excise errors during DNA polymerization (McCulloch and Kunkel 2008). Misincorporations left behind the replication fork are recognized by MMR (Iyer *et al.* 2006; Kolodner and Marsischky 1999). Heterodimers of MutS homologs (Msh2-Msh6 or Msh2-Msh3) bind mismatches, insertions and deletions and recruit MutL homologs (Mlh1-Pms1 or Mlh1-Mlh3) that initiate excision and re-synthesis of the mismatched strand. Thus, pol base selectivity, proofreading and MMR are the main determinants of replication fidelity.

Combined defects in polymerase proofreading and MMR are synthetically lethal in haploid yeast due to unrestrained mutagenesis during DNA replication (Greene and Jinks-Robertson 2001; Herr *et al.* 2011a; Morrison *et al.* 1993). Random mutations in essential genes undermine colony formation, resulting in error-induced extinction. We recently exploited this lethality to screen for mutants that escape error-induced extinction. The first screen isolated suppressors of Pol δ error-induced lethality (*pol3-01 msh6Δ*) (Herr *et al.* 2011a). Thirty-five percent of recovered suppressor mutations encoded variants in Pol δ that reduced mutation rates (Herr *et al.* 2011a). These antimutator alleles were scattered throughout the polymerase domains, implicating multiple mechanisms of error suppression. The remaining sixty-five percent were extragenic to *pol3*. In a second screen for *eex* mutants, we isolated suppressors of Pol ε error-induced extinction (*pol-4 msh2Δ*). Six percent of these mutants encoded antimutator variants of Pol ε, while the remaining ninety-four percent were extragenic to *pol2* (Table 2.1). Both screens isolated antimuator

polymerase variants, underscoring the importance of polymerase base selectivity in mutation avoidance (Herr *et al.* 2011a) (Figure 2.1). However, the preponderance of extragenic suppressors implicates pathways other than polymerase fidelity in antimutagenesis (Herr *et al.* 2011a), (Table 2.1).

To identify novel pathways of DNA replication fidelity, we wanted to map extragenic mutations that suppress error-induced extinction. The classic techniques of complementation and cloning are generally used to map recessive and dominant alleles, respectively. These methods are advantageous with respect to time and effort, but unfortunately, cannot be applied to the unique circumstances of *eex* mutants. First, since combined defects in polymerase proofreading and MMR drive error-induced extinction only in haploids, it would be difficult to determine whether extragenic *eex* alleles are dominant or recessive. We could determine whether *eex* allele suppress mutation rates in diploids, but would have to extrapolate what degree of suppression constitutes a dominant or recessive phenotype. Complicating this matter is that fact that many mutator alleles are semi-dominant (Albertson *et al.* 2009; Goldsby *et al.* 2002; Morrison *et al.* 1993). Complementation of the *eex* phenotype (escape from error-induced extinction) would kill clones, precluding recovery of the complementing plasmid. Lastly, an abundance of *de novo* suppressors would arise while cloning the mutations, creating an excess of false positives (Figure 2.3). Thus, we decided to use an alternative approach to identify extragenic *eex* pathways using the Synthetic Genetic Array (SGA).

In *Saccharomyces cerevisiae*, a complete set of gene deletion mutants has been constructed for each of 5,916 predicted yeast genes. 1,105 essential genes were identified, resulting in the generation of 4,811 viable deletion mutants that comprise the SGA (Giaever *et al.* 2002; Winzeler *et al.* 1999). SGA analysis allows almost global identification of gene interactions by crossing a query strain to the array and selecting for haploid strains containing

both the query mutation and array deletions through a series of replica pinning procedures (Tong *et al.* 2001; Tong *et al.* 2004). Here, we use the SGA to systematically and comprehensively screen for deletions that suppress error-induced extinction. We hypothesized that this approach would be fruitful because several gene deletion mutants impart an antimutator phenotype under certain circumstances. Deletion of *REV3* (*rev3Δ*), encoding the catalytic subunit of Pol ζ, lowers the background mutation rates in WT cells ~70% (Lawrence and Christensen 1979; Quah *et al.* 1980) and suppresses the mutator phenotype of various mutator alleles (Aksenova *et al.* 2010; Pavlov *et al.* 2001; Shcherbakova *et al.* 1996). Deletion of *DUN1* (*dun1Δ*) suppresses the mutator phenotype of proofreading-defective Pol δ (encoded by *pol3-01*) (Datta *et al.* 2000). In spite of these precedents, we found no single gene deletion capable of suppressing *pol3-01 msh2Δ* error-induced extinction.

RESULTS

The Synthetic Genetic Array (SGA) is primarily used to identify gene interactions by crossing a mutant query strain with SGA strains and selecting for haploid spores that inherit both the introduced mutation and SGA deletions. Gene interactions are inferred when double-mutant spores fail to form colonies (Tong *et al.* 2001). However, the SGA can be adapted for multiple uses (Jorgensen *et al.* 2002). To identify extragenic pathways of antimutagenesis, we employed the SGA to screen for deletions that suppress error-induced extinction.

de novo suppressors of error-induced extinction arise frequently in haploid yeast (Herr *et al.* 2011a) (Figure 2.3). I found that the query strain constructed specifically for SGA analysis is particularly prone to suppression of error-induced extinction (Figure 2.3, Panel B). To reduce the rate of false positives, I performed SGA analysis in quadruplicate. *msh2Δ*

strains lack all MMR activity and fewer *eex* mutants are recovered in screens for *pol3-01 msh2Δ* suppression (Figure 2.3). Therefore, I screened for deletions that could suppress *pol3-01 msh2Δ* synthetic lethality based on the rationale that this combination would reveal the strongest mutator suppressors while reducing false positives.

To screen for deletions that suppress error extinction, I first crossed *msh2Δ* into the array, generating SGA strains that carried both *msh2Δ* and SGA deletions (*sgaΔ*) (Figure 3.1). Following creation of this modified array, I crossed a query strain harboring a *pol3-01* chromosomal mutation with the array and isolated *pol3-01 msh2Δ sgaΔ* haploid spores (Figure 3.1). Although laborious, sequential crosses were required because my previous experiments demonstrated that SGA analysis could not be performed using the shuffling protocol (data not shown). I performed four replicate screens by crossing four independent *pol3-01* strains with the modified SGA (Figure 3.1). *sgaΔ pol3-01 msh2Δ* spores that germinated and formed colonies each of four times were considered *eex* mutants, and the corresponding SGA deletions were considered candidate *eex* mutations. Using this strategy, I identified 40 candidate suppressors of *pol3-01 msh2Δ* synthetic lethality.

Using the list of candidate *eex* deletions, I picked each SGA strain with a candidate suppressor deletion from the modified SGA (*msh2Δ*) and generated a smaller array consisting only of candidate *sgaΔ msh2Δ* strains (Figure 3.2). To increase the rigor of candidate screens, the candidate array was pinned in duplicate so that quadruplicate matings with the candidate array would yield eight independent groups of spores (Figure 3.2). Crosses that resulted in viable *sgaΔ pol3-01 msh2Δ* spores each of eight times would be subject to further analysis. After performing SGA analysis of the candidate array, I observed only one SGA strain that resulted in viable spores for each of eight crosses (Figure 3.2). This strain was notated as harboring a *fes1* deletion. Fes1 is a nucleotide exchange factor localized to the endoplasmic reticulum (www.yeastgenome.org). The possible function of this

protein in DNA replication fidelity was puzzling, but Fes1 abundance has been shown to increase in response to DNA replication stress ((Kabani *et al.* 2002; Tkach *et al.* 2001). To test whether *fes1Δ* could suppress *pol3-01 msh2Δ* error-induced extinction, I constructed a *pol3Δ fes1Δ msh2Δ* strain with the essential *POL3* gene provided on a plasmid and used a plasmid shuffling strategy to introduce the *pol3-01* allele. I observed that *pol3-01 msh2Δ fes1Δ* cells are inviable, suggesting that deletion of Fes1 does not suppress error-induced lethality. Upon further investigation, we discovered that the strain designated as *fes1Δ* in the SGA actually contains no deletion of Fes1, but rather, has acquired spontaneous resistance to aminoglycosides (both nourseothricin and G418), which are used for selection during SGA analysis. Thus, it appears that no single SGA deletion is able to rescue *pol3-01 msh2Δ* synthetic lethality.

DISCUSSION

Synthetic Genetic Array (SGA) analysis has been used extensively to identify genetic interactions (Tong *et al.* 2001; Tong *et al.* 2004). Since approximately 80% of yeast genes are nonessential, SGA analysis can be used to probe the majority of the genome (Giaever *et al.* 2002; Winzeler *et al.* 1999). Combined defects in polymerase proofreading and MMR result in error-induced extinction in haploid yeast (Greene and Jinks-Robertson 2001; Herr *et al.* 2011a; Morrison *et al.* 1993), a lethality suppressed by antimutagenic polymerase variants and other unknown mutations (Figure 2.5) (Herr *et al.* 2011a). We used the Synthetic Genetic Array to comprehensively screen for deletions that suppress error-induced extinction. We failed to identify any single gene deletion that could suppress *pol3-01 msh2Δ* error-inducted extinction.

Two gene deletions have documented antimutator effects: *rev3Δ* and *dun1Δ* (Aksenova *et al.* 2010; Datta *et al.* 2000; Pavlov *et al.* 2001; Shcherbakova *et al.* 1996).

REV3 encodes the catalytic subunit of Pol ζ, which contributes to mutagenesis via error-prone replication past DNA lesions (Prakash and Prakash 2002). *DUN1* encodes a protein kinase that mediates damage-inducible gene expression and up-regulates dNTP synthesis during the S-phase checkpoint (Zhou and Elledge 1993). Why didn't these deletions suppress *pol3-01 msh2Δ* error-induced extinction in our screen? We similarly observed that *rev3Δ* does not suppress *pol2-4 msh2Δ* synthetic lethality (Figure 2.2). These data support the observation that Pol ζ does not extend most mismatches made by proofreading-deficient Pol δ or Pol ε (Figure 2.2, Figure 4.3) (Datta *et al.* 2000; Shcherbakova *et al.* 1996). *dun1Δ* reduces the mutator phenotype of *pol3-01* by 8-fold (Datta *et al.* 2000). Perhaps the mutator phenotype of *pol3-01 msh2Δ* requires a greater than 8-fold decrease in mutation rate to fall below the mutation threshold of error-induced extinction. Our previous studies demonstrated that a modest 3-fold reduction in mutation rate is sufficient to suppress *pol3-01 msh6Δ* error-induced extinction and *pol3-01,eex* alleles with a 10-fold suppressive effect are on the edge of survival when introduced to a *msh2Δ* background (Herr *et al.* 2011a). Alternatively, perhaps Msh2 is involved in antimutagenesis in a *pol3-01 dun1Δ* strain or Dun1 does not contribute to the formation of Pol δ mutations that Msh2 corrects.

The low rate of escape from *pol3-01 msh2Δ* error-induced extinction is a double-edged sword. It reduces the likelihood of false positives during screening, but precludes the detection of weak antimutators. It is entirely possible that deletions could suppress other allele combinations that result in error-induced extinction, such as *pol3-01 msh6Δ* or *pol2-4 msh2Δ*. Nevertheless, our data suggest that the strongest antimutator alleles may be gain-of-function mutations or hypomorphic alleles in essential genes, rather than null alleles of nonessential genes. Whole genome sequencing of spontaneous extragenic *eex* mutants will help us identify extragenic alleles involved in mutator suppression.

MATERIALS AND METHODS

Media and growth conditions

Standard media and growth conditions were used in the propagation of yeast strains (Sherman 2002). Cells were grown non-selectively using YPD or synthetic complete (SC) media with 2% dextrose. Selective growth was on SC media containing 2% dextrose and lacking the appropriate amino acid(s). Pre-formulated SC amino acid supplement was purchased from Bufferad, and supplements lacking defined amino acids were made from individual components as described (Sherman 2002). *URA3*-deficient cells were selected with 5-fluoroorotic acid (FOA, 1 mg/ml, Zymo Research) media (Boeke *et al.* 1984). Unless otherwise specified, reagents were purchased from Sigma-Aldrich or Fisher Scientific.

Query strain construction

Two query strains were constructed to cross into the array. The *msh2Δ* strain was constructed, as previously described in Chapter II, by transforming the *MATα* derivative of the BY4733 strain, also described in Chapter II Materials and Methods. The *pol3-01* query strain was constructed in the Y7092 background (Tong and Boone 2007). The Y7092 strain was transformed with a *pol3-01-URA3* integration plasmid digested with SalI (pAM26 (Morrison and Sugino 1993), kindly provided by Youri Pavlov of University of Nebraska) and transformants were selected on SC-URA. Sixteen transformants were picked and streaked onto SC-URA for further modification. To select for loss of the wild-type *POL3* allele, transformants were plated onto SC supplemented with 5-FOA (Boeke *et al.* 1984). After growth on 5-FOA media, restriction fragment length polymorphism analysis was performed to genotype the *pol3-01* allele as previously described (Herr *et al.* 2011a). Three correct clones were identified. *NAT1* (Stulemeijer *et al.* 2011) was then integrated upstream of *pol3* to make the *pol3-01* allele selectable. *pol3-01* strains were transformed with PCR products containing the *NAT1* gene and homology to the *pol3* locus (PCR template, primers and amplification

conditions: pFvL99 (Stulemeijer *et al.* 2011); NAT1intPOL3F, CACTCTTTCCATTGGCAGAGCGGATCCGCCAAATAGAAATTACATAAAACAAGTAATTTAGACATGGAGGCCCAGAATACCCT; NAT1intPOL3R, AAAAGTACTCGTAATTGTGATTCAATATATAATAAATATTTCGTACTCTGAAAAATAGCAGTATAGCGACCAGCATTCAC; 95°C, 1 min; 30x (95°C, 30 sec; 55°C, 30 sec; 72°C, 1 min); 72°C, 1 min.)

SGA analysis

SGA analysis was performed as detailed in the published protocol for Synthetic Genetic Analysis (Tong and Boone 2007), except for changes to the sporulation protocol. To improve sporulation (up to 15% efficiency), diploids were pinned onto pre-sporulation media (per liter: 10 g yeast extract, 20 g peptone, 20 g potassium acetate, 20 g agar) for two days at 30°C, then transferred to sporulation media (per liter: 1 g yeast extract, 10 g potassium acetate, 0.5 g glucose, 0.1 g of amino acid supplement, 20 g agar. Amino acid supplement: 1 g uracil, 1 g tryptophan, 1 g adenine, 1 g histidine, 3 g lysine, 4 g leucine.). Sporulation plates were incubated at 30°C for 5-7 days.

Figure 3.1

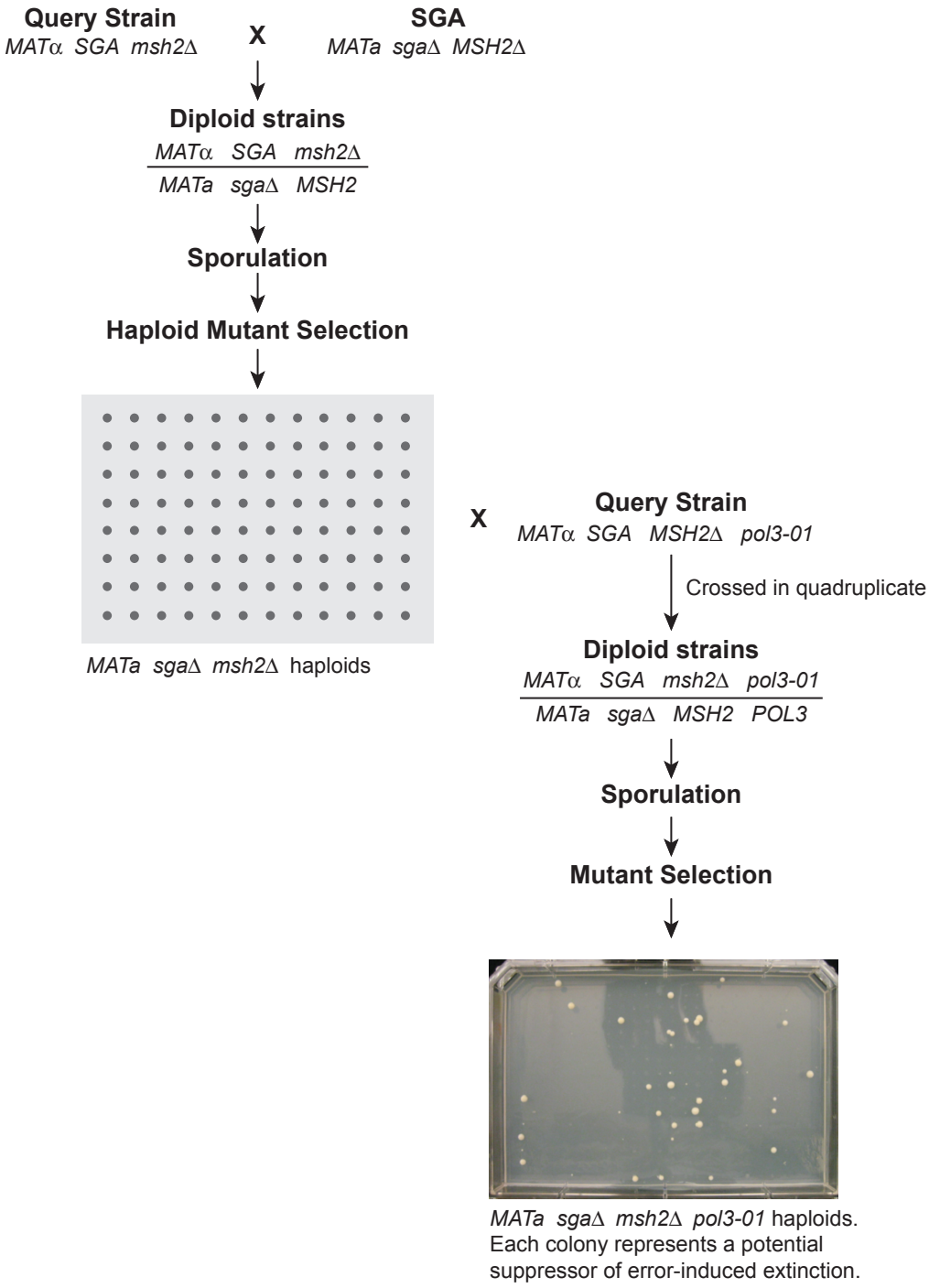
Query Strain
MATα SGA msh2Δ
X
SGA
MATa sgaΔ MSH2Δ
Diploid strains
MATα SGA msh2Δ
MATa sgaΔ MSH2
Sporulation
Haploid Mutant Selection
MATa sgaΔ msh2Δ haploids
X
Query Strain
MATα SGA MSH2Δ pol3-01
Crossed in quadruplicate
Diploid strains
MATα SGA msh2Δ pol3-01
MATa sgaΔ MSH2 POL3
Sporulation
Mutant Selection
MATa sgaΔ msh2Δ pol3-01 haploids.
Each colony represents a potential
suppressor of error-induced extinction.

Figure 3.1 Adapting the Synthetic Genetic Array (SGA) to screen for deletions that suppress error-induced extinction. A mismatch repair deletion (*msh2Δ*) and a Pol δ proofreading-deficient allele (*pol3-01*) were introduced to SGA strains in successive crosses. The final SGA analysis was performed in quadruplicate by crossing four independent *pol3-01* clones with the SGA. Deletions that suppress error-induced extinction should result in viable colonies in four separate replicate crosses.

Figure 3.2

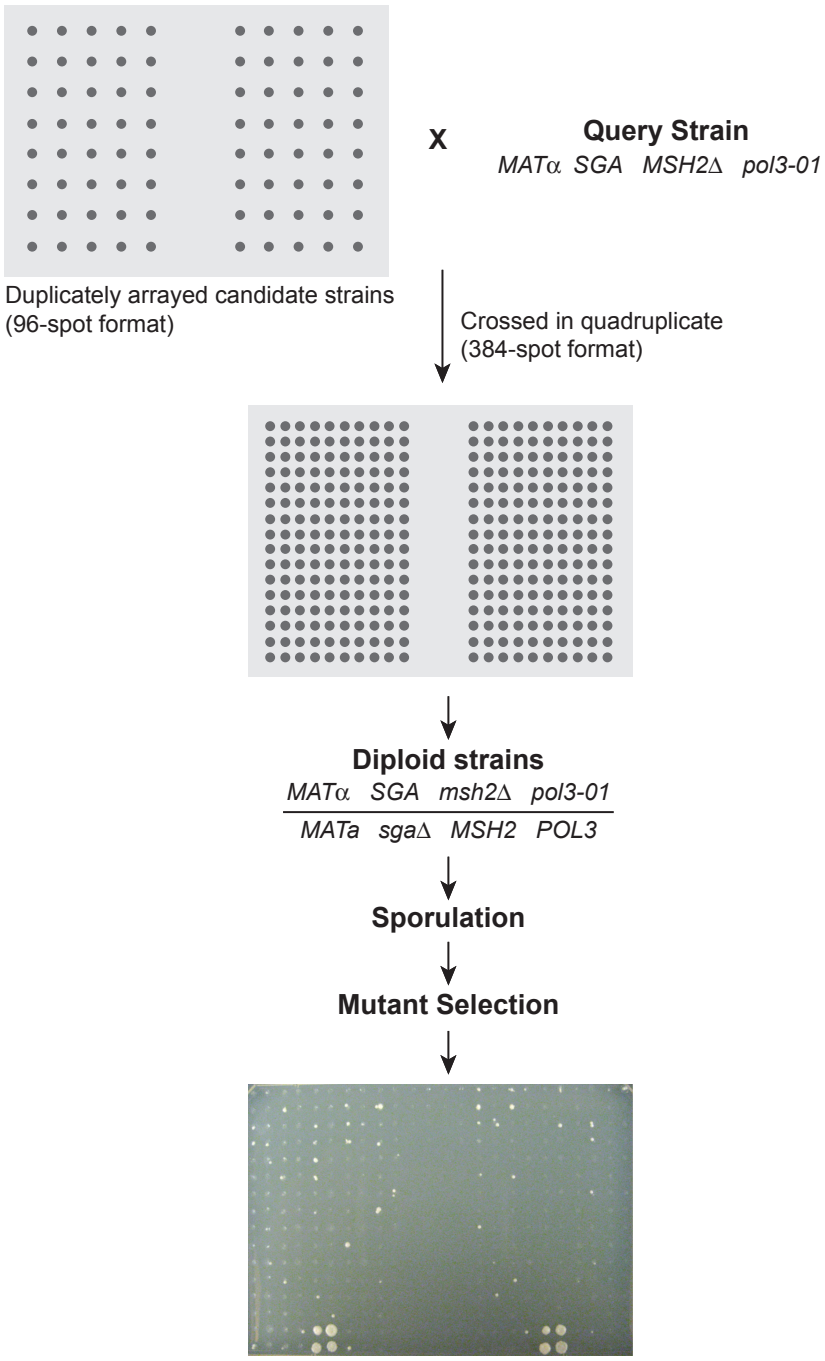
X
Query Strain
MATα SGA MSH2Δ pol3-01
Duplicately arrayed candidate strains
(96-spot format)
Crossed in quadruplicate
(384-spot format)
Diploid strains
MATα SGA msh2Δ pol3-01
MATa sgaΔ MSH2 POL3
Sporulation
Mutant Selection

Figure 3.2 Synthetic Genetic Array analysis of the candidate suppressor array. Candidate strains (*sgaΔ msh2Δ*) were arrayed in duplicate for final SGA analysis. Four independent Pol δ proofreading-deficient (*pol3-01*) strains were crossed to the candidate SGA in quadruplicate. Deletions that suppress error-induced extinction should result in viable colonies in all eight replicate analyses. Only one SGA candidate conferred viability in all eight crosses (bottom panel).

CHAPTER IV: DUN1-DEPENDENT MUTAGENESIS BY ERROR-PRONE DNA POLYMERASE ε VARIANTS

Yeast DNA polymerases (Pols) ε and δ perform the bulk of nuclear DNA replication. Both Pols are high-fidelity enzymes with intrinsic proofreading exonucleases that remove errors during DNA synthesis. *S. cerevisiae* strains defective for Pol δ or ε fidelity exhibit a 'mutator phenotype' characterized by increased rates of spontaneous mutation. Previous studies (Datta *et al.* 2000) demonstrated that the mutator phenotype of proofreading-deficient Pol δ depends on Dun1, a protein kinase that mediates damage-inducible gene expression and up-regulates dNTP synthesis during the S-phase checkpoint. Here, we show that mutator alleles of *POL2* (encoding Pol ε) are also Dun1-dependent. Deletion of *DUN1* (*dun1Δ*) suppressed the mutator phenotypes of *pol2-4* (encoding proofreading-deficient Pol ε) and *pol2-M644G* (encoding a Pol ε variant with altered base selectivity) 7- to 10-fold. Furthermore, *dun1Δ* rescued cells from lethal mutagenesis caused by combined defects in Pol ε proofreading and base selectivity (*pol2-4,M644G*) or Pol ε proofreading and mismatch repair (*pol2-4 msh2Δ*). The checkpoint effectors Mrc1 and Rad9 differentially influenced the checkpoint response to Pol ε errors; *mrc1Δ* weakly suppressed (2-fold) the mutator phenotypes of *pol2-4* and *pol2-M644G*, while *rad9Δ* had no effect on mutation rates. The *pol2-4* and *pol2-M644G* mutator phenotypes were unchanged in *rev3Δ* and *rad30Δ* cells, indicating that Pols ζ and η, respectively, do not extend mispairs in these strains. Surprisingly, the antimutator effect of *dun1Δ* was Mrc1-dependent, suggesting that fixation of Pol ε errors into heritable mutations occurs by more than one mechanism. Our findings, together with those of Datta *et al.*, suggest that Pol ε and Pol δ errors, or the mutator polymerases themselves, are sensed as stressors that trigger the Dun1 activation. We propose that Dun1-dependent elevation of dNTP pools feeds back and enhances mispair extension in an effort to maintain replication fork progression.

INTRODUCTION

Faithful genome transmission requires the cooperation of multiple DNA metabolic pathways. Expression of replication machinery and metabolic enzymes are tightly coupled with DNA replication to provide sufficient enzymes and DNA precursors to complete DNA synthesis. High-fidelity DNA polymerases ensure accurate genome duplication (reviewed in (McCulloch and Kunkel 2008)), while surveillance and repair of DNA damage occurs throughout the cell cycle . Furthermore, cell cycle checkpoints prevent the inheritance of incompletely replicated or damaged chromosomes (reviewed in (Paulovich and Hartwell 1995; Sancar *et al.* 2004). Defects in DNA replication enzymes or cell cycle checkpoint genes result in genomic instability, a hallmark of cancer cells.

In the budding yeast *Saccharomyces cerevisiae*, DNA polymerases (Pols) ε and δ perform the bulk of leading- and lagging-strand synthesis, respectively (Kunkel and Burgers 2008; Larrea *et al.* 2010; Nick Mcelhinny *et al.* 2008; Pursell *et al.* 2007; Shcherbakova and Pavlov 1996). Both enzymes synthesize DNA with extraordinary fidelity and possess exonuclease domains, whose proofreading activity improves fidelity 10-100 fold (Fortune *et al.* 2005; Morrison *et al.* 1991; Shcherbakova *et al.* 2003; Shimizu *et al.* 2002; Simon *et al.* 1991). Mismatch repair (MMR) further enhances faithful replication by targeting mismatches for excision from nascent DNA (reviewed in (Iyer *et al.* 2006). Thus, normal replication machinery can synthesize billions of basepairs without permitting a single mutation. Defects in Pol exonuclease activity, Pol fidelity, or MMR increase the spontaneous mutation rate, resulting in mutator phenotypes (Greene and Jinks-Robertson 2001; Morrison *et al.* 1991; Morrison and Sugino 1994; Simon *et al.* 1991; Tran *et al.* 1999b). Combinations of these defects result in a synergistic increase in mutation rate, suggesting that polymerase fidelity, proofreading and MMR act in series to prevent replication errors (Morrison *et al.* 1993; Nick Mcelhinny *et al.* 2006).

Eukaryotic MMR proteins suppress mutagenesis by facilitating the repair of replication errors (reviewed in (Iyer *et al.* 2006; Modrich 2006)). Heterodimers of MutS homologs (Msh2-Msh6 or Msh2-Msh3) recognize and bind mispaired bases, insertions and deletions. Subsequently, heterodimeric MutL complexes (Mlh1-Pms1 or Mlh1-Mlh3) are recruited to bound lesions. The MutL homologs Pms1 and Mlh3 contain a latent endonuclease activity that nicks the newly replicated strand, providing entry points for excision and re-synthesis (Kadyrov *et al.* 2006; Kadyrov *et al.* 2009). Absence of Msh2, the integral component of both MutS complexes, abrogates all MMR activity. Similarly, deletion of the gene encoding Mlh1 abolishes the formation of all MutL complexes, and thus, all MMR activity.

Haploid yeast cells that exceed a mutation rate threshold undergo error-induced extinction and cease colony formation after a few cell divisions (Herr *et al.* 2011a; Morrison *et al.* 1993). In previous studies, we observed that error-induced extinction results from combined defects in Pol ε proofreading and MMR (Figure 2.1). The *pol2-4* allele, encoding proofreading-deficient Pol ε, is lethal in strains lacking all MMR activity (*msh2Δ, mlh1Δ, msh6Δ msh3Δ,* and *pms1Δ mlh3Δ*). Error-induced extinction was surmounted by mutations affecting the Pol ε catalytic subunit, as well as by unidentified antimutator mutations elsewhere in the genome. Mutants harboring these unidentified mutations constituted the vast majority (96%) of strains that escape Pol ε error-induced extinction, providing tantalizing evidence that factors other than Pol ε and MMR influence leading-strand replication fidelity (Table 2.1).

Cells modulate DNA replication activity during the cell cycle in response to replication blocks or DNA damage by triggering checkpoint signaling cascades (reviewed in (Navadgi-Patil and Burgers 2009; Rouse and Jackson 2002). Single-stranded DNA and double-strand breaks are recognized by sensors, which then trigger effecter kinases that propagate the checkpoint signal and activate an array of target proteins that arrest cell cycle progression,

stabilize replication forks and induce DNA repair. The S-phase checkpoint has two branches: a Mec1-dependent branch activated in response to single-stranded DNA and a Tel1-dependent branch activated by double-strand breaks. Two checkpoint 'mediators' further divide the Mec1-dependent branch (Figure 4.1). Replication stress induced by treatment with hydroxyurea, an inhibitor of dNTP synthesis, is mediated through Mrc1, a Pol ε-associated protein that travels with the replication fork (Alcasabas *et al.* 2001), while Rad9 responds to multiple DNA damage inputs in conjunction with the 9-1-1 complex. The 9-1-1 DNA damage complex, composed of Ddc1-Rad17-Mec3, resembles PCNA and is loaded onto RPA-coated single-stranded DNA resulting from replication stress and DNA damage (Zou *et al.* 2003). Additionally, both S-phase checkpoint pathways signal through Rad53 (mammalian Chk2), which mediates the checkpoint response by activating various targets (Huang *et al.* 1998c; Tercero and Diffley 2001; Zhao and Rothstein 2002) (Figure 4.1). Thus, two S-phase checkpoint signaling pathways, defined by Mrc1 and Rad9, mediate Mec1 activation of Rad53. Whereas Mrc1 only mediates S-phase checkpoint activation, Rad9 can also trigger the G2/M checkpoint by activating Chk1.

Dun1 is a Rad53 target that modulates dNTPs pools by controlling negative regulators of ribonucleotide reductase (RNR), the enzyme responsible for dNTP synthesis (Reichard 1988b; Zhou and Elledge 1993) (Figure 4.1). In budding yeast, the RNR holoenzyme contains a large Rnr1 homodimeric subunit, and a small dimeric subunit of Rnr2 and Rnr4 ((Chabes *et al.* 2000; Elledge and Davis 1987; Elledge and Davis 1990; Huang and Elledge 1997)). A minor isoform contains Rnr3 instead of Rnr1 in the large subunit (Elledge and Davis 1990). Dun1 targets three proteins that repress transcription, assembly and activity of RNR. Crt1 represses transcription of *RNR2, RNR3* and *RNR4* (Elledge and Davis 1990; Huang and Elledge 1997; Huang *et al.* 1998c). Dif1 prevents RNR assembly by mediating import of Rnr2-Rnr4 into the nucleus, where it is sequestered from Rnr1 (Lee *et al.* 2008; Wu and Huang 2008; Zhao and Rothstein 2002). Sml1 binds and inhibits RNR activity.

Phosphorylation of Sml1 and Dif1 results in their proteolysis, releasing the negative regulation of RNR catalysis and allowing cytoplasmic localization of Rnr2 and Rnr4, followed by RNR holoenzyme assembly (Lee *et al.* 2008; Wu and Huang 2008; Zhao and Rothstein 2002). At the same time, phosphorylation of Crt1 increases transcription of *RNR2, RNR3* and *RNR4*. A separate damage-inducible system controls *RNR1* transcription (Tsaponina *et al.* 2011). Overall, dNTP pools increase 6- to 8-fold during the DNA damage response (Chabes *et al.* 2003a). Intriguingly, mutants of the checkpoint proteins Mec1 and Rad53 are inviable, but rescued by deletions of *SML1*, *DIF1*, or *CRT1*, or over-expression of RNR subunits. Thus, regulation of dNTP pools is the essential function of the Mec1-Rad53-Dun1 pathway (Desany *et al.* 1998; Huang *et al.* 1998c; Lee *et al.* 2008; Zhao *et al.* 1998).

Mec1 and Rad53 are the homologs of human ATR and Chk2, respectively, and link checkpoint control to human disease (Cimprich *et al.* 1996; Matsuoka *et al.* 1998). ATR and Chk2 both act upstream of p53 (reviewed in (Navadgi-Patil and Burgers 2009; Zegerman and Diffley 2009)), a tumor suppressor mutated in more than 50% of cancers (Zhou and Elledge 2000). The p53 tumor suppressor activates expression of the mammalian RNR enzyme p53R2 in response to DNA damage (Guittet *et al.* 2001; Tanaka *et al.* 2000; Yamaguchi *et al.* 2001a). Thus, increased dNTP synthesis is an evolutionarily conserved feature of checkpoint activation.

The abundance and relative concentration of dNTPs modulates the fidelity of DNA synthesis. In the presence of fork-blocking lesions, increased dNTP pools facilitate lesion bypass and S-phase progression (Chabes *et al.* 2003a; Zhou and Elledge 1993). Interestingly, increased dNTP concentration confers resistance to UV and the UV mimetic 4-NQO, but not gamma radiation, suggesting that while amplified dNTP pools alleviate replication blocks, they do no resolve double-strand breaks (Chabes *et al.* 2003a). But the ability to bypass replication barriers is not without consequences. Imbalanced or increased dNTP concentrations reduce the fidelity of DNA synthesis *in vitro* and *in vivo* (Fersht 1979;

Weymouth and Loeb 1978). *In vivo*, dNTP imbalances increase mutation rates up to 14-fold over wild type (Kumar *et al.* 2011). The majority of mutations are single base pair substitutions and small insertions or deletions, consistent with DNA polymerase misincorporations (Kumar *et al.* 2011). Even a modest 2-fold increase in dNTP pools confers a mutator phenotype (Chabes *et al.* 2003a). Mammalian cell lines with altered dNTP pools also display a mutator phenotype (Caras and Martin 1988) and transfection of a mouse RNR allele lacking allosteric feedback inhibition increases the mutation rate of cell lines 15- to 25-fold (Weinberg *et al.* 1981).

A previous study observed that the mutator phenotype of proofreading-deficient Pol δ (encoded by the *pol3-01* allele) is partially Dun1-dependent (Datta *et al.* 2000). Deletion of *DUN1* decreased the *pol3-01* mutation rate eight-fold. Datta *et al.* reported that *pol3-01* causes an S-phase progression defect and proposed that mutagenic repair during the checkpoint generates the *pol3-01* mutator phenotype. They hypothesized that *dun1Δ* suppresses mutations by altering DNA repair functions. In the same study, the mutator phenotype of proofreading-deficient Pol ε (encoded by the *pol2-4* allele) was unaffected by the absence of Dun1. This result is surprising, given the role of Pol ε in mediating the S-phase checkpoint (Araki *et al.* 1995; Dua *et al.* 1998; Dua *et al.* 1999; Lou *et al.* 2008; Navas *et al.* 1996; Navas *et al.* 1995; Puddu *et al.* 2011). However, the weak *pol2-4* mutator phenotype observed in this study may have limited the ability to detect a decrease in mutation rate in *dun1Δ* strains.

In the present study, we show that mutator alleles of *POL2* (encoding Pol ε) are also Dun1-dependent (Figure 4.2). Deletion of *DUN1* suppressed the mutator phenotypes of *pol2-4* and *pol2-M644G* (encoding a Pol ε variant with altered base selectivity) 7- to 10-fold (Figure 4.2, Table 4.1). Furthermore, *dun1Δ* rescued cells from error-induced extinction caused by combined defects in Pol ε proofreading and base selectivity (*pol2-4,M644G*) or Pol

ε proofreading and mismatch repair (*pol2-4 msh2Δ*) (Figure 4.2). The *pol2-4* and *pol2-M644G* mutator phenotypes were unchanged in *rev3Δ* and *rad30Δ* cells, indicating that Pols ζ and η, respectively, do not extend replication errors in these strains (Figure 4.3). *pol2-M644G* cells displayed slow S-phase progression and increased *RNR* induction (Figure 4.4 and 4.5) while *po2-4* cells did not, suggesting that Dun1 activity may not be limited to the S-phase checkpoint. Mrc1 and Rad9 differentially influenced the checkpoint response to Pol ε errors; *mrc1Δ* weakly suppressed (2-fold) the mutator phenotypes of *pol2-4* and *pol2-M644G*, while *rad9Δ* had no effect on mutation rates (Figure 4.6). Our findings, together with those of Datta *et al.*, suggest that mutator polymerases or their errors are sensed as replication stressors that trigger Dun1 activation. We propose that Dun1-dependent elevation of dNTP pools enhances mispair extension by replicative DNA polymerases, ensuring continued DNA replication, but also mutagenesis.

RESULTS

Deletion of Dun1 suppresses Pol ε replication errors

To determine the effect of *dun1Δ* on mutator phenotypes, we compared the mutation rates of *pol2-4* and *pol2-M644G* in *DUN1* and *dun1Δ* strains. We observed that the *pol2-4* and *pol2-M644G* alleles increased mutation rates 7- and 13-fold, respectively (Figure 4.2, Panel A and Table 4.1). In contrast, the mutation rates of the *pol2-4 dun1Δ* and *pol2-M644G dun1Δ* strains were indistinguishable from *POL2 DUN1* wild-type strains. Thus, *dun1Δ* suppresses the mutator phenotypes of the *pol2-4* and *pol2-M644G* alleles.

Haploid yeast strains with combined defects in DNA polymerase proofreading and MMR succumb to error extinction and fail to form colonies (Greene and Jinks-Robertson 2001; Herr *et al.* 2011a; Morrison *et al.* 1993; Morrison and Sugino 1992; Sokolsky and Alani 2000; Tran *et al.* 1999b). In screens to isolate mutants that escape Pol ε error-induced

extinction, 96% of suppressors harbored unknown mutations extragenic to *pol2* (Table 2.1). Since *dun1Δ* suppresses the mutator phenotype of *pol2-4*, we predicted that *dun1Δ* would confer escape from *pol2-4 msh2Δ* error extinction. To test this, we introduced the *pol2-4* allele into *msh2Δ dun1Δ* strains. We observed that *pol2-4 msh2Δ dun1Δ* strains are viable, though they have reduced colony-forming capacity compared to wild type (Figure 4.2, Panel B). Additionally, when *pol2-4* was introduced into *msh6Δ dun1Δ* cells, we found the *dun1Δ* mutation rescued the synthetic sick phenotype of *pol2-4 msh6Δ* (Figure 4.2, Panel B).

Substitution of M644 with glycine in the Pol ε active site produces a 3- to13-fold increase in mutation rate ((Pursell *et al.* 2007), Figure 4.2, Panel B and Table 1). Biochemical characterization indicates that the *pol2-M644G* allele encodes a Pol ε variant that retains 44% of wild type polymerase activity and a fully active exonuclease domain (Pursell *et al.* 2007). Mutation of the corresponding residue in the Pol δ active site is lethal in strains that also lack Pol δ proofreading (Venkatesan *et al.* 2005) (Herr *et al.*, unpublished data). This lethality is suppressed by antimutator variants of Pol δ, suggesting it results from error-induced extinction (Herr *et al.*, unpublished data). Similarly, we observed that *pol2-M644G* is synthetically lethal with the *pol2-4* allele (Figure 4.2, Panel B). Since the likely cause of this lethality is error extinction, we tested whether *pol2-4,M644G* lethality is suppressed by *dun1Δ* and found that *dun1Δ* confers survival in the presence of *pol2-4,M644G* (Figure 4.2, Panel B). The *pol2-4,M644G dun1Δ* strain had a mutation rate 23-fold above wild type (Figure 4.2 and Table 4.1), suggesting that not all errors resulting from the *pol2-4,M644G* allele are Dun1-dependent.

Mismatch repair has been implicated in checkpoint activation (Reha-Krantz *et al.* 2011) and cells with checkpoint defects are more sensitive to DNA damage. Thus, we examined the effect of *dun1Δ* on the mutator phenotypes of *pol2-4* and *pol2-M644G* in a MMR-deficient background. As *msh6Δ* is not synthetically lethal with either allele, we

measured *pol2-4 msh6Δ* and *pol2-M644G msh6Δ* mutation rates with and without Dun1. We found *dun1Δ* reduces the mutation rates of these strains only 2- to 3-fold (Figure 4.2, Panel C and Table 1), indicating that only 50-70% of mutations are Dun1-dependent in an MMR-deficient background. This suggests that MMR may mediate Dun1 activation in response to Pol ε errors.

pol2-4 and pol2-M644G mutator phenotypes are not Pol ζ or Pol η dependent

Error-prone synthesis by Pols ζ and η allows bypass of replication-blocking DNA lesions (Prakash and Prakash 2002). Additionally, the mutator phenotype of several DNA mutants is dependent on Pol ζ (Aksenova *et al.* 2010; Kai and Wang 2003; Northam *et al.* 2006; Northam *et al.* 2010; Pavlov *et al.* 2001; Shcherbakova *et al.* 1996). We hypothesized that the mutator phenotypes of *pol2-4* and *pol2-M644G* might be due to mispair extension by Pols ζ or η. To test this, we engineered strains lacking Pol ζ (*rev3Δ*) or Pol η (*rad30Δ*) and measured the mutation rates of *pol2-4* and *pol2-M644G* in these strains. We found that the *pol2-4* and *pol2-M644G* mutator phenotypes were not significantly affected by Pol ζ or Pol η (Figure 4.3, Table 4.1). This suggests that neither Pol ζ nor Pol η is responsible for mismatch formation in these mutator strains.

Cell cycle progression of Pol ε mutator strains

The *pol3-01* allele confers a delayed progression through S-phase that is rescued by *dun1Δ* (Datta *et al.* 2000). To determine whether Pol ε mutator alleles elicit similar S-phase defects, the cell cycle progression of *pol2-4* and *pol2-M644G* strains was monitored by fluorescence-activated cell sorting (FACS). The cell cycle kinetics of the *pol2-4* strain are indistinguishable from wild-type (Figure 4.4). The *dun1Δ* and *pol2-4 dun1Δ* strains both delay initiation of S-phase (Figure 4.4), but appear to divide at the same time as wild type. The

delay in replication initiation in *dun1Δ* strains has been previously observed (Zhao and Rothstein 2002). The *pol2-M644G* strain progresses more slowly though S-phase, finally completing S-phase and dividing 30 minutes later than wild-type. *dun1Δ* exacerbates the *pol2-M644G* S-phase progression defect, extending the S-phase another 15 minutes (Figure 4.4). The majority of asynchronously-dividing cells collected in the log phase samples of the *pol2-M644G* and *pol2-M644G dun1Δ* strains were in S-phase, further demonstrating the cell cycle defects of these mutants. These data suggest the *pol2-M644G* allele, but not *pol2-4*, confers an S-phase progression defect and that deletion of *dun1Δ* aggravates, rather than rescues, the *pol2-M644G* S-phase defect.

To complement the cell cycle studies, we measured the log-phase doubling times of each strain using a precision incubator and growth-monitoring instrument (Bioscreen C MBR). The *dun1Δ* strain has the same growth rate as wild-type (Figure 4.4). The *pol2-4* and *pol2-M644G* strains both have significantly longer doubling times compared to wild-type, at 100 and 115 minutes, respectively. Interestingly, the *dun1Δ* deletion restores the doubling time of the *pol2-4* strain to 90 minutes. In contrast, *dun1Δ* increases the doubling time of the *pol2-M644G* strain to 130 minutes (Figure 4.4).

pol2-M644G, but not pol2-4, induces the expression of RNR1 and RNR3

Since the mutator phenotypes of *pol2-4* and *pol2-M644G* are Dun1-dependent, we expected the S-phase checkpoint to be activated in response to both alleles. Increased expression of RNR-encoding genes is an indicator of checkpoint activation (Elledge and Davis 1990; Huang *et al.* 1998c). *RNR1* expression is independent of Dun1 activity and induced up to 5-fold during checkpoint activation (Elledge and Davis 1990; Tsaponina *et al.* 2011). *RNR3* induction is induced up to 100-fold during checkpoint activation (Elledge and Davis 1990). While initially thought to be Dun1-dependent (Huang *et al.* 1998c), *RNR3*

induction occurs in the absence of Dun1 (Davidson *et al.* 2012). To investigate the checkpoint response to Pol ε mutations, we measured *RNR1* and *RNR3* transcript levels in *pol2-4* and *pol2-M644G* mutant strains. Increased levels ($P \leq 0.05$) of *RNR1* and *RNR3* were detected in *pol2-M644G* cells, but neither transcript was increased in *pol2-4* cells (Figure 4.5) suggesting that the S-phase checkpoint is activated in response to *pol2-M644G*, but not *pol2-4*. However, *RNR3* induction in *pol2-M644G* cells compared to the HU-treated cells is significantly lower. Increased levels of *RNR1* or *RNR3* were detected *pol2-4 dun1Δ* and *pol2-M644G dun1Δ* strains. Surprisingly, increased *RNR1* transcripts were also detected in *dun1Δ* cells, suggesting that loss of Dun1 is sufficient to activate the S-phase checkpoint (Figure 4.5). This is consistent with the delayed S-phase initiation observed in *dun1Δ* strains (Figure 4.4) (Zhao and Rothstein 2002).

The role of Mrc1 and Rad9 in sensing Pol ε mutations

Mrc1 and Rad9 define two pathways of Mec1-activation that respond to stalled replication forks and DNA damage, respectively (Alcasabas *et al.* 2001; Paulovich *et al.* 1997). A polymerase error has the potential to generate either signal type. Polymerases inefficiently extend mispaired primer termini into duplex DNA; a polymerase paused at a mispair would stall a replication fork. Mismatches that are incorporated into duplex DNA are processed by MMR to generate single-stranded DNA, recognized as DNA damage (Reha-Krantz *et al.* 2011). Stalled forks that fail to resume synthesis accumulate abnormal DNA structures as the result of fork collapse (Lopes *et al.* 2001). These possibilities can be distinguished genetically because Mrc1 and Rad9 respond to different lesions. We introduced *pol2-4* and *pol2-M644G* into strains lacking Mrc1 or Rad9 (Figure 4.6) to determine which factor mediates Dun1 activation in response to error-prone Pol ε alleles. We found that *mrc1Δ* and *rad9Δ* strains expressing mutator Pol ε alleles are viable, although

mrc1Δ strains are slow growing. We also tested the requirement of Dun1 in *mrc1Δ* and *rad9Δ* strains and observed that *pol2-M644G mrc1Δ dun1Δ* strains are slow growing and display reduced colony-forming capacity, while the *pol2-M644G rad9Δ dun1Δ* cells are inviable (Figure 4.6, Panel A). Thus, Mrc1 and Rad9 checkpoint responses promote survival of *pol2-M644G dun1Δ* cells. This suggests that in the absence of Dun1, stalled replication forks and DNA damage accumulate in *pol2-M644G* cells and that the DNA damage checkpoint, but not the replication checkpoint, is required to maintain viability.

If Mrc1 or Rad9 mediates the Dun1 stimulation of Pol ε mutators, the corresponding deletion mutations should suppress *pol2-4* and *pol2-M644G* mutation rates. The absence of Mrc1 dampens the Pol ε mutator phenotypes approximately 50-70% (Figure 4.6, Panel B), consistent with Mrc1 contributing to Dun1-dependent mutagenesis. In contrast, *rad9Δ* had no effect on mutation rates of *pol2-4* or *pol2-M644G* (Figure 4.6, Panel C and Table 1). Thus, the stimulatory effect of Dun1 on mutation rates requires Mrc1 and not Rad9.

The failure of *mrc1Δ* to lower mutation rates to the same extent as *dun1Δ* could mean that another pathway of Dun1 activation exists. Alternatively, *mrc1Δ* may synergize independently with the Pol ε mutators at the same time it suppresses the stimulation by Dun1. To distinguish between these hypotheses, we determined whether *dun1Δ* was epistatic to *mrc1Δ* with respect to mutation rates. *POL2 mrc1Δ dun1Δ* strains display a weak mutator phenotype (3-fold over wild-type) (Figure 4.6, Panel B and Table 4.1). In the presence of *pol2-4* or *pol2-M644G,* the *mrc1Δ dun1Δ* mutator phenotype increases 10- and 26-fold above the corresponding *dun1Δ* strains (Figure 4.6, Panel B and Table 4.1). In contrast, in *POL2 rad9Δ dun1Δ* and *pol2-4 rad9Δ dun1Δ* strains display no difference in mutation rate compared to the corresponding *dun1Δ* strains (Figure 4.6, Panel C and Table 4.1). Thus, Mrc1 likely augments Pol ε mutator phenotypes by activating Dun1. The

absence of Mrc1 also augments Pol ε mutator phenotypes, but in a Dun1-independent manner.

DISCUSSION

The eukaryotic cell cycle program safeguards genomic information during DNA replication and division through checkpoints that arrest cell cycle progression in response to DNA damage or replication stress. The Dun1 kinase promotes recovery from DNA damage as part of the S-phase checkpoint by elevating intracellular dNTP pools, which enables polymerases to bypass lesions that would otherwise prevent completion of DNA replication. Elevated dNTP pools increase mutation rates in WT cells. A single study found that Dun1 augmented the mutator phenotype of proofreading-deficient Pol δ, but not proofreading-deficient Pol ε (Datta *et al.* 2000). We wished to determine whether checkpoint activation was truly Pol δ-specific. Therefore, we re-examined the influence between the checkpoint and Pol ε with a broader range of *pol2* mutator alleles.

Here, we report that elimination of Dun1 suppresses the mutator phenotypes of Pol ε proofreading deficiency (encoded by *pol2-4*) or error-prone synthesis (encoded by *pol2-M644G*) and rescues cells from Pol ε error-induced extinction (Figure 4.2). We show that although the *pol2-4* and *pol2-M644G* mutator phenotypes depend on Dun1, only cells expressing *pol2-M644G* transit the S-phase more slowly than WT (Figure 4.4) and exhibit induction of RNR genes (Figure 4.5). The mutator phenotypes of *pol2-4* and *pol2-M644G* are unchanged in cells lacking the translesion synthesis polymerases, Pol ζ or Pol η (Figure 4.3) suggesting that Dun1 influences Pol ε fidelity directly. Lastly, we show that elimination of the Mrc1 checkpoint mediator, but not the Rad9 mediator, suppresses the Pol ε mutator phenotypes (Figure 4.6). Together our findings suggest that Pol ε mutators trigger Dun1

activation through Mrc1, and that Dun1 activation enhances extension of mispaired primer termini by Pol ε mutators.

Error-prone Pol ε replication and the Dun1 kinase

Dun1 was first identified as a regulator of damage-inducible *RNR3* transcription (Zhou and Elledge 1993). Since then it has become one of the most well-characterized targets of the S-phase checkpoint (Allen *et al.* 1994; Andreson *et al.* 2010; Chen *et al.* 2010; Elledge *et al.* 1993; Lee *et al.* 2008; Myung *et al.* 2001; Tsaponina *et al.* 2011; Zhao and Rothstein 2002). In our studies, we found that deletion of *dun1* suppressed the mutator phenotypes of *pol2-4* and *pol2-M644G* between 7- to 10-fold (Figure 4.2, Panel B). Moreover, *dun1Δ* rescued cells from lethal mutagenesis caused by combined defects in Pol ε proofreading and base selectivity (*pol2-4,M644G*) or Pol ε proofreading and mismatch repair (*pol2-4 msh2Δ*) (Figure 4.2, Panel A). The sheer magnitude of random mutations required to extinguish cell populations suggests that Dun1 enhances error-prone replication by Pol ε. We favor a model where Dun1 increases dNTP pools, thereby enhancing the ability of mutator Pol ε to extend mispairs. The mutation rates of *pol2-4* and *pol2-M644G* were suppressed only 2- to 3-fold in an *msh6Δ* strain (Figure 4.2, Panel C). Given recent studies demonstrating MMR involvement in S-phase checkpoint activation, Dun1 may be only partially activated in *msh6Δ* cells (Reha-Krantz *et al.* 2011). Alternatively, Dun1-dependent and Dun1-independent Pol ε errors may be corrected by MMR with difference efficiencies, so that Dun1-dependent Pol ε errors are disproportionately represented until MMR is eliminated.

REV3 and *RAD30* encode the catalytic subunits of lesion bypass Pols ζ and η, respectively. Pol ζ is responsible for most spontaneous mutations in wild type cells (Lawrence and Christensen 1979; Quah *et al.* 1980), as well as the mutator phenotypes of various mutator alleles (Aksenova *et al.* 2010; Pavlov *et al.* 2001; Shcherbakova *et al.* 1996).

The mutator phenotypes of *pol2-4* and *pol2-M644G* are not affected by deletions of either *rev3* or *rad30* (Figure 4.3), suggesting that error-prone Pol ε variants extend their own mispairs. Pol ε can bypass DNA lesions with greater efficiency in the presence of amplified dNTP pools (Sabouri *et al.* 2008). These findings are consistent with a model where activated Dun1 enhances Pol ε mispair extension by augmenting dNTP pools.

pol2-4 cells progress normally through the cell cycle (Figure 4.4) and do not induce *RNR1* or *RNR3* transcription (Figure 4.5), indicators of S-phase checkpoint activation. In contrast, *pol2-M644G* cells progress slowly though S-phase, dividing 30 minutes later than wild-type cells (Figure 4.4) and exhibit increased *RNR1* and *RNR3* transcription (Figure 4.5). These data suggest that *pol2-M644G* cells activate the S-phase checkpoint, while *pol2-4* cells do not. The lower specific activity of the *pol2-M644G* allele (only 45% of wild-type) reported by Pursell *et al.* (Pursell *et al.* 2007) offers one explanation for these differences. A slower polymerase might stall replication forks, or cause increased singled-stranded DNA due to slow polymerization. Interestingly, while Pursell *et al.* reported no growth defect of *pol2-M644G* cells, we find an increased doubling time of 25 minutes relative to wild-type (Figure 4.4, bottom). Differences in growth conditions or genetic background may explain these inconsistencies.

Datta *et al.* noted that *dun1Δ* rescues cell cycle defects of *pol3-01*. In contrast, we observed that *dun1Δ* exacerbated the S-phase progression defects of *pol2-M644G,* suggesting that the presence of Dun1 in *pol2-M644G* strains aids S-phase progression. We also found that *dun1Δ* caused an S-phase initiation delay in the *pol2-4* strain (Figure 4.4). *dun1Δ* also appears to be sufficient for checkpoint activation itself, and elevates *RNR* gene transcription in the *pol2-4* strain. The absence of Dun1 decreased the viability of *pol2-M644G* strains by half in plating efficiency experiments. We interpret this to mean that without enhanced extension of polymerase errors, more deleterious lesions form (Lopes *et al.*

2001). In support of this interpretation, elevated dNTP pools suppress hyper-recombination in S-phase checkpoint mutants (Fasullo *et al.* 2010). Additionally, the viability of a *mec1* mutant is reduced by a *rad52* mutation, defective in homologous recombination, suggesting that destabilization of the replication fork generates lesions subject to recombination (Fasullo *et al.* 2010).

The observation that *pol2-4* does not trigger the checkpoint, but is subject to Dun1-dependent mutagenesis (Figure 4.2, Figure 4.4, Figure 4.3), suggests that Dun1 activation may occur outside of the S-phase checkpoint. Two lines of evidence further suggest that Dun1 is important during an unperturbed S-phase. First, *dun1Δ* mutants are slow to initiate DNA replication (Figure 4.4) (Zhao and Rothstein 2002). Secondly, deletion of any one of three Dun1 targets (*SML1, DIF1* or *CRT1)* restores viability of *mec1* and *rad53* mutants (Desany *et al.* 1998; Huang *et al.* 1998c; Lee *et al.* 2008; Zhao *et al.* 1998). This could support a role for Dun1 activation as a rheostat of dNTP pools. Since dNTP pools are paramount for the progression of the replication fork, it may be that this important function can be triggered without the activation of the S-phase checkpoint. Alternatively, only a subset of *pol2-4* cells, below our level of detection, activate the checkpoint, leading to a transient mutator phenotype.

Role of Dun1 in stabilizing the replication fork

To further investigate the nature of *pol2-4* and *pol2-M644G* mutagenesis, we introduced these mutator alleles to strains with Mrc1 and Rad9 deletions. Mrc1 is thought to stabilize the replication fork, and sense replication stress (Alcasabas *et al.* 2001; Lou *et al.* 2008; Reha-Krantz *et al.* 2011). We find that deletion of Mrc1 weakly suppresses the mutator phenotypes of *pol2-4* and *pol2-M644G* (Figure 4.6). We interpret this to mean that Mrc1 mediates Dun1 mutagenesis, in conjunction with another unknown pathway. Unexpectedly, *mrc1Δ dun1Δ* double mutants exhibit a modest mutator phenotype (2- to 3-fold) in the

absence of any error-prone polymerases. The *mrc1Δ dun1Δ* mutator phenotype increases the *pol2-4* and *pol2-M644G* mutator phenotypes in a more than additive fashion, relative to the *dun1Δ* background, suggesting that the absence of Mrc1 augments mutagenesis in *POL dun1Δ* cells (Figure 4.6, Panel B). This supports a role for both Mrc1 and Dun1 in replication fork stability. In our model, Mrc1 and Dun1 act together to stabilize the replication forks by triggering increased dNTPs that allow Pol ε to extend its own replication errors. In the absence of Mrc1 and Dun1, replication fork collapses trigger Rad9-dependent mechanisms of mutagenic replication.

Deletion of *rad9* did not affect the *pol2-4* or *pol2-M644G* mutator phenotypes, so Rad9 is not involved in Dun1-dependent mutagenesis. This suggests that *pol2-4* and *pol2-M644G* cause replication stress rather than DNA damage, as Rad9 mediates the DNA damage checkpoint (Paulovich *et al.* 1997; Reha-Krantz *et al.* 2011). In the absence of *rad9* and *dun1*, the *pol2-4* mutation rate is still suppressed (Figure 4.6, Panel C). However, the *pol2-M644G rad9Δ dun1Δ* strain is lethal (Figure 4.6, Panel A). Thus, without Dun1, replication stress caused by *pol2-M644G* may lead to catastrophic fork collapse. Though Mrc1 is present, its ability to mediate the checkpoint is limited (Figure 4.6, Panel B), or perhaps the most damaging lesions are not Mrc1 dependent. In absence of fork-stabilizing Dun1-mutagenesis and Rad9, cells accumulate collapsed replication forks, but don't arrest in the S-phase or G2 and enter mitosis with unreplicated DNA or broken chromosomes.

In conclusion, our studies demonstrate that the mutator phenotype of error-prone Pol ε is Dun1-dependent (Figure 4.2). We hypothesize that Pol ε misincorporations activate Dun1, which augments dNTP synthesis to enhance Pol ε mispair extension. This cycle is mutagenic but allows replication fork progression. Future studies will determine whether Dun1 activation is strictly limited to the S-phase checkpoint. Overall, our studies suggest a complex interplay between dNTP pools and replication fidelity. A balance must be stuck to

maintain the highest possible DNA replication fidelity and the ability to promote fork progression during replication stress.

MATERIALS AND METHODS

Media and growth conditions

Standard media and growth conditions were used to culture yeast strains (Sherman 2002). Cells were propagated non-selectively on YPD or synthetic complete (SC) media. Prototrophic clones were selected on SC lacking the appropriate amino acid(s). Pre-formulated SC supplement was purchased from Bufferad and amino acid-limited supplements were mixed from individual amino acids as described (Sherman 2002). Cells lacking *URA3* were selected with media containing 5-fluorootic acid (FOA, 1 mg/mL, Zymo Research) (Boeke *et al.* 1984). *can1* mutants were selected on SC lacking arginine and containing 50 μg/mL of canavanine. Unless otherwise specified, reagents were purchased from Sigma-Aldrich or Fischer Scientific.

Yeast plasmids and strain construction

POL2 plasmids. CEN6/ARS4 plasmids containing *POL2* (*URA3*) and *pol2-4* (*LEU2*) were made as described in Chapter II. The *pol2-M644G* (*LEU2*) plasmid was engineered similarly to *pol2-4*, using the QuikChange protocol (Wang and Malcolm 1999) with the following PCR conditions: Phusion polymerase (New England Biolabs), 95°, 1 min; 16x (95°, 40 sec; 53°, 1 min; 68°, 7 min). The entire *pol2* gene was then sequenced to confirm the presence of the *pol2-M644G* mutation.

Strains. All strains used in this study were derived from the BY4733 background described in Brachmann *et al*. (Brachmann *et al.* 1998). Table 4.2 contains a comprehensive list of strains used in this study. Chromosomal gene disruptions were made using PCR products generated with Phusion polymerase and the primers and PCR conditions indicated in Table

4.3. Yeast were transformed using the resulting PCR products (lithium acetate transformation, [find]) and correct clones were identified by Zymolyase-treatment (MP Biomedicals) and genotyped using junction-specific PCR primers that recognize the transgene and endogenous locus (primer and PCR conditions available upon request).

Plasmid shuffling

Plasmid shuffling was performed in strains containing either a *pol2Δ::KANMX* or *pol3Δ::HIS3* gene replacement. The *URA3* plasmids pRS416*POL2* (described in Chapter II methods) or pGL310 (*POL3*) (Herr *et al.* 2011a) provide the essential activity of Pol ε or Pol δ. Strains were transformed with CEN/LEU2 plasmids encoding wild-type or mutant polymerases (*pol2-4*, *pol2-M644G*, or *pol3-01*). Transformants were selected on SC-URA-LEU and colonies were picked and suspended in water and plated onto media containing FOA to select for the loss of the *URA3* plasmid (carrying the wild-type gene).

Mutation rates

Detailed methods describing the measurement of canavanine resistance (Can^r) mutation rates can be found in (Herr *et al.* 2011a). Briefly, cells containing plasmids encoding wild-type (*URA3*) and mutant (*LEU2*) polymerases were plated onto media containing FOA to select for the loss of the wild-type plasmid. Twenty-four FOA-resistant colonies were then picked and suspended in water. Aliquots of each colony were plated onto SC and canavinine selection plates to estimate the number of cell divisions during colony formation and the frequency of Can^r mutants per colony, respectively. Plates were incubated at 30°C and colonies were counted after 3-4 days. The web-based program FALCOR (Fluctuation AnaLysis CalculatOR, http://www.keshavsingh.org/protocols/FALCOR.html) was used to calculate mutation rates with 95% confidence intervals.

Cell cycle analysis

Cell synchonization. Cells were synchronized using alpha factor (Zymo Research) (Breeden 1997). Strains were grown overnight in 50 mL of YPD at 30°C to an optical density (A600) of 0.2-0.3. Alpha factor was diluted in methanol and added at a final concentration of 5μM. Cells were checked for synchrony after 90 minutes (10 μl of culture was sonicated for 10 seconds and examined on the microscope for unbudded cells). If unbudded cells remained, more alpha factor was added and cells were re-examined every 30 minutes. When only unbudded cells were present, cultures were collected in 50 mL Falcon tubes and centrifuged to pellet cells. Cells were rinsed once in water and re-suspended into 25 mL of warm YPD containing Pronase E (10 μg/ml) to release from alpha factor arrest.

Cell collection and ethanol fixation. One mL of cells was collected prior to alpha factor arrest (log phase sample) and prior to release from arrest (0 min sample). Following release, 1 mL of cells was collected every 15 minutes for 210 minutes. Immediately following collection, cells were spun down in 1.5 mL microcentrufuge tubes. YPD was aspirated and cells were rinsed once in water. The cell pellet was then resuspended in 300 μl of water and vigorously vortexed. 700 μl of 95% ethanol was immediately added and cells were vortexed again. Cells were fixed overnight at 4°C.

SYTOX green staining. Fixed cells were spun down and washed in 500 μl of water, then resuspended in 500μl of sodium citrate (50 mM) solution containing RNase (10 μg/ml, Thermo Scientific). Samples were heated to 95°C for 15 minutes and then placed in 37°C for at least 2 hours. Samples were spun down and resuspended in 500μl of 50mM sodium citrate without RNase and probe sonicated for 20 seconds. Finally samples were spun down and stained with 500 μl of 50mM sodium citrate containing SYTOX green (2μM, Invitrogen) and immediately run on the FACS machine

(http://www.pathology.washington.edu/research/labs/rabinovitch/flowroom/). FACS data was analyzed using WinCycle and FCS express.

Doubling time. Strain doubling times were measured using a precision incubator and growth-monitoring instrument (Bioscreen C MBR). Five colonies of each genotype were inoculated and grown overnight to saturation. Cultures were then diluted 1:200 and incubated in the Bioscreen, which monitored growth by measuring by optical density. Doubling times were calculated as previously described in Olsen *et al.* (Olsen *et al.* 2010).

Quantitative reverse transcriptase PCR

cDNA preparation. Cells were grown at 30°C in 25 mL of YPD until they reached log phase, as determined by OD measurements. Cells were then pelleted by centrifugation and frozen in -80°C without re-suspension until ready for RNA extraction.

Q-PCR. cDNA levels were measured using quantitative PCR. *RNR1* and *RNR3* transcripts were measured, using *ACT1* as a reference control. cDNA was amplified using the following primers: Rnr1F 5'-TGCCCCAACTATGGGTAAACTAACA-3'and Rnr1R 5'-CACTGGAAGGCATATATGA-3'; Rnr3F 5'- GATCGTCCAGTTTATGTTCCAAAGGGTA-3' and Rnr3R 5'- TATTGTTTCCGTTGGAACTGCT-3'; Act1: Act1F, 5'-GAAATGCAAACCGCTGCTCA-3' and Act1R 5'-TACCGGCAGATTCCAAACCC-3'

Q-PCRs were performed using Brilliant III Ultra-Fast QPCR Master Mix (Agilent Technologies).

Figure 4.1

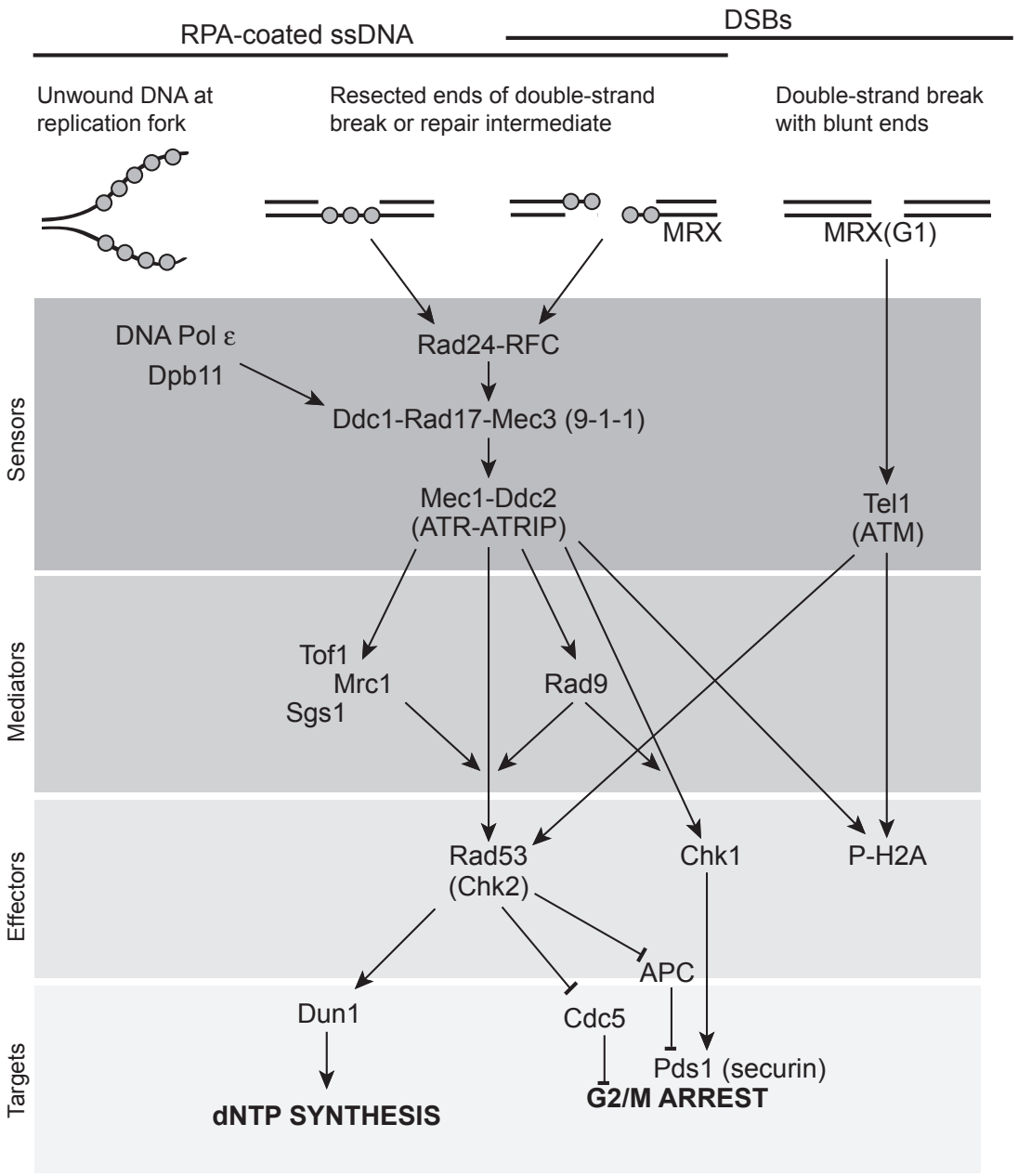
RPA-coated ssDNA
DSBs
Unwound DNA at replication fork
Resected ends of double-strand break or repair intermediate
Double-strand break with blunt ends
MRX
MRX(G1)
Sensors
DNA Pol ε
Dpb11
Rad24-RFC
Ddc1-Rad17-Mec3 (9-1-1)
Mec1-Ddc2 (ATR-ATRIP)
Tel1 (ATM)
Mediators
Tof1
Mrc1
Sgs1
Rad9
Effectors
Rad53 (Chk2)
Chk1
P-H2A
APC
Targets
Dun1
Cdc5
Pds1 (securin)
dNTP SYNTHESIS
G2/M ARREST

Figure 4.1 The S-phase and DNA damage checkpoints in *S. cerevisiae*. RPA (show as grey circles) coated DNA and double-strand breaks with blunt ends trigger the S-phase and DNA damage checkpoints. RPA-coated DNA can be generated by stalled replication forks, replication-blocking lesions, repair intermediates or resected ends of double-strand breaks. [Adapted from Reha-Krantz *et al.* (Reha-Krantz *et al.* 2011)]

Figure 4.2

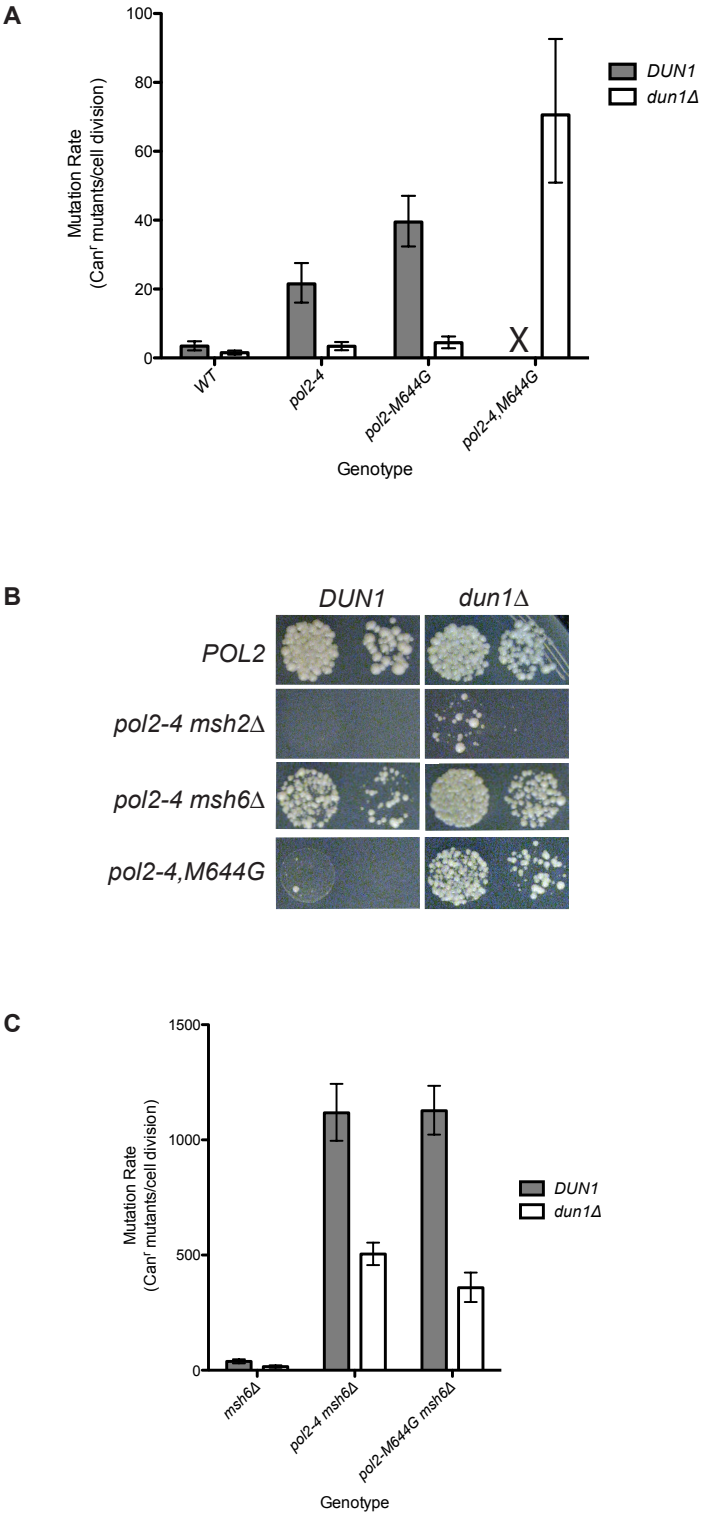
A
100
80
60
40
20
0
Mutation Rate
(Can^r mutants/cell division)
DUN1
dun1Δ
X
WT
pol2-4
pol2-M644G
pol2-4,M644G
Genotype
B
DUN1
dun1Δ
POL2
pol2-4 msh2Δ
pol2-4 msh6Δ
pol2-4,M644G
C
1500
1000
500
0
Mutation Rate
(Can^r mutants/cell division)
DUN1
dun1Δ
msh6Δ
pol2-4 msh6Δ
pol2-M644G msh6Δ
Genotype

Figure 4.2 Effect of Dun1 on Pol ε error-prone replication and error-induced extinction. (A) *dun1Δ* suppresses error extinction. Strains with the indicated genotypes were transformed with *LEU2* plasmids carrying Pol ε alleles (*POL2, pol2-4 or pol2-4,M644G*) and plated onto FOA media to select for loss of the complementing *POL2-URA3* plasmid. Plates were incubated at 30°C and photographed after 3 days. (B) and (C) *dun1Δ* confers an antimutator phenotype. Rates of spontaneous mutation (shown as number of mutants per cell division (x 10^{-7})) were determined from multiple independent fluctuation analyses of each strain and reported as canavanine resistant mutants per cell division. 95% confidence intervals for each mutation rate are shown as error bars. Gray and white columns represent *DUN1* and *dun1Δ* strains, respectively. Lethality of the *pol2-4,M644G* allele precludes rate measurement in a *DUN1* strain.

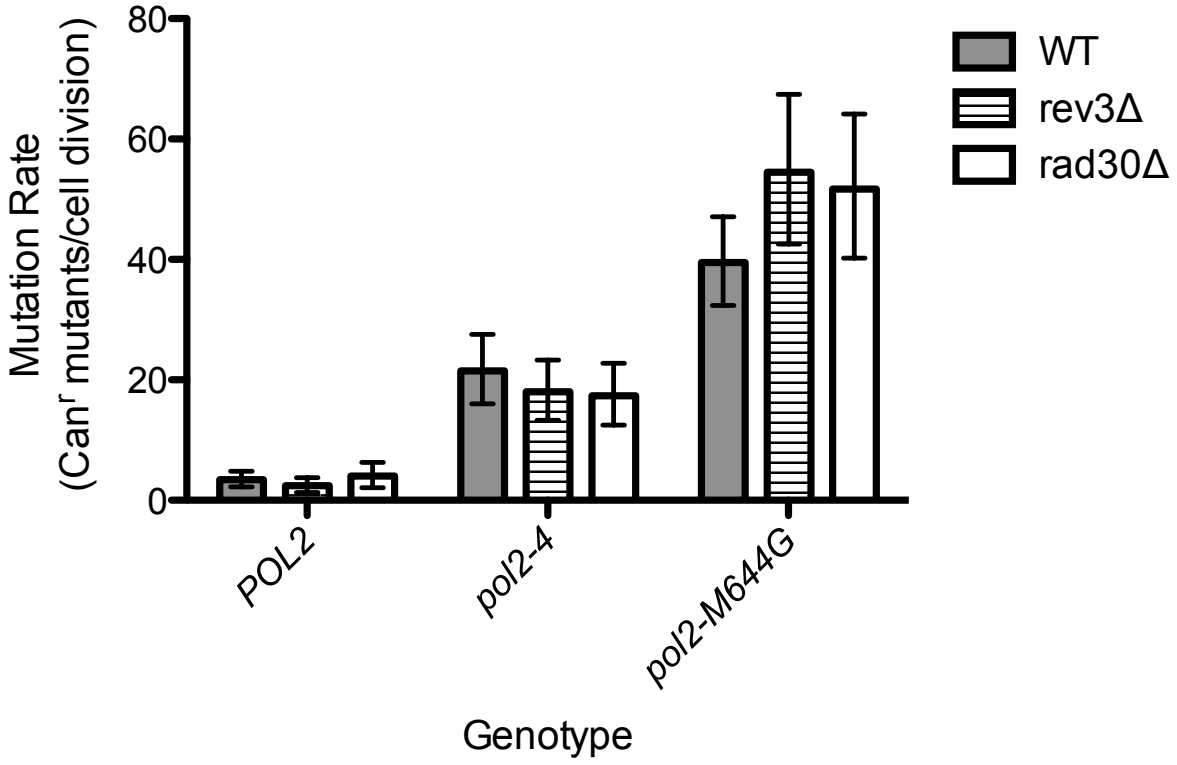

Figure 4.3 Rev3 and Rad30 do not participate in Pol ε error-prone replication. *POL2, pol2-4* and *pol2-M644G* alleles were introduced into wild-type, *rev3Δ* and *rad30Δ* strains and rates of spontaneous mutation were determined from multiple independent fluctuation analyses. Mutation rates (shown as number of mutants per cell division (x 10^{-7})) are reported as canavanine resistant mutants per cell division. 95% confidence intervals for each mutation rate are shown as error bars. Gray, striped and white columns represent, wild-type, *rev3Δ* and *rad30Δ*, strains respectively.

Figure 4.4

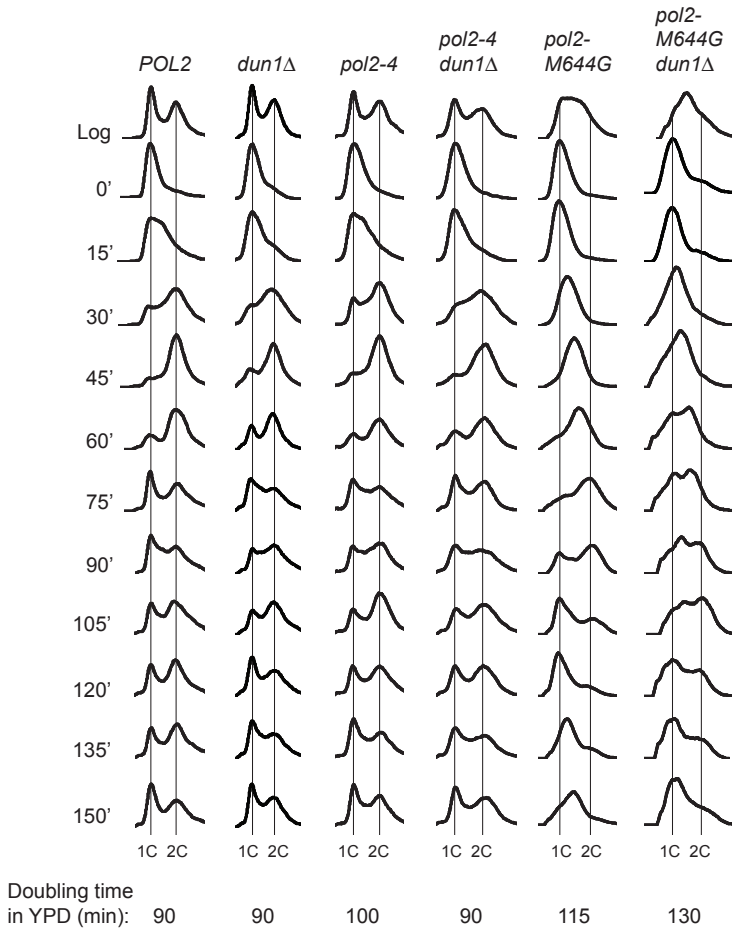
POL2
dun1Δ
pol2-4
pol2-4 dun1Δ
pol2-M644G
pol2-M644G dun1Δ
Log
0'
15'
30'
45'
60'
75'
90'
105'
120'
135'
150'
1C 2C
Doubling time in YPD (min):
90
90
100
90
115
130

Figure 4.4 Cell cycle progression and doubling times of *pol2-4* and *pol2-M644G* strains. Wild-type and mutant strains were synchronized with alpha-factor, released into rich medium, and examined for cell cycle progression by FACS. The X-axis represents relative DNA content and the Y-axis represents cell number at the indicated time points. Vertical lines indicate ploidy (1C and 2C). Log phase doubling time in rich media was measured using a precision incubator and growth-monitoring instrument (Bioscreen C MBR). Five colonies of each genotype were inoculated and grown overnight to saturation. Cultures were then diluted 1:200 and incubated in the Bioscreen, which monitored growth by measuring by optical density.

Figure 4.5

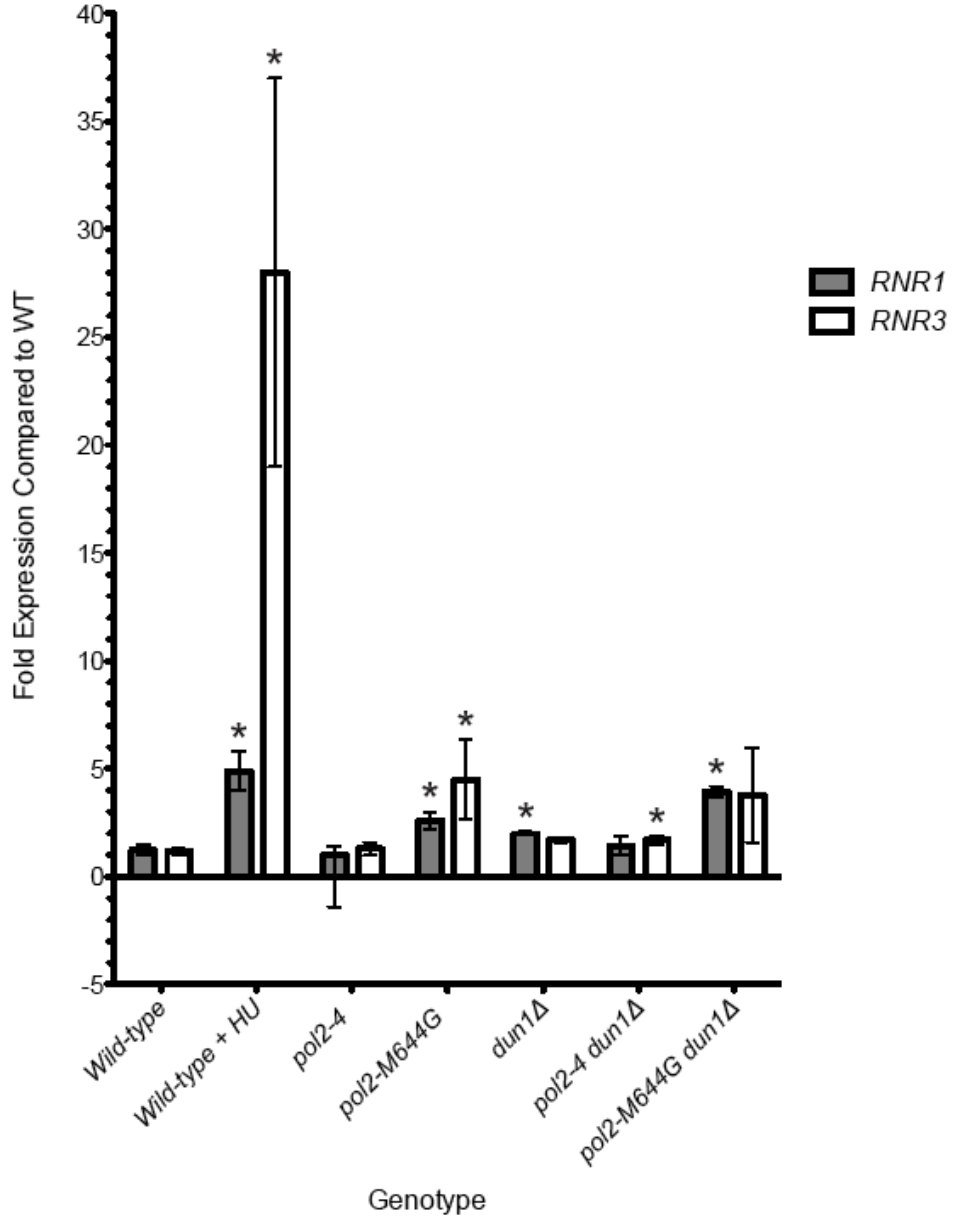
Fold Expression Compared to WT
40
35
30
25
20
15
10
5
0
-5
RNR1
RNR3
Wild-type
Wild-type + HU
pol2-4
pol2-M644G
dun1Δ
pol2-4 dun1Δ
pol2-M644G dun1Δ
Genotype

Figure 4.5 Expression of *RNR* transcripts in *pol2-4* and *pol2-M644G* strains.
Transcript levels of *RNR1* and *RNR3* were measured by quantitative PCR to ascertain checkpoint induction. Measurements were normalized to actin expression. Transcript levels are reported as fold increases compared to wild-type. A wild-type strain treated with 200mM hydroxyurea for two hours was used as a positive control for potent checkpoint activation. Error bars show 95% confidence intervals for transcript expression. Gray and white columns indicate *RNR1* and *RNR3* expression, respectively. An asterisk denotes expression levels that are significantly different ($P \leq 0.05$) from wild-type.

Figure 4.6

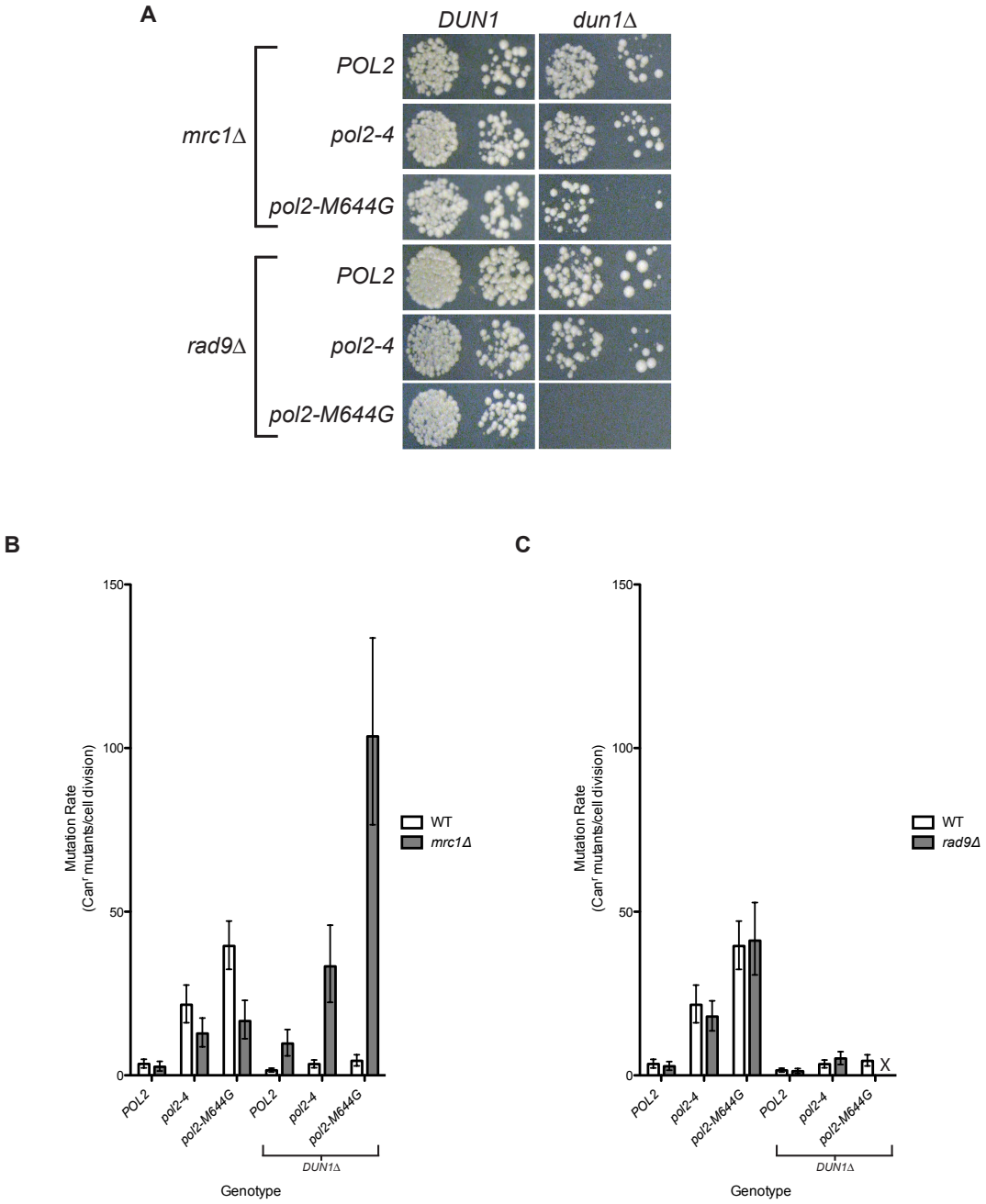
A
DUN1
dun1Δ
mrc1Δ
rad9Δ
POL2
pol2-4
pol2-M644G
B
Mutation Rate
(Canr mutants/cell division)
150
100
50
0
WT
mrc1Δ
POL2
pol2-4
pol2-M644G
DUN1Δ
Genotype
C
rad9Δ
X

Figure 4.6 Effects of Mrc1 and Rad9 on viability and mutator phenotype of *pol2-4* and *pol2-M644G* strains. (A) As in Figure 1, strains with the indicated genotypes were transformed with *LEU2* plasmids carrying Pol ε alleles (*POL2, pol2-4 or pol2-M644G*) and plated onto FOA media to select for loss of the complementing *POL2-URA3* plasmid. Plates were incubated at 30°C and photographed after 3 days. (B) and (C) Rates of spontaneous mutation (shown as number of mutants per cell division (x 10^{-7})) in *mrc1Δ* and *rad9Δ* strains were determined and reported as canavanine resistant mutants per cell division. 95% confidence intervals for each mutation rate are shown as error bars.

Table 4.1 Rates of spontaneous *CAN1* mutations in *POL2, pol2-4* and *pol2-M644G* strains

Genotype	*DUN1*		*dun1Δ*	
	Rate	95% CI	Rate	95% CI
POL2	3	5, 2	2	2, 2
pol2-4	22	28, 16	3	5, 2
pol2-M644G	40	47, 32	4	6 ,3
pol2-4,M644G	-		71	93, 51
msh6Δ	38	48, 30	16	22, 11
pol2-4 msh6Δ	1117	1243, 996	504	554, 456
pol2-M644G msh6Δ	1127	1235, 1023	358	424, 297
POL2 rev3Δ	2	4, 1	ND	
POL2 rad30Δ	3	4, 2	ND	
pol2-4 rev3Δ	18	23, 13	ND	
pol2-4 rad30Δ	17	23, 13	ND	
pol2-M644G rev3Δ	55	67, 43	ND	
pol2-M644G rad30Δ	52	64, 40	ND	
mrc1Δ	3	4, 1	10	14, 6
pol2-4 mrc1Δ	13	18, 9	33	46, 22
pol2-M644G mrc1Δ	17	23, 11	104	134, 77
rad9Δ	3	4, 2	1	2, 1
pol2-4 rad9Δ	18	23, 14	5	7, 3
pol2-M644G rad9Δ	41	53, 31	-	

Mutation rates are expressed as the number Can^r mutants per cell division (x 10^{-7}). "-" denotes an inviable strain. ND: mutation rates were not determined.

Table 4.2 Yeast strains

Strain[a]	Relevant Genotype	Reference
LW01	*pol2::kanMX msh2::HIS3* + pRS416*POL2*	Chapter II
LW03	*pol2::kanMX msh6::HIS3* + pRS416*POL2*	Chapter II
LW14	*pol2::kanMX* + pRS416*POL2*	This study
LW15	*pol2::kanMX dun1::TRP1* + pRS416*POL2*	This study
LW16	*pol2::kanMX msh6::HIS3 dun1::TRP1* + pRS416*POL2*	This study
LW17	*pol2::kanMX rev3::TRP1* + pRS416*POL2*	This study
LW18	*pol2::kanMX rad30::TRP1* + pRS416*POL2*	This study
LW19	*pol2::kanMX mrc1::HIS3* + pRS416*POL2*	This study
LW20	*pol2::kanMX mrc1::HIS3 dun1::TRP1* + pRS416*POL2*	This study
LW21	*pol2::kanMX rad9::HIS3* + pRS416*POL2*	This study
LW21	*pol2::kanMX rad9::HIS3 dun1::TRP1* + pRS416*POL2*	This study

[a] Strains engineered from the BY4733 strain (*MATa leu2Δ0 ura3Δ0 met15Δ0 trp1Δ63 his3Δ200*), an S288C descendent (Brachmann *et al.* 1998) that we re-derived via sporulation of a BY4733 X BY4734 diploid (kindly provided by Tim Formosa, University of Utah). The *pol2::kanMX* strains were constructed from this re-derived BY4733 strain by first introducing pRS416*POL2* (to provide a wild-type plasmid copy of *POL2*) and then replacing the entire chromosomal *POL2* gene with a *kanMX* cassette. pRS416*POL2* is the *CEN6/ARSH4/URA3* plasmid pRS416 (Brachmann *et al.* 1998) carrying wild-type *POL2* with its natural promoter.

Table 4.3 Oligonucleotides used for construction of chromosomal gene disruptions

Allele	PCR Primer Name	PCR Primer Sequence	PCR Template [a]
pol2Δ::kanMX	Pol2-kanMXkoF	5'-ATGATGTTTGGCAAGAAAAAAAACAACGGAGGATCTTCCACTGCAAGATATTCAGCTGGCGAAGTTATTAGGTCTAGAGATCTG-3'	pUG6 (Guldener *et al.* 1996)
	Pol2-kanMXkoR	5'-TCATATGGTCAAATCAGCAATACAACTCAATAATATATCAAAACCGTAATACTTGGCTACTACGAAGTTATATTAAGGGTTCTCG-3'	
msh2Δ::HIS3	Msh2U	5'-AAAAATCTCTTTATCTGCTGACCTAACATCAAAATCCTCAGATTAAAAGTAGATTGTACTGAGAGTGCAC-3'	pRS413 (Brachmann *et al.* 1998)
	Msh2D	5'-TTATAACAACAAGGCTTTTATATATTTCAGGTAATTATCGTTTTCCTTTTCTGTGCGGTATTTCACACCG-3'	
msh6Δ::HIS3	Msh6U	5'-TTTAATTGGAGCAACTAGTTAATTTTGACAAAGCCAATTTGAACTCCAAAGAAGTTATTAGGTCTAGAGATCTG-3'	pRS413 (Brachmann *et al.* 1998)
	Msh6D	5'-ACTTTAAAAAAAATAAGTAAAAATCTTACATACATCGTAAATGAAAATACACGAAGTTATATTAAGGGTTCTCG-3'	
dun1Δ::TRP1	Dun1Ftko	5'-ATGAGTTTGTCCACGAAAAGAGAGCACTCTGGTGATGTAACTGACTCTTCAGATTGTACTGAGAGTGCAC-3'	pRS414 (Brachmann *et al.* 1998)
	Dun1Rtko	5'-AGAGGCAAGATAATTCTGAGTATGTTTTGGGTATTTTATTGTCAGTAATTCTGTGCGGTATTTCACACCG-3'	
rev3Δ::TRP1	Rev3U	5'-ATTTGAGTCAATACAAAACTACAAGTTGTGGCGAAATAAAATGTTTGGAAAGATTGTACTGAGAGTGCAC-3'	pRS414 (Brachmann *et al.* 1998)
	Rev3D	5'-TTACCAATCATTTAGAGATATTAATGCTTCTTCCCTTTGAACAGATTGATCTGTGCGGTATTTCACACCG-3'	
rad30Δ::TRP1	Rev3D	5'-TTACCAATCATTTAGAGATATTAATGCTTCTTCCCTTTGAACAGATTGATCTGTGCGGTATTTCACACCG-3'	pRS414 (Brachmann *et al.* 1998)
	Rad30U	5'-TAGCGCAGGCCTGCTCATTTTTGAACGGCTTTGATAAAACAAGACAAAGCAGATTGTACTGAGAGTGCAC-3'	
mrc1Δ::HIS3	Mrc1ko-for	5'-TAGCATTTCAAACACATTATGTTGGAAAAAAACCAAGAACAGACAAACAACTAAGGAAGTTCGTTATTCGCTTTTGAACTTATCACCAAATATTTTAGTGAGATTGTACTGAGAGTGCAC-3'	pRS413 (Brachmann *et al.* 1998)
	Mrc1ko-rev	5'-CCTAGACTCGGGTGCCATCTTTTTTAATGCGACTACTTCAAGACAGCTTCTGGAGTTCAATCAACTTCTTCGGAAAAGATAAAAAACCATCTGTGCGGTATTTCACACCG-3'	
rad9Δ::HIS3	Rad9ko-for	5'-TTTGTTCGTGGATATTTGCAACGATGAGCAATGTGAAGTGAGCAAGATAGAGAAACGCCATAGAAAAGAGCATAGTGAGAAAATCTTCAACATCAGGGCTAGATTGTACTGAGAGTGCAC -3'	pRS413 (Brachmann *et al.* 1998)

	Rad9ko-rev	5'-TGGCGTGTGGGAGGATGTTCTTAGACTTAATTAAGAA TCTCTAAATTTTTTTTTATTTAATCGTCCCTTTCTATCAAT TATGAGTTTATATATTTTTATAATTTCTGTGCGGTATTTC ACACC-3'	

[a] pRS411 was used as template for gene replacement with *MET15*; pRS413 with *HIS3;* pRS414 with *TRP1*; pRS415 with *LEU2*.

Mutations were introduced into yeast using PCR products generated with the indicated primers and template DNAs. The PCR conditions for all primers used here were: 98°, 1 min.; 30x (98°, 10 sec.; 55°, 30 sec.; 72°, 90 sec.); 72°, 60 sec.

CHAPTER V: CONCLUSIONS AND PERSPECTIVES

In this dissertation, I have presented data that augments the understanding of DNA replication fidelity. By clarifying the synthetic interactions between Pol ε and mismatch repair (MMR), I provided an in-depth view of dynamics that maintain fidelity. Analysis of Pol ε and Pol δ antimutator variants suggests multiple mechanisms of mutation suppression by polymerases, and reinforces the importance of polymerase fidelity during DNA replication. I have also provided evidence that factors other than polymerase base selectivity, proofreading and MMR operate to suppress replication errors. In my quest to identify these factors, I discovered that Dun1, a checkpoint kinase, augments mutagenesis by error-prone Pol ε. Paradoxically, this implies that triggering the S-phase checkpoint can be mutagenic. Below, I highlight my major conclusions and suggest further experimental directions.

Chapter II: Emergence of DNA Polymerase ε antimutators that escape error-induced extinction in yeast

Almost 20 years ago, Morrison and Sugino reported that combined defects in Pol δ proofreading and MMR were lethal due to error-induced extinction (Morrison *et al.* 1993). Soon after, they showed that a similar combination in Pol ε proofreading (encoded by *pol2-4*) and MMR was viable (Morrison and Sugino 1994). Several years later, the Resnick group affirmed this finding by isolating viable *pol2-4 msh2Δ* mutants (Tran *et al.* 1999b). However, Greene and Jinks-Robinson later reported that they could not obtain a viable *pol2-4 msh2Δ* strain using either gene disruption or plasmid shuffling methods (Greene and Jinks-Robertson 2001). Thus, it remained unclear whether the magnitude of Pol ε errors was sufficient to trigger error-induced extinction.

While clarifying the synthetic interactions between proofreading-deficient Pol ε and MMR, I discovered that Pol ε proofreading-deficiency (encoded by *pol2-4*) is only lethal in the complete absence of MMR (Figure 2.1). This suggests that the MutS-homolog Msh3 and the MutL-homolog Mlh3 both contribute substantially to mutation avoidance during Pol ε DNA synthesis. The role of both proteins in mutation avoidance is underappreciated in the literature (Harrington and Kolodner 2007; Palombo *et al.* 1996; Peltomäki 2005). In contrast, Pol δ proofreading deficiency (encoded by *pol3-01*) is lethal in strains where Msh3- and Mlh3-mediated repair is still active (Figure 2.1) (Morrison *et al.* 1993). This could be due to the severity of the *pol3-01* mutator phenotype, which is up to 30-fold greater than the *pol2-4* mutator phenotype (Datta *et al.* 2000; Greene and Jinks-Robertson 2001; Karthikeyan *et al.* 2000; Morrison and Sugino 1994; Pavlov *et al.* 2004; Shcherbakova *et al.* 1996; Tran *et al.* 1999b). Alternatively, perhaps *pol2-4* creates more mutations that are repaired by Msh3- and Mlh3-dependent mechanisms.

Although complete abrogation of both Pol ε proofreading and MMR is lethal, mutants that suppressed this error-induced extinction (*eex*) frequently emerged. Five percent of *eex* mutants encoded antimutator variants of Pol ε (Table 2.1, Figure 2.5). *Eex* alleles were scattered throughout the Pol ε sequence, suggesting multiple antimutator mechanisms. Biochemical analyses will help determine these mechanisms. The remaining *eex* mutants were extragenic to *pol2*, implicating factors other than polymerase fidelity and MMR in mutation suppression. Interestingly, a smaller proportion of Pol δ *eex* alleles are extragenic to *pol3*, suggesting polymerase-specific pathways of mutation suppression. Discovering the reason for this difference between Pol ε and Pol δ may help clarify the roles of these polymerases at the replication fork.

Chapter III: Synthetic Genetic Array (SGA) analysis to identify deletions that suppress error-induced extinction

Suppression of error-induced extinction occurs commonly through mutations in DNA polymerase (pol) genes that confer an antimutator phenotype (Figure 2.5) (Herr *et al.* 2011a). However, mutations extragenic to pol genes are more common, suggesting pathways other than polymerase base selectivity, proofreading, and MMR contribute to DNA replication fidelity. To identify these pathways, I performed Synthetic Genetic Array (SGA) analysis to screen for deletions that suppress error-induced lethality. The SGA is a collection of approximately 5,000 budding yeast strains, each containing one deletion of a nonessential gene. Altogether, the SGA comprises a powerful tool to probe almost the entire yeast genome (~80%) (Winzeler *et al.* 1999). I used the SGA to screen for deletions that could suppress *pol3-01 msh2Δ* error-induced extinction. Suppressors of this allelic combination emerge at a low rate, reducing the chances of false positives during screening. However, this low rate of suppression has disadvantages, as it limits detection of suppressors to only the strongest antimutators. Compatible with idea, I discovered that no SGA deletion could suppress *pol3-01 msh2Δ* lethality. This suggests that the strongest suppressors of error-induced extinction are either gain-of-function alleles or hypomorphic alleles in essential genes. Whole genome sequencing of spontaneous *eex* mutants will help reveal extragenic pathways of mutation suppression.

Chapter VI: Checkpoint-dependent mutagenesis by error-prone DNA polymerase ε variants

In 2000, Datta and colleagues discovered that the mutator phenotype of proofreading-deficient Pol δ (*pol3-01*) is Dun1-dependent (Datta *et al.* 2000). Deletion of *dun1*, encoding a protein kinase that mediates damage-inducible gene expression and up-regulates dNTP

synthesis during the S-phase checkpoint, suppressed the mutator phenotype of *pol3-01* 8-fold. In the same study, no difference in the mutation rate of proofreading-deficient Pol ε was observed. We used Pol ε mutants deficient in proofreading (*pol2-4*) and base selectivity (*pol2-M644G*) to investigate the interaction between Pol ε mutators and the S-phase checkpoint. We found that *dun1Δ* suppresses mutagenesis of error-prone Pol ε (Figure 4.1, Panel B). Moreover, *dun1Δ* suppresses Pol ε mediated error-induced extinction (Figure 4.1, Panel A). These data suggest that Dun1 has a mutagenic role during error-prone replication. We propose that Dun1 activation triggers an increase in dNTP synthesis, leading to mutagenic DNA synthesis by Pol ε. Interestingly, while the *pol2-4* strain does not appear to have an activated S-phase checkpoint, the mutator phenotype is Dun1-dependent, suggesting that Dun1 can be activated independently of the checkpoint. Detection of replication errors appears to progress mainly through Mrc1 (Figure 4.5, Panel B). However, in the absence of fork stabilization by either Mrc1 or Dun1, Rad9 triggers a mutagenic error-prone replication pathway (Figure 4.5, Panel B). Cumulatively, our data suggest that during times of replication stress, a Dun1-dependent mechanism promotes mutation fixation, likely to progress the replisome and avoid replication fork collapse.

Broader implications

By investigating mutator phenotypes, we hope to elucidate pathways of cancer progression. The budding yeast *Saccharomyces cerevisiae* provides a flexible system to investigate DNA replication fidelity. As many components of DNA metabolism are highly conserved, our studies should be applicable to mammalian cells. We have observed that mutator phenotypes are inherently unstable and frequently suppressed (Figure 2.3) (Herr *et al.* 2011a). These data are consistent with a model where mutator phenotypes provide the

genetic diversity required for adaptation, but are suppressible during periods of steady-state growth when mutations are unfavorable. A transient mutator phenotype has been speculated to drive cancer progression (Loeb 1997b). Malignant clones would emerge after repeated cycles of natural selection, resulting from the rise and fall of mutator phenotypes as cells overcome barriers to cell growth. We speculate that antimutators moderate high mutation rates and minimize deleterious mutations during mammalian oncogenesis.

REFERENCES

Aksenova, A., K. Volkov, J. Maceluch, Z. F. Pursell, I. B. Rogozin *et al.*, 2010 Mismatch repair-independent increase in spontaneous mutagenesis in yeast lacking non-essential subunits of DNA polymerase epsilon. PLoS Genet. **6:** e1001209.

Albertson, T. M., M. Ogawa, J. M. Bugni, L. E. Hays, Y. Chen *et al.*, 2009 DNA polymerase ε and δ proofreading suppress discrete mutator and cancer phenotypes in mice. Proc. Natl. Acad. Sci. USA **106:** 17101-17104.

Albertson, T. M., and B. D. Preston, 2006 DNA replication fidelity: proofreading *in trans*. Curr. Biol. **16:** R209-211.

Alcasabas, A. A., A. J. Osborn, J. Bachant, F. Hu, W. P. J. H. *et al.*, 2001 Mrc1 transduces signals of DNA replication stress to activate Rad53. Nat Cell Biol **3:** 958-965.

Allen, J. B., Z. Zhou, W. Siede, E. C. Friedberg and S. J. Elledge, 1994 The SAD1/RAD53 protein kinase controls multiple checkpoints and DNA damage-induced transcription in yeast.

10.1101/gad.8.20.2401. Genes Dev. **8:** 2401-2415.

Andreson, B. L., A. Gupta, B. P. Georgieva and R. Rothstein, 2010 The ribonucleotide reductase inhibitor, Sml1, is sequentially phosphorylated, ubiquitylated and degraded in response to DNA damage. Nucleic Acids Res. **38:** 6490-6501.

Araki, H., S. H. Leem, A. Phongdara and A. Sugino, 1995 Dpb11, which interacts with DNA polymerase II(epsilon) in Saccharomyces cerevisiae, has a dual role in S-phase progression and at a cell cycle checkpoint. Proc. Natl. Acad. Sci. USA **92:** 11791-11795.

Bailey, S., R. A. Wing and T. A. Steitz, 2006 The structure of *T. aquaticus* DNA polymerase III is distinct from eukaryotic replicative DNA polymerases. Cell **126:** 893-904.

Bardwell, A. J., L. Bardwell, A. E. Tomkinson and E. C. Friedberg, 1994 Specific cleavage of model recombination and repair intermediates by the yeast Rad1-Rad10 DNA endonuclease. Science **265:** 2082-2085.

Barlow, J. H., M. Lisby and R. Rothstein, 2008 Differential regulation of the Cellular Response to DNA Double-strand Breaks in G1. Mol. Cell **30:** 73-85.

Bastin-Shanower, S. A., W. M. Fricke, J. R. Mullen and S. J. Brill, 2003 The mechanism of Mus81-Mms4 cleavage site selection distinguishes it from the homologous endonuclease Rad1-Rad10. Mol. Cell. Biol. **23:** 3487-3496.

Beard, W. A., and S. H. Wilson, 2003 Structural Insights into the origins of DNA polymerase fidelity. Structure **11:** 489-496.

Bebenek, K., and T. A. Kunkel, 1995 Analyzing fidelity of DNA polymerases. Methods Enzymol. **262:** 217-232.

Beese, L. S., V. Derbyshire and T. A. Steitz, 1993 Structure of DNA polymerase I Klenow fragment bound to duplex DNA. Science **260:** 352-355.

Bernad, A., L. Blanco, J. M. Lazaro, G. Martin and M. Salas, 1989 A conserved 3′→5′ exonuclease active site in prokaryotic and eukaryotic DNA polymerases. Cell **59:** 219-228.

Bielas, J. H., and L. A. Loeb, 2005 Mutator phenotype in cancer: timing and perspectives. Environ. Mol. Mutagen. **45:** 206-213.

Boddy, M. N., P. H. Gaillard, W. H. Mcdonald, P. Shanahan, J. R. Yates, 3rd *et al.*, 2001 Mus81-Eme1 are essential components of a Holliday junction resolvase. Cell **107:** 537-548.

Boeke, J. D., F. Lacroute and G. R. Fink, 1984 A positive selection for mutants lacking orotidine-5'-phosphate decarboxylase activity in yeast: 5-fluoro-orotic acid resistance. Mol. Gen. Genet. **197:** 345-346.

Brachmann, C. B., A. Davies, G. J. Cost, E. Caputo, J. Li *et al.*, 1998 Designer deletion strains derived from *Saccharomyces cerevisiae* S288C: a useful set of strains and plasmids for PCR-mediated gene disruption and other applications. Yeast **14:** 115-132.

Breeden, L. L., 1997 Alpha-factor synchronization of budding yeast. Methods Enzymol. **283:** 332-341.

Caras, I. W., and D. W. J. Martin, 1988 Molecular cloning of the cDNA for a mutant mouse ribonucleotide reductase M1 that produces a dominant mutator phenotype in mammalian cells. Mol. Cell. Biol. **8:** 2698-2704.

Chabes, A., V. Domkin, N.-G. Larsson, A. Liu, A. Graslund *et al.*, 2000 Yeast ribonucleotide reductase has a heterodimeric iron-radical-containing subunit. Proc. Natl. Acad. Sci. USA **97:** 2474-2479.

Chabes, A., B. Georgieva, V. Domkin, X. Zhao, R. Rothstein *et al.*, 2003a Survival of DNA damage in yeast directly depends on increased dNTP levels allowed by relaxed feedback inhibition of ribonucleotide reductase. Cell **112:** 391-401.

Chabes, A., B. Georgieva, V. Domkin, X. Zhao, R. Rothstein *et al.*, 2003b Survival of DNA damage in yeast directly depends on increased dNTP levels allowed by relaxed feedback inhibition of ribonucleotide reductase. Cell **112:** 391-401.

Chao, L., and E. C. Cox, 1983 Competition between high and low mutating strains of *Escherichia coli*. Evolution **37:** 125-134.

Chen, S.-H., C. P. Albuquerque, J. Liang, R. T. Suhandynata and H. Zhou, 2010 A Proteome-wide Analysis of Kinase-Substrate Network in the DNA Damage Response. J. Biol. Chem. **285:** 12803-12812.

Chen, X. B., R. Melchionna, C. M. Denis, P. H. Gaillard, A. Blasina *et al.*, 2001 Human Mus81-associated endonuclease cleaves Holliday junctions in vitro. Mol. Cell **8:** 1117-1127.

Cimprich, K. A., T. B. Shin, C. T. Keith and S. L. Schreiber, 1996 cDNA cloning and gene mapping of a candidate human cell cycle checkpoint protein. Proc. Natl. Acad. Sci. USA **93:** 2850-2855.

Datta, A., J. L. Schmeits, N. S. Amin, P. J. Lau, K. Myung *et al.*, 2000 Checkpoint-dependent activation of mutagenic repair in *Saccharomyces cerevisiae pol3-01* mutants. Mol. Cell **6:** 593-603.

Davidson, M. B., Y. Katou, A. Keszthelyi, T. L. Sing, T. Xia *et al.*, 2012 Endogenous DNA replication stress results in expansion of dNTP pools and a mutator phenotype. EMBO J. **31:** 895-907.

De Wind, N., M. Dekker, A. Berns, M. Radman and H. Te Riele, 1995 Inactivation of the mouse Msh2 gene results in mismatch repair deficiency, methylation tolerance, hyperrecombination, and predisposition to cancer. Cell **82:** 321-330.

Denver, D. R., S. Feinberg, S. Estes, W. K. Thomas and M. Lynch, 2005 Mutation rates, spectra and hotspots in mismatch repair-deficient Caenorhabditis elegans. Genetics **170:** 107-113.

Desai, M. M., D. S. Fisher and A. W. Murray, 2007 The speed of evolution and maintenance of variation in asexual populations. Curr. Biol. **17:** 385-394.
Desany, B. A., A. A. Alcasabas, J. B. Bachant and S. J. Elledge, 1998 Recovery from DNA replicational stress is the essential function of the S-phase checkpoint pathway. Genes Dev. **12:** 2956-2970.
Ding, J., K. Das, Y. Hsiou, S. G. Sarafianos, A. D. Clark *et al.*, 1998 Structure and functional implications of the polymerase active site region in a complex of HIV-1 RT with a double-stranded DNA template-primer and an antibody fab fragment at 2.8 Å resolution. J. Mol. Biol. **284:** 1095-1111.
Domkin, V., L. Thelander and A. Chabes, 2002 Yeast DNA damage-inducible Rnr3 has a very low catalytic activity strongly stimulated after the formation of a cross-talking Rnr1/Rnr3 complex. The Journal of biological chemistry **277:** 18574-18578.
Doublie, S., M. R. Sawaya and T. Ellenberger, 1999 An open and closed case for all polymerases. Structure **7:** R31-35.
Doublie, S., S. Tabor, A. M. Long, C. C. Richardson and T. Ellenberger, 1998 Crystal structure of a bacteriophage T7 DNA replication complex at 2.2 A resolution. Nature **391:** 251-258.
Drake, J. W., 1993 General antimutators are improbable. J. Mol. Biol. **229:** 8-13.
Drake, J. W., and E. F. Allen, 1968 Antimutagenic DNA polymerases of bacteriophage T4. Cold Spring Harb. Symp. Quant. Biol. **33:** 339-344.
Drake, J. W., E. F. Allen, S. A. Forsberg, R. M. Preparata and E. O. Greening, 1969 Genetic control of mutation rates in bacteriophage T4. Nature **221:** 1128-1132.
Drake, J. W., B. Charlesworth, D. Charlesworth and J. F. Crow, 1998 Rates of spontaneous mutation. Genetics **148:** 1667-1686.
Dua, R., D. L. Levy and J. L. Campbell, 1998 Role of the putative zinc finger domain of Saccharomyces cerevisiae DNA polymerase epsilon in DNA replication and the S/M checkpoint pathway. J. Biol. Chem. **273:** 30046-30055.
Dua, R., D. L. Levy and J. L. Campbell, 1999 Analysis of the essential functions of the C-terminal protein/protein interaction domain of *Saccharomyces cerevisiae* Pol ε and its unexpected ability to support growth in the absence of the DNA polymerase domain. J. Biol. Chem. **274:** 22283-22288.
Echols, H., and M. F. Goodman, 1991 Fidelity mechanisms in DNA replication. Annu. Rev. Biochem. **60:** 477-511.
Elena, S. F., and R. E. Lenski, 2003 Evolution experiments with microorganisms: the dynamics and genetic bases of adaptation. Nat Rev Genet **4:** 457-469.
Elledge, S. J., and R. W. Davis, 1987 Identification and isolation of the gene encoding the small subunit of ribonucleotide reductase. Mol. Cell. Biol. **9:** 2783-2793.
Elledge, S. J., and R. W. Davis, 1990 Two genes differentially regulated in the cell cycle and by DNA-damaging agents encode alternative regulatory subunits of ribonucleotide reductase. Genes Dev. **4:** 740-751.
Elledge, S. J., Z. Zhou, J. B. Allen and T. A. Navas, 1993 DNA damage and cell cycle regulation of ribonucleotide reductase. Bioessays **15:** 333-339.
Eom, S. H., J. Wang and T. A. Steitz, 1996 Structure of Taq polymerase with DNA at the polymerase active site. Nature **382:** 278-281.

Estes, S., P. C. Phillips, D. R. Denver, W. K. Thomas and M. Lynch, 2004 Mutation accumulation in populations of varying size: the distribution of mutational effects for fitness correlates in *Caenorhabditis elegans*. Genetics **166:** 1269-1279.

Fasullo, M., O. Tsaponina, M. Sun and A. Chabes, 2010 Elevated dNTP levels suppress hyper-recombination in Saccharomyces cerevisiae S-phase checkpoint mutants. Nucleic Acids Res. **38:** 1195-1203.

Feng, W., and G. D'urso, 2001 *Schizosaccharomyces pombe* cells lacking the amino-terminal catalytic domains of DNA polymerase epsilon are viable but require the DNA damage checkpoint control. Mol. Cell. Biol. **21:** 4495-4504.

Fersht, A. R., 1979 Fidelity of replication of phage phi X174 DNA by DNA polymerse III holoenzyme: spontaneous mutation by misincorporation. Proc. Natl. Acad. Sci. USA **76:** 4946-4950.

Fijalkowska, I. J., R. L. Dunn and R. M. Schaaper, 1993 Mutants of *Escherichia coli* with increased fidelity of DNA replication. Genetics **134:** 1023-1030.

Fijalkowska, I. J., and R. M. Schaaper, 1993 Antimutator mutations in the α subunit of *Escherichia coli* DNA polymerase III: identification of the responsible mutations and alignment with other DNA polymerases. Genetics **134:** 1039-1044.

Fijalkowska, I. J., and R. M. Schaaper, 1995 Effects of *Escherichia coli dnaE* antimutator alleles in a proofreading-deficient *mutD5* strain. J. Bacteriol. **177:** 5979-5986.

Fijalkowska, I. J., and R. M. Schaaper, 1996 Mutants in the Exo I motif of *Escherichia coli dnaQ*: defective proofreading and inviability due to error catastrophe. Proc. Natl. Acad. Sci. USA **93:** 2856-2861.

Finette, B., A. C. Homans, J. Rivers, T. Messier and R. J. Albertini, 2001 Accumulation of somatic mutations in proliferating T cell clones from children treated for leukemia. Leukemia **15:** 1898-1905.

Fishel, R., M. K. Lescoe, M. R. Rao, N. G. Copeland, N. A. Jenkins *et al.*, 1993 The human mutator gene homolog MSH2 and its association with hereditary nonpolyposis colon cancer. Cell **75:** 1027-1038.

Flores-Rozas, H., and R. D. Kolodner, 1998 The *Saccharomyces cerevisiae MLH3* gene functions in *MSH3*-dependent suppression of frameshift mutations. Proc. Natl. Acad. Sci. USA **95:** 12404-12409.

Fortune, J. M., Y. I. Pavlov, C. M. Welch, E. Johansson, P. M. Burgers *et al.*, 2005 *Saccharomyces cerevisiae* DNA polymerase δ: high fidelity for base substitutions but lower fidelity for single- and multi-base deletions. J. Biol. Chem. **280:** 29980-29987.

Fox, E. J., J. J. Salk and L. A. Loeb, 2009 Cancer genome sequencing—an interim analysis. Cancer Res. **69:** 4948-4950.

Franklin, M. C., J. Wang and T. A. Steitz, 2001 Structure of the replicating complex of a pol α family DNA polymerase. Cell **105:** 657-667.

Friedberg, E. C., and L. B. Meira, 2003 Database of mouse strains carrying targeted mutations in genes affecting biological responses to DNA damage. Version 5. DNA Repair (Amst) **2:** 501-530.

Friedberg, E. C., G. C. Walker, W. Siede, R. D. Wood, R. A. Schultz *et al.*, 2006 *DNA Repair and Mutagenesis*. ASM Press, Washington, D.C.

Funchain, P., A. Yeung, J. L. Stewart, R. Lin, M. M. Slupska *et al.*, 2000 The consequences of growth of a mutator strain of *Escherichia coli* as measured by loss of function among multiple gene targets and loss of fitness. Genetics **154:** 959-970.

Garg, P., C. M. Stith, N. Sabouri, E. Johansson and P. M. Burgers, 2004 Idling by DNA polymerase δ maintains a ligatable nick during lagging-strand DNA replication. Genes Dev. **18:** 2764-2773.

Giaever, G., A. M. Chu, L. Ni, C. Connelly, L. Riles *et al.*, 2002 Functional profiling of the *Saccharomyces cerevisiae* genome. **418:** 387-391.

Gietz, R. D., and R. A. Woods, 2002 Transformation of yeast by lithium acetate/single-stranded carrier DNA/polyethylene glycol method, pp. 87-96 in *Part B: Guide to Yeast Genetics and Molecular and Cell Biology*, edited by C. GUTHRIE and G. R. FINK. Academic Press.

Gillin, F. D., and N. G. Nossal, 1976a Control of mutation frequency by bacteriophage T4 DNA polymerase. I. The CB120 antimutator DNA polymerase is defective in strand displacement. J. Biol. Chem. **251:** 5219-5224.

Gillin, F. D., and N. G. Nossal, 1976b Control of mutation frequency by bacteriophage T4 DNA polymerase. II. Accuracy of nucleotide selection by the L88 mutator, CB120 antimutator, and wild type phage T4 DNA polymerases. J. Biol. Chem. **251:** 5225-5232.

Giraud, A., I. Matic, O. Tenaillon, A. Clara, M. Radman *et al.*, 2001a Costs and benefits of high mutation rates: adaptive evolution of bacteria in the mouse gut. Science **291:** 2606-2608.

Giraud, A., M. Radman, I. Matic and F. Taddei, 2001b The rise and fall of mutator bacteria. Curr. Opin. Microbiol. **4:** 582-585.

Goldsby, R. E., L. E. Hays, X. Chen, E. A. Olmsted, W. B. Slayton *et al.*, 2002 High incidence of epithelial cancers in mice deficient for DNA polymerase δ proofreading. Proc. Natl. Acad. Sci. USA **99:** 15560-15565.

Goldsby, R. E., N. A. Lawrence, L. E. Hays, E. A. Olmsted, X. Chen *et al.*, 2001 Defective DNA polymerase-δ proofreading causes cancer susceptibility in mice. Nat. Med. **7:** 638-639.

Goodman, M. F., S. Creighton, L. B. Bloom and J. Petruska, 1993 Biochemical basis of DNA replication fidelity. Crit. Rev. Biochem. Mol. Biol. **28:** 83-126.

Greene, C. N., and S. Jinks-Robertson, 1997 Frameshift intermediates in homopolymer runs are removed efficiently by yeast mismatch repair proteins. Mol. Cell. Biol. **17:** 2844-2850.

Greene, C. N., and S. Jinks-Robertson, 2001 Spontaneous frameshift mutations in *Saccharomyces cerevisiae*: accumulation during DNA replication and removal by proofreading and mismatch repair activities. Genetics **159:** 65-75.

Guittet, O., P. Hakansson, N. Voevodskaya, S. Fridd, A. Graslund *et al.*, 2001 Mammalian p53R2 protein forms an active ribonucleotide reductase in vitro with the R1 protein, which is expressed both in resting cells in response to DNA damage and in proliferating cells. J. Biol. Chem. **276:** 40647-40651.

Guldener, U., S. Heck, T. Fielder, J. Beinhauer and J. H. Hegemann, 1996 A new efficient gene disruption cassette for repeated use in budding yeast. Nucleic Acids Res. **24:** 2519-2524.

Hadjimarcou, M. I., R. J. Kokoska, T. D. Petes and L. J. Reha-Krantz, 2001 Identification of a mutant DNA polymerase δ in *Saccharomyces cerevisiae* with an antimutator phenotype for frameshift mutations. Genetics **158:** 177-186.

Hall, B. M., C. X. Ma, P. Liang and K. K. Singh, 2009 Fluctuation AnaLysis CalculatOR: a web tool for the determination of mutation rate using Luria-Delbrück fluctuation analysis. Bioinformatics **25:** 1564-1565.

Hanawalt, P. C., 2002 Subpathways of nucleotide excision repair and their regulation. Oncogene **21:** 8949-8956.

Harrington, J. M., and R. D. Kolodner, 2007 *Saccharomyces cerevisiae* Msh2-Msh3 acts in repair of base-base mispairs. Mol. Cell. Biol. **27:** 6546-6554.

Herr, A. J., M. Ogawa, N. A. Lawrence, L. N. Williams, J. M. Eggington *et al.*, 2011a Mutator suppression and escape from replication error–induced extinction in yeast. PLoS Genet. **7:** e1002282.

Herr, A. J., L. N. Williams and B. D. Preston, 2011b Antimutator variants of DNA polymerases. Crit. Rev. Biochem. Mol. Biol. **46:** 548-570.

Hombauer, H., C. S. Campbell, C. E. Smith, A. Desai and R. D. Kolodner, 2011 Visualization of eukaryotic DNA mismatch repair reveals distinct recognition and repair intermediates. Cell **147:** 1040-1053.

Huang, D., R. Knuuti, H. Palosaari, H. Pospiech and J. E. Syväoja, 1999 cDNA and structural organization of the gene *Pole1* for the mouse DNA polymerase ε catalytic subunit. Biochim. Biophys. Acta **1445:** 363-371.

Huang, H., R. Chopra, G. L. Verdine and S. C. Harrison, 1998a Structure of a Covalently Trapped Catalytic Complex of HIV-1 Reverse Transcriptase: Implications for Drug Resistance. Science **282:** 1669-1675.

Huang, M., and S. J. Elledge, 1997 Identification of RNR4, encoding a second essential small subunit of ribonucleotide reductase in Saccharomyces cerevisiae. Mol. Cell. Biol. **17:** 6105-6113.

Huang, M., Z. Zhou and S. J. Elledge, 1998b The DNA replication and damage checkpoint pathways induce transcription by inhibition of the Crt1 repressor. Cell **94:** 595-605.

Huang, M., Z. Zhou and S. J. Elledge, 1998c The DNA replication and damage checkpoint pathways induce transcription by inhibition of the Crt1 repressor. Cell **94:** 595-605.

Hubscher, U., G. Maga and S. Spadari, 2002 Eukaryotic DNA polymerases. Annu. Rev. Biochem. **71:** 133-163.

Iyer, R. R., A. Pluciennik, V. Burdett and P. L. Modrich, 2006 DNA mismatch repair: functions and mechanisms. Chem. Rev. **106:** 302-323.

Johnson, A., and M. O'Donnell, 2005 Cellular DNA replicases: components and dynamics at the replication fork. Annu. Rev. Biochem. **74:** 283-315.

Johnson, K. A., 1993 Conformational coupling in DNA polymerase fidelity. Annu. Rev. Biochem. **62:** 685-713.

Johnson, K. A., 2010 The kinetic and chemical mechanism of high-fidelity DNA polymerases. Biochim. Biophys. Acta **1804:** 1041-1048.

Johnson, R. E., G. K. Kovvali, L. Prakash and S. Prakash, 1996 Requirement of the yeast *MSH3* and *MSH6* genes for *MSH2*-dependent genomic stability. J. Biol. Chem. **271:** 7285-7288.

Johnson, R. E., M. T. Washington, L. Haracska, S. Prakash and L. Prakash, 2000 Eukaryotic polymerases iota and zeta act sequentially to bypass DNA lesions. Nature **406:** 1015-1019.
Johnson, S. J., J. S. Taylor and L. S. Beese, 2003 Processive DNA synthesis observed in a polymerase crystal suggests a mechanism for the prevention of frameshift mutations. Proc. Natl. Acad. Sci. USA **100:** 3895-3900.
Jorgensen, P., B. Nelson, M. D. Robinson, Y. Chen, B. Andrews *et al.*, 2002 High-resolution genetic mapping with ordered arrays of Saccharomyces cerevisiae deletion mutants. Genetics **162:** 1091-1099.
Joyce, C. M., and S. J. Benkovic, 2004 DNA polymerase fidelity: kinetics, structure, and checkpoints. Biochemistry (Mosc). **43:** 14317-14324.
Kabani, M., J. M. Beckerich and J. L. Brodsky, 2002 Nucleotide exchange factor for the yeast Hsp70 molecular chaperone Ssa1p. Mol. Cell. Biol. **22:** 4677-4689.
Kadyrov, F. A., L. Dzantiev, N. Constantin and P. Modrich, 2006 Endonucleolytic function of MutLα in human mismatch repair. Cell **126:** 297-308.
Kadyrov, F. A., J. Genschel, Y. Fang, E. Penland, W. Edelmann *et al.*, 2009 A possible mechanism for exonuclease 1-independent eukaryotic mismatch repair. Proc. Natl. Acad. Sci. USA **106:** 8495-8500.
Kai, M., and T. S. Wang, 2003 Checkpoint activation regulates mutagenic translesion synthesis. Genes Dev. **17:** 64-76.
Kaliraman, V., J. R. Mullen, W. M. Fricke, S. A. Bastin-Shanower and S. J. Brill, 2001 Functional overlap between Sgs1-Top3 and the Mms4-Mus81 endonuclease. Genes Dev. **15:** 2730-2740.
Karthikeyan, R., E. J. Vonarx, A. F. Straffon, M. Simon, G. Faye *et al.*, 2000 Evidence from mutational specificity studies that yeast DNA polymerases δ and ε replicate different DNA strands at an intracellular replication fork. J. Mol. Biol. **299:** 405-419.
Kesti, T., K. Flick, S. Keranen, J. E. Syväoja and C. Wittenberg, 1999 DNA polymerase ε catalytic domains are dispensable for DNA replication, DNA repair, and cell viability. Mol. Cell **3:** 679-685.
Kiefer, J. R., C. Mao, J. C. Braman and L. S. Beese, 1998 Visualizing DNA replication in a catalytically active Bacillus DNA polymerase crystal. Nature **391:** 304-307.
Kolodner, R. D., and G. T. Marsischky, 1999 Eukaryotic DNA mismatch repair. Curr. Opin. Genet. Dev. **9:** 89-96.
Kool, E. T., 2002 Active site tightness and substrate fit in DNA replication. Annu. Rev. Biochem. **71:** 191-219.
Kumar, D., A. L. Abdulovic, J. Viberg, A. K. Nilsson, T. A. Kunkel *et al.*, 2010a Mechanisms of mutagenesis in vivo due to imbalanced dNTP pools. Nucleic Acids Res. **39:** 1360-1371.
Kumar, D., A. L. Abdulovic, J. Viberg, A. K. Nilsson, T. A. Kunkel *et al.*, 2011 Mechanisms of mutagenesis *in vivo* due to imbalanced dNTP pools. Nucleic Acids Res. **39:** 1360-1371.
Kumar, D., J. Viberg, A. K. Nilsson and A. Chabes, 2010b Highly mutagenic and severely imbalanced dNTP pools can escape detection by the S-phase checkpoint. Nucleic Acids Res. **38:** 3975-3983.

Kunkel, T. A., and K. Bebenek, 2000 DNA replication fidelity. Annu. Rev. Biochem. **69:** 497-529.
Kunkel, T. A., and P. M. Burgers, 2008 Dividing the workload at a eukaryotic replication fork. Trends Cell Biol. **18:** 521-527.
Kunkel, T. A., and D. A. Erie, 2005 DNA mismatch repair. Annu. Rev. Biochem. **74:** 681-710.
Larrea, A. A., S. A. Lujan, S. A. Nick Mcelhinny, P. A. Mieczkowski, M. A. Resnick *et al.*, 2010 Genome-wide model for the normal eukaryotic DNA replication fork. Proc. Natl. Acad. Sci. USA **107:** 17674-17679.
Lawrence, C. W., and R. B. Christensen, 1979 Ultraviolet-induced reversion of cyc1 alleles in radiation-sensitive strains of yeast. III. rev3 mutant strains. Genetics **92:** 397-408.
Lee, Y. D., J. Wang, J. Stubbe and S. J. Elledge, 2008 Dif1 is a DNA-damage-regulated facilitator of nuclear import for ribonucleotide reductase. Mol. Cell **32:** 70-80.
Li, L., K. M. Murphy, U. Kanevets and L. J. Reha-Krantz, 2005 Sensitivity to phosphonoacetic acid: a new phenotype to probe DNA polymerase δ in *Saccharomyces cerevisiae*. Genetics **170:** 569-580.
Li, Y., S. Korolev and G. Waksman, 1998 Crystal structures of open and closed forms of binary and ternary complexes of the large fragment of Thermus aquaticus DNA polymerase I: structural basis for nucleotide incorporation. EMBO J. **17:** 7514-7525.
Ling, H., F. Boudsocq, R. Woodgate and W. Yang, 2001 Crystal Structure of a Y-Family DNA Polymerase in Action: A Mechanism for Error-Prone and Lesion-Bypass Replication. Cell **107:** 91-102.
Loeb, L. A., 1997a CARCINOGENESIS: Transient Expression of a Mutator Phenotype in Cancer Cells. Science **277:** 1449-1450.
Loeb, L. A., 1997b Transient expression of a mutator phenotype in cancer cells. Science **277:** 1449-1450.
Loeb, L. A., 2011 Human cancers express mutator phenotypes: origin, consequences and targeting. Nat Rev Cancer **11:** 450-457.
Loeb, L. A., J. H. Bielas and R. A. Beckman, 2008 Cancers exhibit a mutator phenotype: clinical implications. Cancer Res. **68:** 3551-3557.
Loeb, L. A., C. F. Springgate and N. Battula, 1974 Errors in DNA replication as a basis of malignant changes. Cancer Res. **34:** 2311-2321.
Loh, E., J. Choe and L. A. Loeb, 2007 Highly tolerated amino acid substitutions increase the fidelity of *Escherichia coli* DNA polymerase I. J. Biol. Chem. **282:** 12201-12209.
Lopes, M., C. Cotta-Ramusino, A. Pellicioli, G. Liberi, P. Plevani *et al.*, 2001 The DNA replication checkpoint response stabilizes stalled replication forks. Nature **412:** 557-561.
Lou, H., M. Komata, Y. Katou, Z. Guan, C. C. Reis *et al.*, 2008 Mrc1 and DNA polymerase epsilon function together in linking DNA replication and the S phase checkpoint. Mol. Cell **32:** 106-117.
Mao, E. F., L. Lane, J. Lee and J. H. Miller, 1997 Proliferation of mutators in a cell population. J. Bacteriol. **179:** 417-422.

Marsischky, G. T., N. Filosi, M. F. Kane and R. Kolodner, 1996 Redundancy of *Saccharomyces cerevisiae MSH3* and *MSH6* in *MSH2*-dependent mismatch repair. Genes Dev. **10:** 407-420.

Matsuoka, S., M. Huang and S. J. Elledge, 1998 Linkage of ATM to cell cycle regulation by the Chk2 protein kinase. Science **282:** 1893-1897.

McCulloch, S. D., and T. A. Kunkel, 2008 The fidelity of DNA synthesis by eukaryotic replicative and translesion synthesis polymerases. Cell Res. **18:** 148-161.

Memisoglu, A., and L. Samson, 2000 Base excision repair in yeast and mammals. Mutat. Res. **451:** 39-51.

Miller, J. H., A. Suthar, J. Tai, A. Yeung, C. Truong *et al.*, 1999 Direct selection for mutators in Escherichia coli. J. Bacteriol. **181:** 1576-1584.

Modrich, P., 2006 Mechanisms in eukaryotic mismatch repair. J. Biol. Chem. **281:** 30305-30309.

Morgan, C., and P. D. Lewis, 2006 iMARS—mutation analysis reporting software: an analysis of spontaneous *cII* mutation spectra. Mutat. Res. **603:** 15-26.

Morrison, A., J. B. Bell, T. A. Kunkel and A. Sugino, 1991 Eukaryotic DNA polymerase amino acid sequence required for 3′ → 5′ exonuclease activity. Proc. Natl. Acad. Sci. USA **88:** 9473-9477.

Morrison, A., A. L. Johnson, L. H. Johnston and A. Sugino, 1993 Pathway correcting DNA replication errors in *Saccharomyces cerevisiae*. EMBO J. **12:** 1467-1473.

Morrison, A., and A. Sugino, 1992 Roles of POL3, POL2 and PMS1 genes in maintaining accurate DNA replication. Chromosoma **102:** S147-149.

Morrison, A., and A. Sugino, 1993 DNA polymerase II, the epsilon polymerase of *Saccharomyces cerevisiae*. Prog. Nucleic Acid Res. Mol. Biol. **46:** 93-120.

Morrison, A., and A. Sugino, 1994 The 3′→5′ exonucleases of both DNA polymerases δ and ε participate in correcting errors of DNA replication in *Saccharomyces cerevisiae*. Mol. Gen. Genet. **242:** 289-296.

Muzyczka, N., R. L. Poland and M. J. Bessman, 1972 Studies on the biochemical basis of spontaneous mutation. I. A comparison of the deoxyribonucleic acid polymerases of mutator, antimutator, and wild type strains of bacteriophage T4. J. Biol. Chem. **247:** 7116-7122.

Myung, K., A. Datta and R. D. Kolodner, 2001 Suppression of spontaneous chromosomal rearrangements by S phase checkpoint functions in Saccharomyces cerevisiae. Cell **104:** 397-408.

Navadgi-Patil, V. M., and P. M. Burgers, 2009 A tale of two tails: activation of DNA damage checkpoint kinase Mec1/ATR by the 9-1-1 clamp and by Dpb11/TopBP1. DNA Repair (Amst) **8:** 996-1003.

Navas, T. A., Y. Sanchez and S. J. Elledge, 1996 RAD9 and DNA polymerase epsilon form parallel sensory branches for transducing the DNA damage checkpoint signal in Saccharomyces cerevisiae. Genes Dev. **10:** 2632-2643.

Navas, T. A., Z. Zhou and S. J. Elledge, 1995 DNA polymerase epsilon links the DNA replication machinery to the S phase checkpoint. Cell **80:** 29-39.

Nick Mcelhinny, S. A., D. A. Gordenin, C. M. Stith, P. M. J. Burgers and T. A. Kunkel, 2008 Division of labor at the eukaryotic replication fork. Mol. Cell **30:** 137-144.

Nick Mcelhinny, S. A., Pavlov, Y.I., Kunkel, T.A., 2006 Evidence for extrinsic exonucleolytic proofreading. Cell Cycle **5:** 958-962.
Nick Mcelhinny, S. A., C. M. Stith, P. M. J. Burgers and T. A. Kunkel, 2006 Inefficient proofreading and biased error rates during inaccurate DNA synthesis by a mutant derivative of Saccharomyces cerevisiae DNA polymerase delta. J. Biol. Chem.**:** M609591200.
Nilsson, A. I., E. Kugelberg, O. G. Berg and D. I. Andersson, 2004 Experimental adaptation of *Salmonella typhimurium* to mice. Genetics **168:** 1119-1130.
Northam, M. R., P. Garg, D. M. Baitin, P. M. Burgers and P. V. Shcherbakova, 2006 A novel function of DNA polymerase zeta regulated by PCNA. EMBO J. **25:** 4316-4325.
Northam, M. R., H. A. Robinson, O. V. Kochenova and P. V. Shcherbakova, 2010 Participation of DNA Polymerase ζ in Replication of Undamaged DNA in Saccharomyces cerevisiae. Genetics **184:** 27-42.
Notley-Mcrobb, L., S. Seeto and T. Ferenci, 2002 Enrichment and elimination of *mutY* mutators in *Escherichia coli* populations. Genetics **162:** 1055-1062.
Olsen, B., C. J. Murakami and M. Kaeberlein, 2010 YODA: software to facilitate high-throughput analysis of chronological life span, growth rate, and survival in budding yeast. BMC Bioinformatics **11**.
Palombo, F., I. Iaccarino, E. Nakajima, M. Ikejima, T. Shimada *et al.*, 1996 hMutSβ, a heterodimer of hMSH2 and hMSH3, binds to insertion/deletion loops in DNA. Curr. Biol. **6:** 1181-1184.
Parsons, R., G. M. Li, M. J. Longley, W. H. Fang, N. Papadopoulos *et al.*, 1993 Hypermutability and mismatch repair deficiency in RER+ tumor cells. Cell **75:** 1227-1236.
Paulovich, A. G., and L. H. Hartwell, 1995 A checkpoint regulates the rate of progression through s phase in S. cerevisiae in response to DNA damage. Cell **82:** 841-847.
Paulovich, A. G., R. U. Margulies, B. M. Garvik and L. H. Hartwell, 1997 RAD9, RAD17, and RAD24 are required for S phase regulation in Saccharomyces cerevisiae in response to DNA damage. Genetics **145:** 45-62.
Pavlov, Y. I., C. Frahm, S. A. Mcelhinny, A. Niimi, M. Suzuki *et al.*, 2006a Evidence that errors made by DNA polymerase α are corrected by DNA polymerase δ. Curr. Biol. **16:** 202-207.
Pavlov, Y. I., S. Maki, H. Maki and T. A. Kunkel, 2004 Evidence for interplay among yeast replicative DNA polymerases alpha, delta and epsilon from studies of exonuclease and polymerase active site mutations. BMC Biol. **2:** 11.
Pavlov, Y. I., I. M. Mian and T. A. Kunkel, 2003 Evidence for preferential mismatch repair of lagging strand DNA replication errors in yeast. Curr. Biol. **13:** 744-748.
Pavlov, Y. I., C. S. Newlon and T. A. Kunkel, 2002 Yeast origins establish a strand bias for replicational mutagenesis. Mol. Cell **10:** 207-213.
Pavlov, Y. I., and P. V. Shcherbakova, 2010 DNA polymerases at the eukaryotic fork—20 years later. Mutat. Res. **685:** 45-53.
Pavlov, Y. I., P. V. Shcherbakova and T. A. Kunkel, 2001 In vivo consequences of putative active site mutations in yeast DNA polymerases alpha, epsilon, delta, and zeta. Genetics **159:** 47-64.
Pavlov, Y. I., P. V. Shcherbakova and I. B. Rogozin, 2006b Roles of DNA polymerases in replication, repair, and recombination in eukaryotes. Int. Rev. Cytol. **255:** 41-132.

Peltomäki, P., 2005 Lynch syndrome genes. Fam. Cancer **4:** 227-232.
Poli, J., O. Tsaponina, L. Crabbe, A. Keszthelyi, V. Pantesco *et al.*, 2012 dNTP pools determine fork progression and origin usage under replication stress. The EMBO journal **31:** 883-894.
Prakash, S., and L. Prakash, 2002 Translesion DNA synthesis in eukaryotes: a one- or two-polymerase affair. Genes Dev. **16:** 1872-1883.
Preston, B. D., T. M. Albertson and A. J. Herr, 2010 DNA replication fidelity and cancer. Semin. Cancer Biol. **20:** 281-293.
Prolla, T. A., D. M. Christie and R. M. Liskay, 1994 Dual requirement in yeast DNA mismatch repair for *MLH1* and *PMS1*, two homologs of the bacterial *mutL* gene. Mol. Cell. Biol. **14:** 407-415.
Puddu, F., G. Piergiovanni, P. Plevani and M. Muzi-Falconi, 2011 Sensing of replication stress and Mec1 activation act through two independent pathways involving the 9-1-1 complex and DNA polymerase epsilon. PLoS Genet. **7:** e1002022.
Pursell, Z. F., I. Isoz, E. B. Lundstrom, E. Johansson and T. A. Kunkel, 2007 Yeast DNA polymerase ε participates in leading-strand DNA replication. Science **317:** 127-130.
Pursell, Z. F., and T. A. Kunkel, 2008 DNA polymerase ε: a polymerase of unusual size (and complexity). Prog. Nucleic Acid Res. Mol. Biol. **82:** 101-145.
Quah, S. K., R. C. Von Borstel and P. J. Hastings, 1980 The origin of spontaneous mutation in *Saccharomyces cerevisiae*. Genetics **96:** 819-839.
Raghuraman, M. K., E. A. Winzeler, D. Collingwood, S. Hunt, L. Wodicka *et al.*, 2001 Replication dynamics of the yeast genome. Science **294:** 115-121.
Reenan, R. A., and R. D. Kolodner, 1992 Characterization of insertion mutations in the *Saccharomyces cerevisiae MSH1* and *MSH2* genes: evidence for separate mitochondrial and nuclear functions. Genetics **132:** 975-985.
Reha-Krantz, L. J., 1988 Amino acid changes coded by bacteriophage T4 DNA polymerase mutator mutants. Relating structure to function. J. Mol. Biol. **202:** 711-724.
Reha-Krantz, L. J., 1995 Learning about DNA polymerase function by studying antimutator DNA polymerases. Trends Biochem. Sci. **20:** 136-140.
Reha-Krantz, L. J., 2010 DNA polymerase proofreading: Multiple roles maintain genome stability. Biochim. Biophys. Acta **1804:** 1049-1063.
Reha-Krantz, L. J., and R. L. Nonay, 1994 Motif A of bacteriophage T4 DNA polymerase: role in primer extension and DNA replication fidelity. Isolation of new antimutator and mutator DNA polymerases. J. Biol. Chem. **269:** 5635-5643.
Reha-Krantz, L. J., M. S. Siddique, K. Murphy, A. Tam, M. O'carroll *et al.*, 2011 Drug-sensitive DNA polymerase δ reveals a role for mismatch repair in checkpoint activation in yeast. Genetics **189:** 1211-1224.
Reichard, P., 1988a Interactions between deoxynucleotide and DNA synthesis. Annu. Rev. Biochem. **57:** 349-374.
Reichard, P., 1988b Interactions Between Deoxyribonucleotide and DNA Synthesis. Annu. Rev. Biochem. **57:** 349-374.
Reitmair, A. H., R. Risley, R. G. Bristow, T. Wilson, A. Ganesh *et al.*, 1997 Mutator phenotype in Msh2-deficient murine embryonic fibroblasts. Cancer Res. **57:** 3765-3771.

Rouse, J., and S. P. Jackson, 2002 Interfaces between the dectection, signaling and repair of DNA damage. Science **297:** 547-551.
Sabouri, N., J. Viberg, D. K. Goyal, E. Johansson and A. Chabes, 2008 Evidence for lesion bypass by yeast replicative DNA polymerases during DNA damage. Nucleic Acids Res. **36:** 5660-5667.
Saenger, W., 1984 *Principles of Nucleic Acid Structure*. Springer-Verlag, New York.
Sancar, A., L. A. Lindsey-Boltz, K. Unsal-Kacmaz and S. Linn, 2004 Molecular mechanisms of mammalian DNA repair and the DNA damage checkpoints. Ann Rev Biochem **73:** 39-85.
Sanchez, Y., J. Bachant, H. Wang, F. Hu, D. Liu *et al.*, 1999 Control of the DNA Damage Checkpoint by Chk1 and Rad53 Protein Kinases Through Distinct Mechanisms. Science **286:** 1166-1171.
Sawaya, M. R., R. Prasad, S. H. Wilson, J. Kraut and H. Pelletier, 1997 Crystal structures of human DNA polymerase beta complexed with gapped and nicked DNA: evidence for an induced fit mechanism. Biochemistry (Mosc). **36:** 11205-11215.
Schaaper, R. M., 1993 Base selection, proofreading, and mismatch repair during DNA replication in *Escherichia coli*. J. Biol. Chem. **268:** 23762-23765.
Schaaper, R. M., 1996 Suppressors of *Escherichia coli mutT*: antimutators for DNA replication errors. Mutat. Res. **350:** 17-23.
Schaaper, R. M., 1998 Antimutator mutants in bacteriophage T4 and *Escherichia coli*. Genetics **148:** 1579-1585.
Schaaper, R. M., and R. Cornacchio, 1992 An *Escherichia coli dnaE* mutation with suppressor activity toward mutator *mutD5*. J. Bacteriol. **174:** 1974-1982.
Schmitt, M. W., R. N. Venkatesan, M. J. Pillaire, J. S. Hoffmann, J. M. Sidorova *et al.*, 2010 Active site mutations in mammalian DNA polymerase delta alter accuracy and replication fork progression. J. Biol. Chem. **285:** 32264-32272.
Shamoo, Y., and T. A. Steitz, 1999 Building a replisome from interacting pieces: sliding clamp complexed to a peptide from DNA polymerase and a polymerase editing complex. Cell **99:** 155-166.
Shcherbakova, P. V., V. N. Noskov, M. R. Pshenichnov and Y. I. Pavlov, 1996 Base analog 6-N-hydroxylaminopurine mutagenesis in the yeast *Saccharomyces cerevisiae* is controlled by replicative DNA polymerases. Mutat. Res. **369:** 33-44.
Shcherbakova, P. V., and Y. I. Pavlov, 1996 3'-->5' exonucleases of DNA polymerases epsilon and delta correct base analog induced DNA replication errors on opposite DNA strands in Saccharomyces cerevisiae. Genetics **142:** 717-726.
Shcherbakova, P. V., Y. I. Pavlov, O. Chilkova, I. B. Rogozin, E. Johansson *et al.*, 2003 Unique error signature of the four-subunit yeast DNA polymerase ε. J. Biol. Chem. **278:** 43770-43780.
Sherman, F., 2002 Getting started with yeast, pp. 3-41 in *Part B: Guide to Yeast Genetics and Molecular and Cell Biology*, edited by C. GUTHRIE and G. R. FINK. Academic Press, San Diego.
Shimizu, K., K. Hashimoto, J. M. Kirchner, W. Nakai, H. Nishikawa *et al.*, 2002 Fidelity of DNA polymerase ε holoenzyme from budding yeast *Saccharomyces cerevisiae*. J. Biol. Chem. **277:** 37422-37429.

Simon, M., L. Giot and G. Faye, 1991 The 3' to 5' exonuclease activity located in the DNA polymerase δ subunit of *Saccharomyces cerevisiae* is required for accurate replication. EMBO J. **10:** 2165-2170.

Siow, C. C., S. R. Nieduszynska, C. A. Müller and C. A. Nieduszynski, 2012 OriDB, the DNA replication origin database updated and extended. Nucleic Acids Res. **40:** D682-D686.

Smith, R. A., L. A. Loeb and B. D. Preston, 2005 Lethal mutagenesis of HIV. Virus Res. **107:** 215-228.

Sniegowski, P. D., P. J. Gerrish and R. E. Lenski, 1997 Evolution of high mutation rates in experimental populations of *E. coli*. Nature **387:** 703-705.

Sokolsky, T., and E. Alani, 2000 *EXO1* and *MSH6* are high-copy suppressors of conditional mutations in the *MSH2* mismatch repair gene of *Saccharomyces cerevisiae*. Genetics **155:** 589-599.

Steitz, T. A., S. J. Smerdon, J. Jager and C. M. Joyce, 1994 A unified polymerase mechanism for nonhomologous DNA and RNA polymerases. Science **266:** 2022-2025.

Stocki, S. A., R. L. Nonay and L. J. Reha-Krantz, 1995 Dynamics of bacteriophage T4 DNA polymerase function: identification of amino acid residues that affect switching between polymerase and 3' → 5' exonuclease activities. J. Mol. Biol. **254:** 15-28.

Strand, M., T. A. Prolla, R. M. Liskay and T. D. Petes, 1993 Destabilization of tracts of simple repetitive DNA in yeast by mutations affecting DNA mismatch repair. Nature **365:** 274-276.

Stulemeijer, I. J., B. L. Pike, A. W. Faber, K. F. Verzijlbergen, T. Van Welsem *et al.*, 2011 Dot1 binding induces chromatin rearrangements by histone methylation-dependent and -independent mechanisms. Epigenetics Chromatin. **4:** 2-15.

Swan, M. K., R. E. Johnson, L. Prakash, S. Prakash and A. K. Aggarwal, 2009 Structural basis of high-fidelity DNA synthesis by yeast DNA polymerase δ. Nat. Struct. Mol. Biol. **16:** 979-986.

Taddei, F., M. Radman, J. Maynard-Smith, B. Toupance, P. H. Gouyon *et al.*, 1997 Role of mutator alleles in adaptive evolution. Nature **387:** 700-702.

Tanaka, H., H. Arakawa, T. Yamaguchi, K. Shiraishi, S. Fukuda *et al.*, 2000 A ribonucleotide reductase gene involved in p53-dependent cell cycle checkpoint for DNA damage. Nature **404:** 42-49.

Tercero, J. A., and J. F. X. Diffley, 2001 Regulation of DNA replication fork progression through damaged DNA by the Mec1/Rad53 checkpoint. **412:** 553-557.

Thompson, D. A., M. M. Desai and A. W. Murray, 2006 Ploidy controls the success of mutators and nature of mutations during budding yeast evolution. Curr. Biol. **16:** 1581-1590.

Tkach, J. M., A. Yimit, A. Y. Lee, M. Riffle, M. Costanzo *et al.*, 2001 Dissecting DNA damage response pathways by analysing protein localization and abundance changes during DNA replication stress. Nat Cell Biol **14:** 966-976.

Tomlinson, I., P. Sasieni and W. Bodmer, 2002 How many mutations in a cancer? Am. J. Pathol. **160:** 755-758.

Tong, A. H., M. Evangelista, A. B. Parsons, H. Xu, G. D. Bader *et al.*, 2001 Systematic genetic analysis with ordered arrays of yeast deletion mutants. Science **294:** 2364-2368.

Tong, A. H., G. Lesage, G. D. Bader, H. Ding, H. Xu *et al.*, 2004 Global mapping of the yeast genetic interaction network. Science **303:** 808-813.

Tong, A. H. Y., and C. Boone, 2007 High-throughput strain construction and systematic synthetic lethal screening in *Saccaromyces cerevisiae*, pp. 369-386, 706-707 in *Methods in Microbiology*, edited by I. STANSFIELD and M. J. R. STARK. Academic Press.

Tran, H. T., N. P. Degtyareva, D. A. Gordenin and M. A. Resnick, 1999a Genetic factors affecting the impact of DNA polymerase δ proofreading activity on mutation avoidance in yeast. Genetics **152:** 47-59.

Tran, H. T., N. P. Degtyareva, N. N. Koloteva, A. Sugino, H. Masumoto *et al.*, 1995 Replication slippage between distant short repeats in Saccharomyces cerevisiae depends on the direction of replication and the RAD50 and RAD52 genes. Mol. Cell. Biol. **15:** 5607-5617.

Tran, H. T., D. A. Gordenin and M. A. Resnick, 1999b The 3′→5′ exonucleases of DNA polymerases δ and ε and the 5′→3′ exonuclease Exo1 have major roles in postreplication mutation avoidance in *Saccharomyces cerevisiae*. Mol. Cell. Biol. **19:** 2000-2007.

Tröbner, W., and R. Piechocki, 1984 Selection against hypermutability in *Escherichia coli* during long term evolution. Mol. Gen. Genet. **198:** 177-178.

Trujillo, K. M., and P. Sung, 2001 DNA Structure-specific Nuclease Activities in the Saccharomyces cerevisiae Rad50·Mre11 Complex. J. Biol. Chem. **276:** 35458-35464.

Tsai, Y.-C., and K. A. Johnson, 2006 A new paradigm for DNA polymerase specificity. Biochemistry (Mosc). **45:** 9675-9687.

Tsaponina, O., E. Barsoum, S. U. Astrom and A. Chabes, 2011 Ixr1 is required for the expression of the ribonucleotide reductase Rnr1 and maintenance of dNTP pools. PLoS Genet. **7:** e1002061.

Unk, I., L. Haracska, S. Prakash and L. Prakash, 2001 3'-Phosphodiesterase and 3′→5′ Exonuclease Activities of Yeast Apn2 Protein and Requirement of These Activities for Repair of Oxidative DNA Damage. Mol. Cell. Biol. **21:** 1656-1661.

Venkatesan, R. N., J. J. Hsu, N. A. Lawrence, B. D. Preston and L. A. Loeb, 2005 Mutator phenotypes caused by substitution at a conserved motif A residue in eukaryotic DNA polymerase δ. J. Biol. Chem. **281:** 4486-4494.

Viguera E., C. D., Ehrlich S.D., 2001 Replication slippage involves DNA polymerase pausing and dissociation. EMBO J. **20:** 2587-2595.

Wang, J., A. K. Sattar, C. C. Wang, J. D. Karam, W. H. Konigsberg *et al.*, 1997 Crystal structure of a pol α family replication DNA polymerase from bacteriophage RB69. Cell **89:** 1087-1099.

Wang, T. L., C. Rago, N. Silliman, J. Ptak, S. Markowitz *et al.*, 2002 Prevalence of somatic alterations in the colorectal cancer cell genome. Proc. Natl. Acad. Sci. USA **99:** 3076-3080.

Wang, T. S.-F., S. W. Wong and D. Korn, 1989 Human DNA polymerase α: predicted functional domains and relationships with viral DNA polymerases. FASEB J. **3:** 14-21.

Wang, W., and B. A. Malcolm, 1999 Two-stage PCR protocol allowing introduction of multiple mutations, deletions and insertions using QuikChange Site-Directed Mutagenesis. Biotechniques **26:** 680-682.
Wei, K., R. Kucherlapati and W. Edelmann, 2002 Mouse models for human DNA mismatch-repair gene defects. Trends Mol. Med. **8:** 346-353.
Weinberg, G., B. Ullman and D. W. J. Martin, 1981 Mutator phenotypes in mammalian cell mutants with distinct diochemical defects and abnormal deoxyribonucleoside triphosphate pools. Proc. Natl. Acad. Sci. USA **78:** 2447-2451.
Weymouth, L. A., and L. A. Loeb, 1978 Mutagenesis during in vitro DNA synthesis. Proc. Natl. Acad. Sci. USA **75:** 1924-1928.
Williamson, M. S., J. C. Game and S. Fogel, 1985 Meiotic gene conversion mutants in *Saccharomyces cerevisiae*. I. Isolation and characterization of *pms1-1* and *pms1-2*. Genetics **110:** 609-646.
Wing, R. A., S. Bailey and T. A. Steitz, 2008 Insights into the replisome from the structure of a ternary complex of the DNA polymerase III α-subunit. J. Mol. Biol. **382:** 859-869.
Winzeler, E. A., D. D. Shoemaker, A. Astromoff, H. Liang, K. Anderson *et al.*, 1999 Functional characterization of the *S. cerevisiae* genome by gene deletion and parallel analysis. Science **285:** 901-906.
Wloch, D. M., K. Szafraniec, R. H. Borts and R. Korona, 2001 Direct estimate of the mutation rate and the distribution of fitness effects in the yeast *Saccharomyces cerevisiae*. Genetics **159:** 441-452.
Wu, X., and M. Huang, 2008 Dif1 controls subcellular localization of ribonucleotide reductase by mediating nuclear import of the R2 subunit. Mol. Cell. Biol. **28:** 7156-7167.
Yabuki, N., H. Terashima and K. Kitada, 2002 Mapping of early firing origins on a replication profile of budding yeast. Genes Cells **7:** 781-789.
Yamaguchi, T., K. Matsuda, Y. Sagiya, M. Iwadate, M. A. Fujino *et al.*, 2001a p53R2-dependent Pathway for DNA Synthesis in a p53-regulated Cell Cycle Checkpoint. Cancer Res. **61:** 8256-8262.
Yamaguchi, T., K. Matsuda, Y. Sagiya, M. Iwadate, M. A. Fujino *et al.*, 2001b p53R2-dependent pathway for DNA synthesis in a p53-regulated cell cycle checkpoint. Cancer Res. **61:** 8256-8262.
Yu, L., L. Pena Castillo, S. Mnaimneh, T. R. Hughes and G. W. Brown, 2006 A survey of essential gene function in the yeast cell division cycle. Mol. Biol. Cell **17:** 4736-4747.
Zegerman, P., and J. F. Diffley, 2009 DNA replication as a target of the DNA damage checkpoint. DNA Repair (Amst) **8:** 1077-1088.
Zeyl, C., and J. a. G. M. De Visser, 2001 Estimates of the rate and distribution of fitness effects of spontaneous mutation in *Saccharomyces cerevisiae*. Genetics **157:** 53-61.
Zhao, X., E. G. Muller and R. Rothstein, 1998 A suppressor of two essential checkpoint genes identifies a novel protein that negatively affects dNTP pools. Mol. Cell **2:** 329-340.

Zhao, X., and R. Rothstein, 2002 The Dun1 checkpoint kinase phosphorylates and regulates the ribonucleotide reductase inhibitor Sml1. Proc. Natl. Acad. Sci. USA **99:** 3746-3751.

Zhou, B. B., and S. J. Elledge, 2000 The DNA damage response: putting checkpoints in perspective. Nature **408:** 433-439.

Zhou, Z., and S. J. Elledge, 1993 DUN1 encodes a protein kinase that controls the DNA damage response in yeast. Cell **75:** 1119-1127.

Zou, L., D. Liu and S. J. Elledge, 2003 Replication protein A-mediated recruitment and activation of Rad17 complexes. Proc. Natl. Acad. Sci. USA **100:** 13827-13832.